USGS
science for a changing world

2016 National Park Service CENTENNIAL

Prepared in Cooperation with the National Park Service

# Geologic Map of Great Sand Dunes National Park, Colorado

By Richard F. Madole, D. Paco VanSistine, and Joseph H. Romig

Pamphlet to accompany Scientific Investigations Map 3362
Version 1.1, August 2018

**U.S. Department of the Interior**
**U.S. Geological Survey**

Prepared in Cooperation with the National Park Service

# Geologic Map of Great Sand Dunes National Park, Colorado

By Richard F. Madole, D. Paco VanSistine, and Joseph H. Romig

Pamphlet to accompany Scientific Investigations Map 3362
Version 1.1, August 2018

**U.S. Department of the Interior**
**U.S. Geological Survey**

**U.S. Department of the Interior**
SALLY JEWELL, Secretary

**U.S. Geological Survey**
Suzette M. Kimball, Director

U.S. Geological Survey, Reston, Virginia: 2016
First release: 2016
Revised: August 2018 (ver 1.1)



**Suggested citation:**
Madole, R.F, VanSistine, D. Paco, and Romig, J.H., 2016, Geologic map of Great Sand Dunes National Park, Colorado (ver. 1.1, August 2018): U.S. Geological Survey Scientific Investigations Map 3362, 58 p., scale 1:35,000, https://doi.org/10.3133/sim3362.

ISSN 2329-1311 (print)
ISSN 2329-132X (online)
ISBN 978-1-4113-4072-5

# Acknowledgments

*Major funding sources include the Bradley Scholar Program of the U.S. Geological Survey (USGS), the project "Effects of Climatic Variability and Land Use on American Drylands" directed by Rich Reynolds (USGS), the National Park Service (NPS), and the Colorado State Historic Fund through The Friends of the Dunes, Inc. The Nature Conservancy also gave material support and access to their properties. The Great Sand Dunes National Park staff provided significant logistical support, and we are particularly grateful to Fred Bunch, Andrew Valdez, Patrick Myers, and Bruce Heise of the NPS for assistance and support in a variety of ways. We thank Margaret Berry and Cal Ruleman (USGS) for reviewing the map and the accompanying pamphlet and for providing constructive comments and suggestions that improved both documents. In addition, we thank the many individuals who helped in various ways, including Lisa Binder, Eric Fisher, Rick Forester (deceased), Jonathan Friedman, Harland Goldstein, Tien Grauch, Jeff Honke, Shannon Mahan, Carol Quesenberry, Rich Reynolds, Lisa Ramirez Rukstales, Randy Schumann, and Gary Skipp (all of the USGS); Jeremy Havens (ADC Management Services, Inc.); Paula Hansley (Petrographic Consultants International, Inc.); Margaret A. Jodry (Smithsonian Museum of Natural History); and Bob Rozinski (International League of Conservation Photographers).*

# Contents



## Figures

## Sheet



## Tables

## Conversion Factors

Inch/Pound to International System of Units

| Multiply | By | To obtain |
|---|---|---|
| | Length | |
| inch | 2.54 | centimeter |
| foot (ft) | 0.3048 | meter (m) |
| mile (mi) | 1.609 | kilometer (km) |
| | Area | |
| square mile ($mi^2$) | 2.590 | square kilometer ($km^2$) |
| | Volume | |
| cubic mile ($mi^3$) | 4.168 | cubic kilometer ($km^3$) |

International System of Units to Inch/Pound

| Multiply | By | To obtain |
|---|---|---|
| | Length | |
| centimeter (cm) | 0.3937 | inch (in.) |
| meter (m) | 3.281 | foot (ft) |
| kilometer (km) | 0.6214 | mile (mi) |
| | Area | |
| square kilometer ($km^2$) | 0.3861 | square mile ($mi^2$) |
| | Volume | |
| cubic kilometer ($km^3$) | 0.2399 | cubic mile ($mi^3$) |

Temperature in degrees Celsius (°C) may be converted to degrees Fahrenheit (°F) as °F = (1.8 × °C) + 32.

Temperature in degrees Fahrenheit (°F) may be converted to degrees Celsius (°C) as °C = (°F – 32) / 1.8.

## Datum

Horizontal coordinate information is referenced to the North American Datum of 1983 (NAD 83).

Vertical coordinate information is referenced to the North American Vertical Datum of 1988 (NAVD 88)

Altitude, as used in this report, refers to distance above sea level.

## Supplemental Information

1 micrometer (µm) = 1 $x10^{-6}$ meters or 1 millionth of a meter

Calibrated and radiocarbon ages are reported relative to AD 1950 (calibrated years before the present; cal yr BP).

Specific conductance is given in microsiemens per centimeter at 25 degrees Celsius (µS/cm at 25 °C).

$\delta$ $^{13}C$ value—Refers to the ratio between the $^{13}C/^{12}C$ of the radiocarbon sample and the $^{13}C/^{12}C$ of the PDB standard (a fossil belemnite from the Peedee Formation in South Carolina) expressed as per mil (‰). This value indicates the degree to which the isotopic composition of the sample varies from the PDB standard. It is used to adjust $^{14}C$ ages to correct for isotopic fractionation. Plants fractionate atmospheric $CO_2$, and have less $^{13}C$ than the atmosphere; hence, the negative delta $^{13}C$ values listed in table 1.

## Divisions of Quaternary, Neogene, and Paleogene Time Used in This Report

| Period or subperiod | Epoch | | Age |
|---|---|---|---|
| Quaternary | Holocene[1] | late | present–4.0 ka |
| | | middle | 4.0–8.0 ka |
| | | early | 8.0–11.7 ka |
| | Pleistocene | late | 11.7–126 ka |
| | | middle | 126–781 ka |
| | | early | 781 ka–2.58 Ma |
| Neogene | Pliocene | | 2.58–5.33 Ma |
| | Miocene | | 5.33–23.03 Ma |
| Paleogene | Oligocene | | 23.03–33.9 Ma |
| | Eocene | | 33.9–56.0 Ma |
| | Paleocene | | 56.0–66.0 Ma |

[1]Except for the subdivisions of the Holocene epoch, ages of time boundaries are those of the International Commission on Stratigraphy (Cohen and others, 2015). Ages are expressed in ka for kilo-annum (thousand years ago) and Ma for mega-annum (million years ago).

## Useful Web Sites

U.S. Geological Survey (USGS)
http://www.usgs.gov/

National Park Service (NPS)
http://www.nps.gov/index.htm

Great Sand Dunes National Park
http://www.nps.gov/grsa/index.htm

Great Sand Dunes National Park location map
http://www.nps.gov/grsa/planyourvisit/maps.htm

Great Sand Dunes National Park visitor guide
http://www.nps.gov/grsa/planyourvisit/upload/visitor_guide-2014-final-webversion.pdf

# Geologic Map of Great Sand Dunes National Park, Colorado

By Richard F. Madole,[1] D. Paco VanSistine,[1] and Joseph H. Romig[2]

## Introduction

The purpose of this map and pamphlet is to provide the public and the National Park Service (NPS) with a detailed geologic map and information about the age, origin, and evolution of the landscape of which the Great Sand Dunes National Park is a part (fig. 1). The Great Sand Dunes National Park is covered almost entirely by surficial deposits (loose, uncemented sediment as opposed to rock) of Quaternary age. Quaternary is the term for the geologic period that spans the time between 2.58 Ma (million years ago) and the present. Prior to this study, the area encompassed by the park and the complex array of Quaternary deposits in it (divided here into 19 different units) had never been mapped or studied in detail. The impetus for mapping evolved in the aftermath of a range fire that burned a large area in the southeastern part of the park in April 2000. The temporary absence of vegetation following the fire presented opportunities to discover archeological sites that would greatly expand knowledge of the prehistory of the area. However, reconstructing the paleoenvironments of these sites begins with understanding their geologic setting and recent geologic history, information that was lacking at the time. Hence, geologic mapping began at select locations in support of archeological studies.

[1]U.S. Geological Survey
[2]Ponderosa Associates Ltd., Lafayette, Colo.

Eventually, the scope of the mapping was broadened to include the entire park because even before the archeological program was initiated, it was recognized that a detailed geologic map would be useful to address management issues in areas within and adjacent to the park. Chief among these issues are concerns about groundwater withdrawals, maintenance of natural vegetation, environmental restoration, and preservation of cultural resources. As Mast (2007) noted, the principal threat to water resources in the Great Sand Dunes National Park are surface water and groundwater withdrawals and climate change. These threats also extend to the Baca National Wildlife Refuge and the San Luis State Park and San Luis Lakes Wildlife Area, which border the Great Sand Dunes National Park on the west, and to the Blanca Wildlife Habitat Area (administered by the Bureau of Land Management) and the Alamosa National Wildlife Refuge south of the park (see the regional index map on pages 2–3). Also, the Closed Basin Project, which mostly coincides with the area referred to here as the trough (fig. 2), overlaps the western part of the park. This project, operated by the Bureau of Reclamation, maintains a large network of wells and a canal to extract groundwater from the closed basin and export it to the Rio Grande to comply with the terms of the Rio Grande Compact (Public Act No. 96, 76th Congress). This compact, which was adopted in 1939, assures availability of Rio Grande water to States downstream from Colorado. The compact also allows water to be provided when needed to the Alamosa Wildlife Refuge, the Blanca Wildlife Habitat area, and the San Luis Lakes State Park and Wildlife Area.

# Regional Index Map for Great Sand Dunes National Park, Colorado

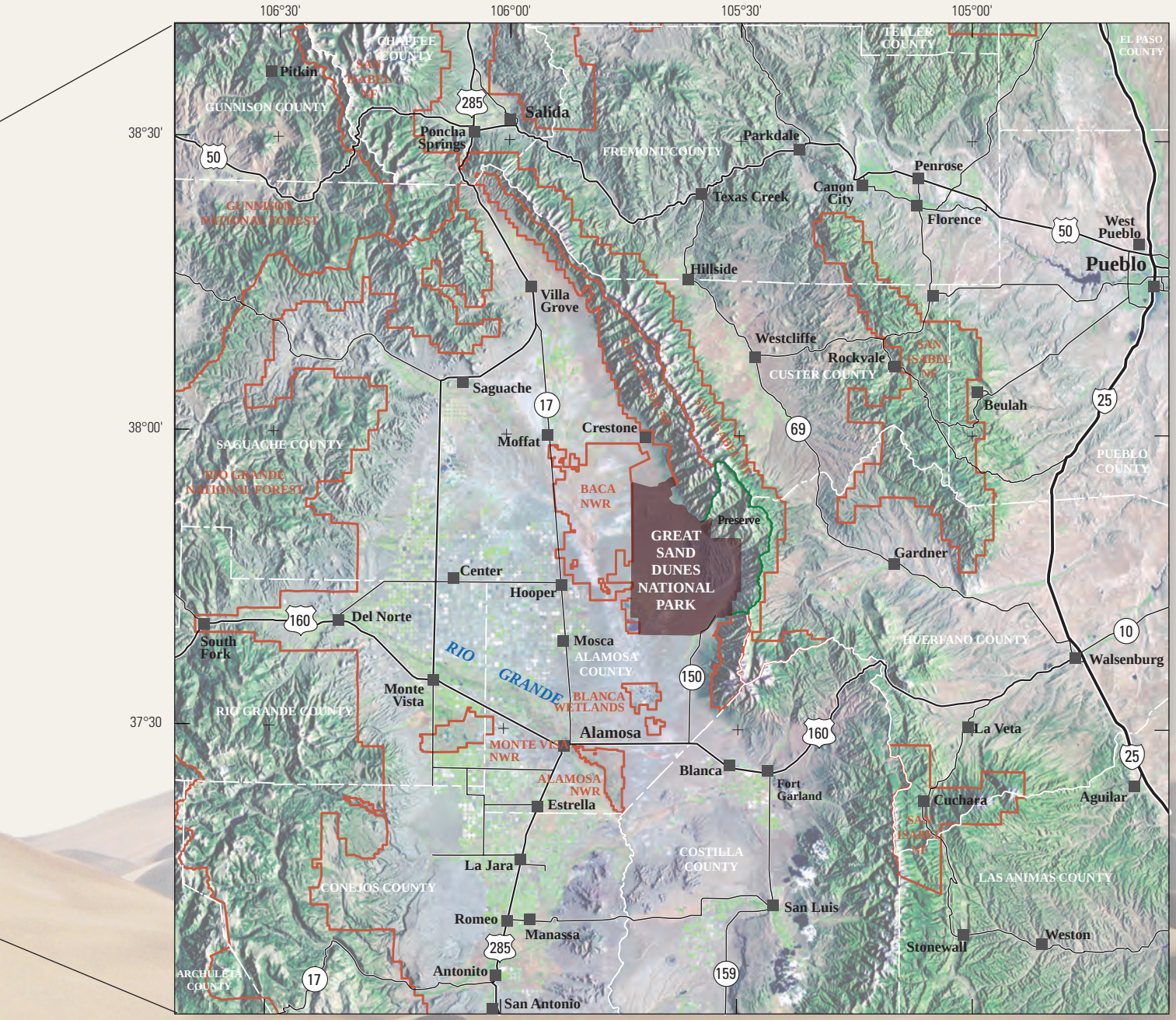


Base Image from U.S. Geological Survey 30-meter Landsat
National Park and Preserve, and other boundaries from Data.gov
and other sources as listed on main map.

0 5 10 15 20 MILES
0 5 10 15 20 KILOMETERS

**EXPLANATION**

- 25 — Interstate route
- 160 — U.S. route
- 69 — County road
- National or State park, area, forest, or other boundary
- Great Sand Dunes National Park
- County boundary

# Geologic Setting

## Structure and Pre-Quaternary Geology

The San Luis Valley in south-central Colorado and north-central New Mexico is a major component of the Rio Grande rift (figs. 3*A* and 3*B*), which is one of the more important geologic structures of its kind in the world (Chapin, 1971; Tweto, 1979; Chapin and Cather, 1994; Keller and Cather, 1994; Hudson and Grauch, 2013). The rift extends from northern Mexico to the Southern Rocky Mountains in central Colorado, a distance of more than 1,000 kilometers (km). The San Luis Valley segment of the rift (San Luis basin) is about 220 km long and as much as 70–75 km wide. It is closed off on the north by the convergence of the Sangre de Cristo Range on the east and the San Juan Mountains on the west, and on the south by the convergence of the Sangre de Cristo Range and the Tusas Mountains.

Like other structural basins in the Rio Grande rift, the San Luis basin is a half-graben (fig. 3*B*). In the San Luis basin, the dominant displacement was down on the east. Sediment aggraded in the basin as rifting proceeded, and in the process produced a relatively flat surface that conceals a complex, highly faulted subsurface terrain (Brister and Gries, 1994; Kluth and Schaftenaar, 1994). Within the first-order half graben are several second-order grabens and horsts (fig. 3*B*). Lipman and Mehnert (1975) placed the onset of rifting in the San Luis basin at about 26 Ma, and Wallace (2004) concluded that rifting in the Culebra re-entrant, the eastward recess in the rift margin south of Blanca Peak (fig. 1), began about 25 Ma. However, the pronounced topographic relief that exists today between the San Luis Valley floor and adjacent mountains (about 2,100 meters [m]) most likely did not develop until well after 15 Ma (Chapin and Cather, 1994).

The ages and kinds of rock in the mountains flanking the San Luis Valley are distinctly different. The San Juan Mountains on the west side of the valley consist almost entirely of upper Eocene and lower Miocene volcanic rocks ranging in age from about 35 Ma to about 18 Ma (Lipman, 2007). In contrast, the core rocks of the Sangre de Cristo Range exposed in the vicinity of the Great Sand Dunes are mostly gneiss and quartz monzonite of Paleoproterozoic age (2,500–1,600 Ma) (Johnson and others, 1989). The San Luis Hills are a cluster of upthrown, tilted fault blocks of Oligocene volcanic rock, similar to that in the nearby San Juan Mountains, which more or less divide the San Luis Valley into halves (fig. 4). Volcanic rock (mostly the Pliocene Servilleta Basalt capping the Taos Plateau volcanic field) and lesser amounts of sedimentary rock (the Tertiary Santa Fe Group) cover most of the southern half of the San Luis Valley. Conversely, the northern half of the valley contains only a small amount of volcanic rock and is covered almost entirely by sediment of Quaternary age. This sediment is estimated to be as much as 610 m thick (Huntley, 1976), and most of the upper 75 m or more is poorly sorted alluvium that includes various combinations of sand, silt, clay, and some gravel derived from adjacent mountains (Madole and others, 2013) (fig. 5).

## Closed Basin

That part of the San Luis Valley between Poncha Pass on the north and the small city of Alamosa on the south, a distance of a little more than 100 km, is a closed basin; which is to say, there is no outflow of surface water from this area. High mountains bound the basin on all sides except the south (fig. 2). On the south, only an ill-defined topographic divide and a low groundwater divide (Powell, 1958) separate the closed basin from the Rio Grande drainage basin. On the west side of the San Luis Valley, this topographic divide is practically adjacent to the Rio Grande, but southeastward from where the river exits the mountains, the trends of the river and the topographic divide diverge. Thus, in the vicinity of Alamosa, the divide bounding the southern end of the closed-basin floor is about 5 km north of the Rio Grande. On the east side of the valley, this boundary terminates on the foot slopes of Blanca Peak.

The lowest part of the closed basin, the trough (fig. 2), is closer to the east side of the San Luis Valley than to the west side, and its axis trends northwest-southeast approximately parallel to the Sangre de Cristo Range. In the northernmost part of the closed basin, from Poncha Pass southward to about 8 km beyond Villa Grove, piedmont-slope deposits derived from opposing sides of the San Luis Valley converge along San Luis Creek. Near its confluence with the eastward flowing Saguache Creek, which originates in the San Juan Mountains, San Luis Creek also is joined by several westward-flowing tributaries that originate in the cluster of exceptionally high peaks east of Crestone. These streams more or less converge at the northern end of an ill-defined shallow trough that is bounded on the west by the distal edge of the large Rio Grande fan (about 1,150 square kilometers [km$^2$] or 444 square miles [mi$^2$]) and on the east by the distal edge of the piedmont slope that flanks the Sangre de Cristo Range (fig. 2). This shallow trough was one of the features that caught Hayden's (1873) attention during his preliminary survey of the area. He described it (p. 176) as

> a singular depression, about 10 miles wide and thirty miles long; it looks like one vast thicket of 'greasewood' *Sarcobatus vermicularis*, and other chenopiaceous shrubs. Into it flow some twelve or fifteen good sized streams [sic], and yet there is no known outlet, neither is there any large body of water visible. It seems to be one vast swamp or bog, with a few small lakes, one of which is said to be three miles in length.

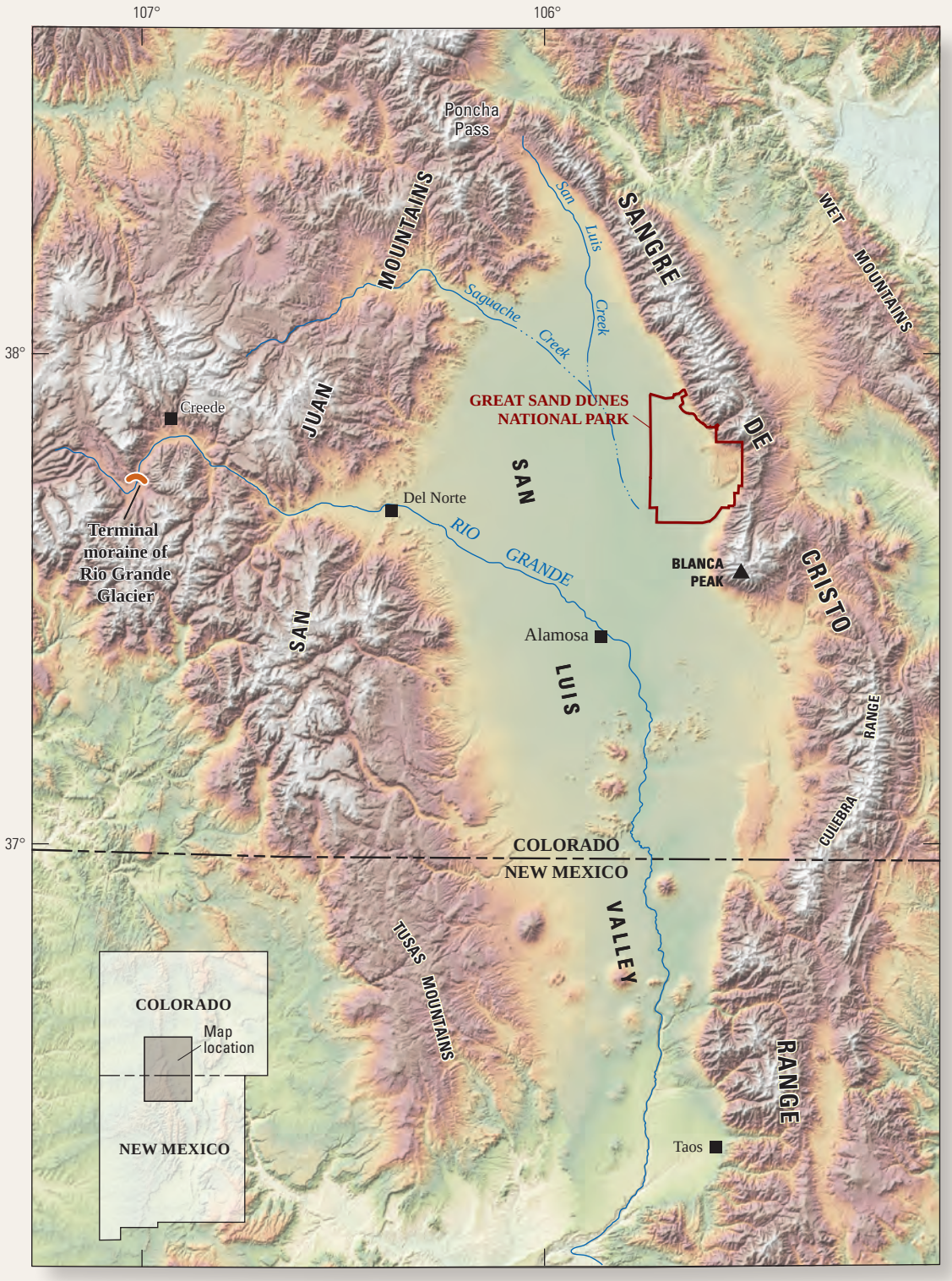


**Figure 1.** Map showing the location of the Great Sand Dunes National Park and the principal landforms in and adjacent to the San Luis Valley in south-central Colorado and north-central New Mexico.

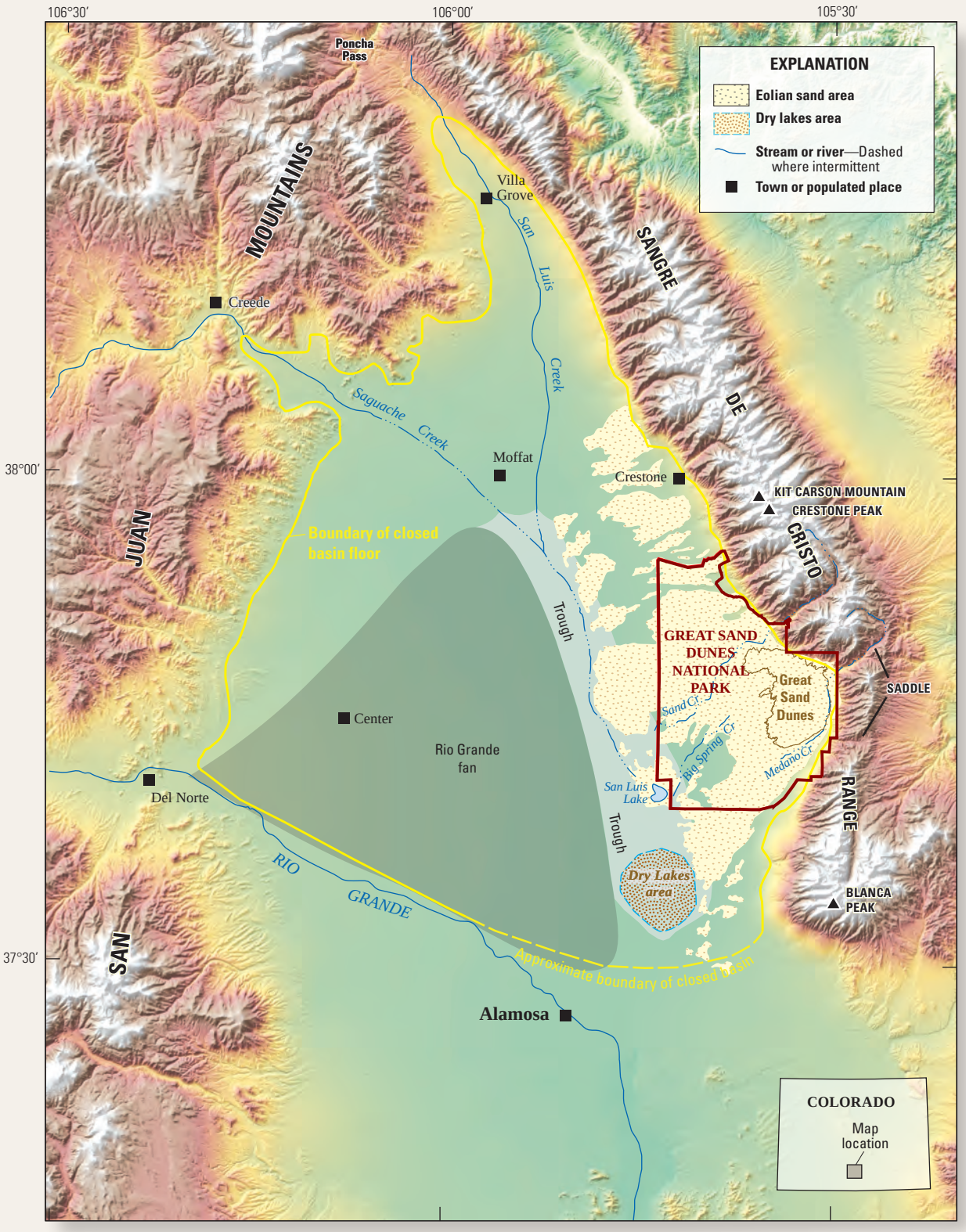
106°30′
106°00′
105°30′
38°00′
37°30′
EXPLANATION
Eolian sand area
Dry lakes area
Stream or river—Dashed where intermittent
Town or populated place
Poncha Pass
SAN JUAN MOUNTAINS
SANGRE DE CRISTO RANGE
Villa Grove
San Luis Creek
Creede
Saguache Creek
Moffat
Crestone
KIT CARSON MOUNTAIN
CRESTONE PEAK
Boundary of closed basin floor
Trough
GREAT SAND DUNES NATIONAL PARK
Great Sand Dunes
SADDLE
Sand Cr.
Big Spring Cr.
Medano Cr.
Center
Rio Grande fan
San Luis Lake
Del Norte
Trough
Dry Lakes area
BLANCA PEAK
RIO GRANDE
Approximate boundary of closed basin
Alamosa
COLORADO
Map location
Shaded relief base from 30-meter National Elevation Dataset (NED, http://nationalmap.gov/elevation.html)
Projection: Universal Transverse Mercator, zone 13
North American Datum 1983 (NAD 83)
0 5 10 15 MILES
0 5 10 15 KILOMETERS

The "singular depression," referred to here as the trough (fig. 2), is nearly 50 km long and varies in width from 5–6 km in the north to 11–12 km in the south. However, its margins are only 3–6 m higher than its axis, and the southern end of the trough is only 8–10 m lower than its northern end, thus it slopes southward at a mere 1 m/3,000 m. Consequently, a small change in the water-table level here can affect a large area, a fact that is of great importance to understanding the history of eolian sand deposition discussed later. The trough contains a variety of palustrine, lacustrine, and alluvial deposits including the wetlands that make up the Baca National Wildlife Refuge, which is the newest (2003) and one of the largest (about 376 km$^2$) refuges in the National Wildlife Refuge system, and the Blanca Wildlife Habitat Area (Blanca Wetlands). Because the water table is shallow and the soils are saline throughout this lowland, most of the area is non-arable. These conditions contributed to the selection of this area for the Closed Basin Project, which mostly coincides with the area referred to here as the trough and overlaps the western part of the park (fig. 2). This project, operated by Reclamation, maintains a large network of wells and a canal to extract groundwater from the closed basin and export it to the Rio Grande to comply with the terms of the Rio Grande Compact (Public Act No. 96, 76$^{th}$ Congress). This compact, which was adopted in 1939, assures availability of Rio Grande water to States downstream from Colorado. The compact also allows for water to be provided when needed to the Alamosa Wildlife Refuge, the Blanca Wildlife Habitat area, and the San Luis Lakes State Park and Wildlife Area.

**Figure 2 (facing page).** Map showing the locations of the principal geomorphic features discussed in the text. These include the boundary of the closed basin floor (yellow line); the extent of eolian sand (625 square kilometers [km$^2$]; Madole and others, 2008) flanking the Sangre de Cristo Range (stipple pattern). Within the area covered by eolian sand, there is a smaller area (72 km$^2$) referred to as the "Great Sand Dunes" outlined in brown; the area of the Rio Grande fan (about 1,150 km$^2$); the trough, a term used here for a relatively narrow (5–12 km wide), 50-km long, shallow lowland whose margins are only 3–6 meters (m) higher than its axis and the southern end of which includes the "sump" (defined by Powell,1958) as the lowest part of the closed basin; and the location of the Dry Lakes area, named for several deflation basins of various sizes on the floor of the closed basin between San Luis Lake on the north and the Blanca Wetlands to the south.

## Groundwater and Surface Water Hydrology

The mountains flanking the San Luis Valley intercept most of the precipitation coming from both the west (the dominant moisture source) and the east. Therefore, the San Luis Valley is in the rain shadow of two highlands, which is why it contains the largest area of truly arid land in Colorado (www.wrcc.dri.edu/precip.html). Arid land, by definition, receives less than 250 millimeters (mm) of annual precipitation. Near the center of the San Luis Valley, mean annual precipitation for the period 1948–2000 ranged from 177 mm at the town of Center to 181 mm at Alamosa. However, in spite of its aridity, the region also contains the largest area of wetland in Colorado (Walton-Day, 1996). This is because much of the precipitation intercepted by the mountains eventually reaches the San Luis Valley floor via streams draining from the mountains and groundwater transfer from bedrock along the basin margins.

Water-table maps (Emery and others, 1971; Rupert and Plummer, 2004) show that groundwater flows westward from the west edge of the Sangre de Cristo Range through or beneath eolian (windblown) sand to discharge points (springs and marshes) west of the Great Sand Dunes. The slope of the water table at the mountain front is less than 2°, and near the basin floor 12–15 km to the west, it is less than 0.5°. In contrast, the slope of the piedmont surface at and near the mountain front is typically about 6°, but it decreases westward to the extent that within a few kilometers it is 2° or less. The convergence and eventual intersection of the more steeply sloping piedmont surface with the gently sloping (nearly flat) water-table surface results in the formation of cienegas (marshy areas caused by springs or seepage) and instream wetlands (map units Qai and Qw). At present, these groundwater discharge points tend to occur beyond about 14 km west of the mountain front. However, changes in groundwater level at times in the past caused the loci of discharge points to shift toward or away from the basin center. When the water table was high, the intersection of the piedmont slope and the water table occurred closer to the mountain front and vice-versa when the water table was low. Hence, deposits of Qw (wetland or marsh sediment) are present mainly in the southwestern part of the map area in a zone that is 3–6 km wide.

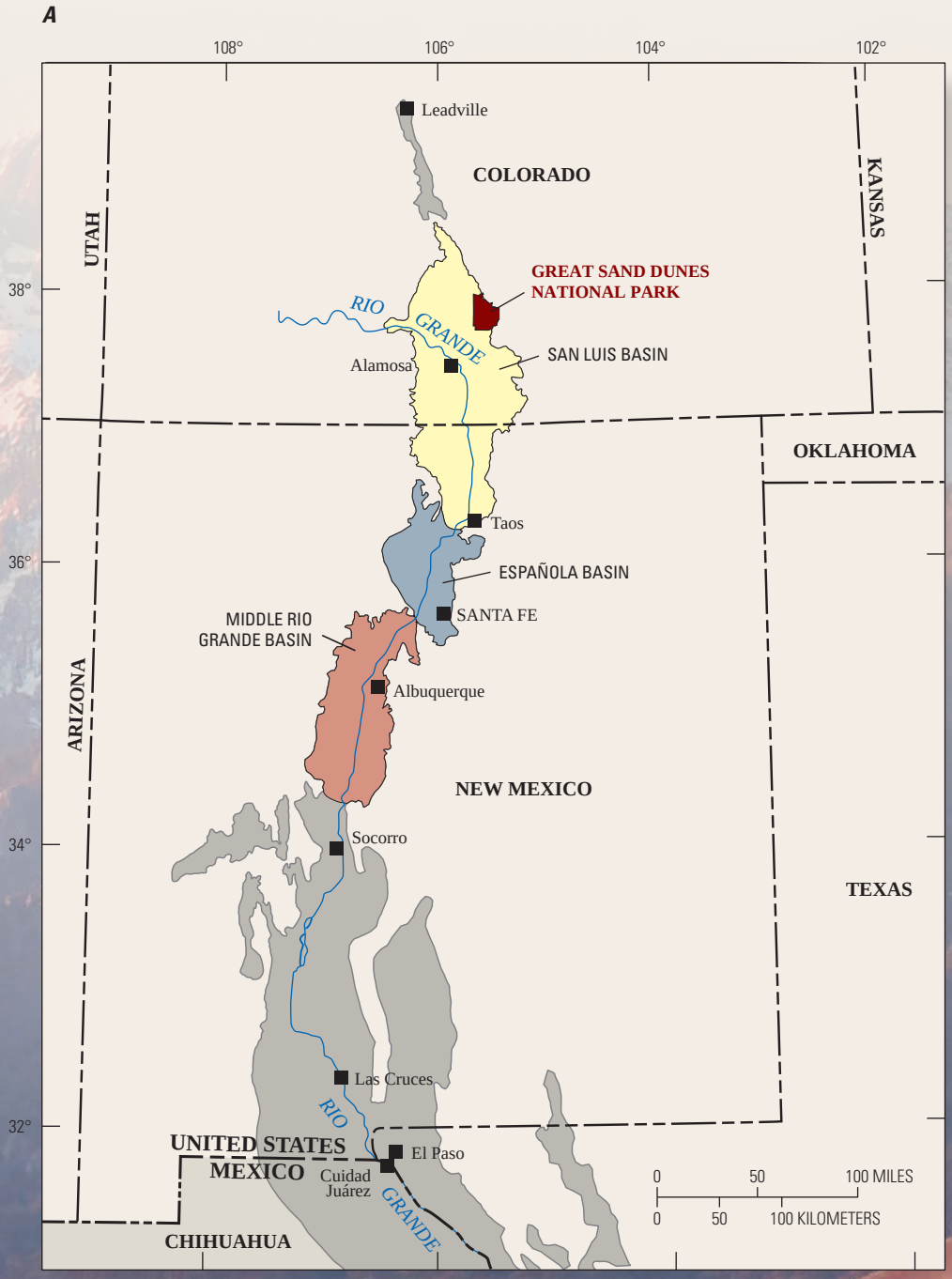


**Figure 3 (pages 8 and 9).** *A,* Map of the Rio Grande rift in Colorado, New Mexico, Texas, and northern Mexico showing the principal basins in the northern part of the rift (modified from Hudson and Grauch, 2013). *B,* Generalized cross section of the San Luis Basin (adapted from Brister, 1990; Brister and Gries, 1994). The basin is a half graben, hinged on the west and dropped down on the east. It contains several second-order half grabens and horsts (shown with gray dashed lines). Sediment (shown in orange) aggraded as rifting progressed, ultimately forming a relatively flat valley floor. Deposits of Quaternary age (time between the present and 2.58 million years ago [Ma]) blanket most of the valley floor in the northern part of the basin (see fig. 4).

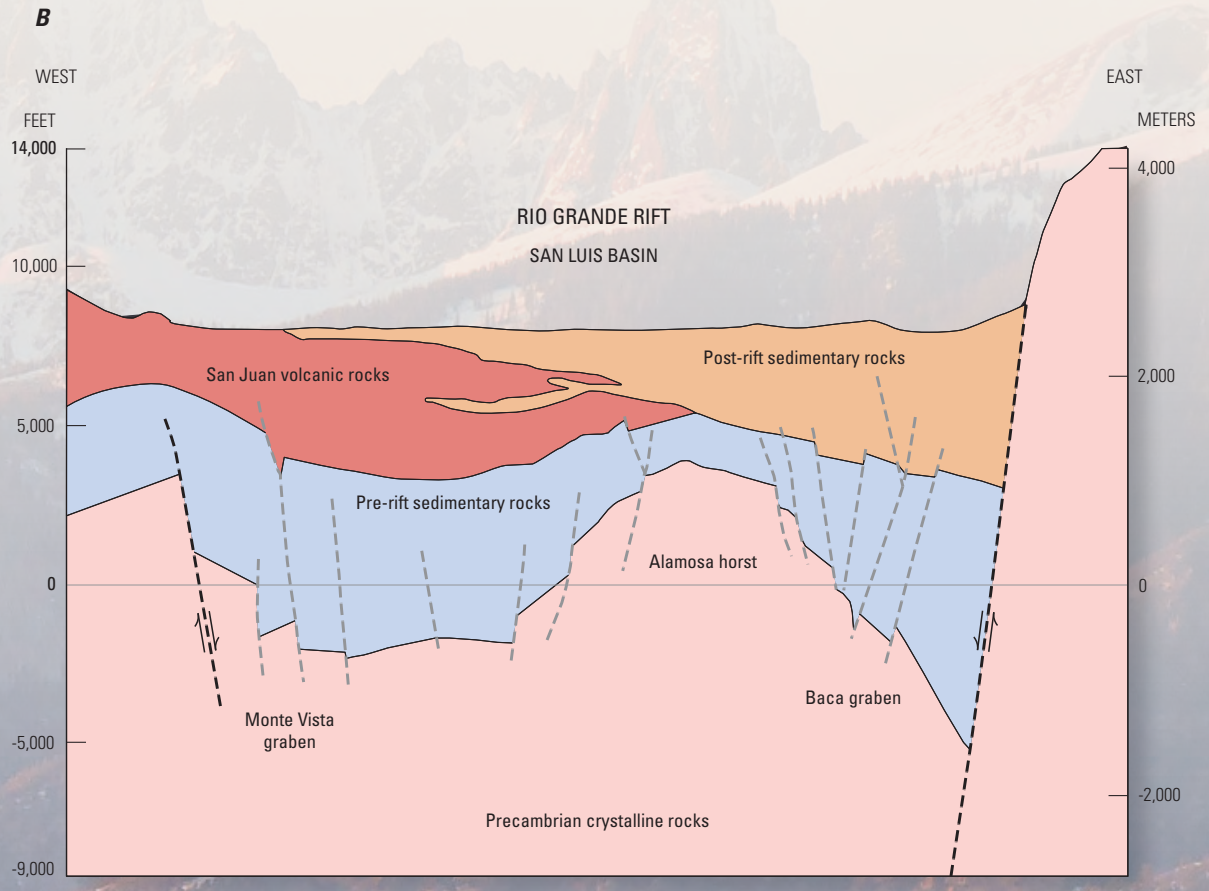
B
WEST
EAST
FEET
METERS
14,000
10,000
5,000
0
-5,000
-9,000
4,000
2,000
0
-2,000
RIO GRANDE RIFT
SAN LUIS BASIN
San Juan volcanic rocks
Post-rift sedimentary rocks
Pre-rift sedimentary rocks
Alamosa horst
Monte Vista graben
Baca graben
Precambrian crystalline rocks

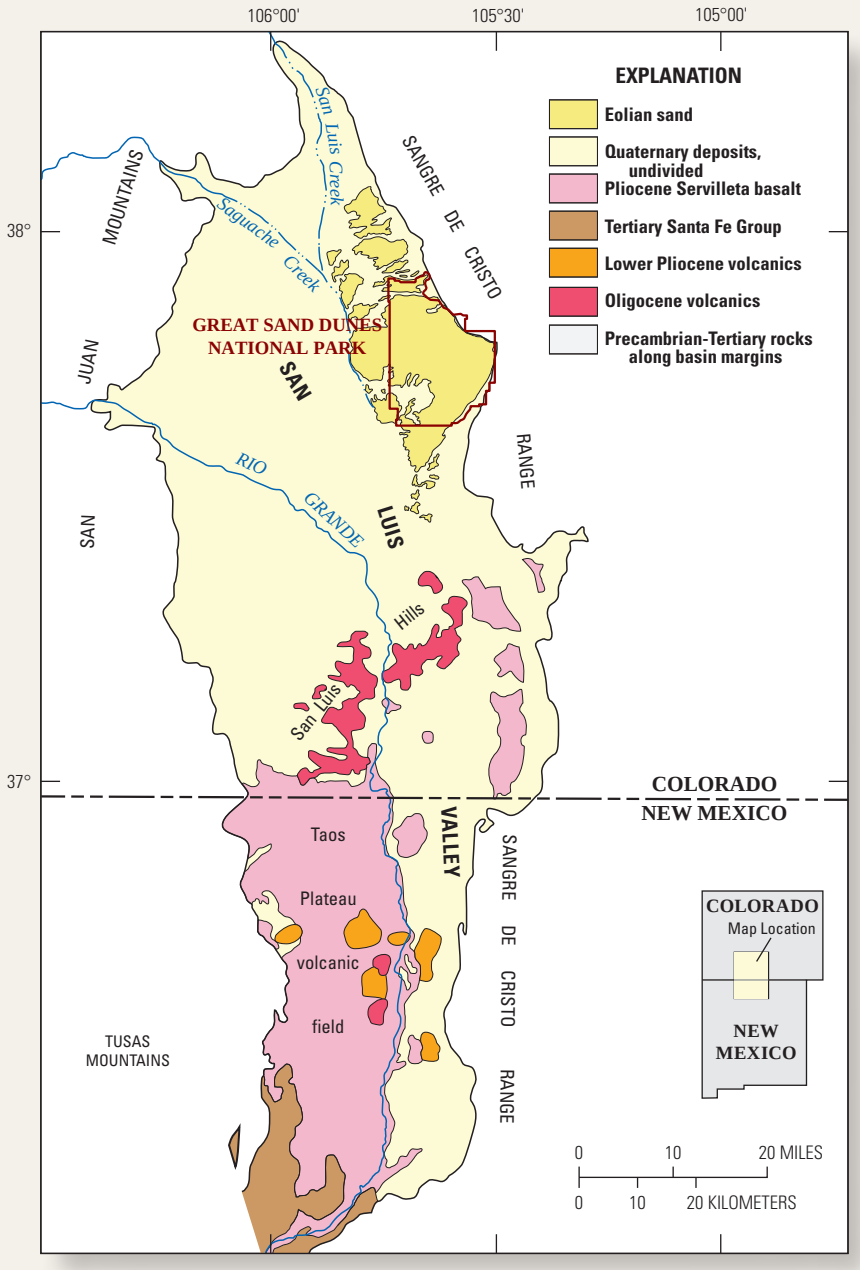


**Figure 4.** Generalized geologic map of the San Luis Valley floor (modified from Machette and others, 2007). Brown line indicates the location of the Great Sand Dunes National Park.

**Figure 5 (facing page).** Electric logs of wells V and Y (see figs. 7 and 9 for locations) and a lithologic log constructed using well cuttings primarily from well Y (modified from Madole and others, 2013). Wells X and Y are just 8 meters (m) apart; well logs were provided by HRS Water Consultants, Inc. (http://www.hrswater.com/). The lithologic log is an extremely generalized depiction of strata that are mostly thin and lithologically diverse, similar to those described by Powell (1958) in a well just north of the Great Sand Dunes where beds of sand, silty and clayey sediment, and gravel alternate in vertical succession 164 times between the surface and a depth of 305 m. The water table is near the surface at both wells V and Y; thus, sediment is water saturated. Water saturated sediment, whose resistivity is between 300 and 1,000 ohm-m (ohm-meter) and conductivity is less than 30 mS/m (millisiemens/meter), likely consists mostly of sand and fine pebble gravel (that is, relatively coarse, permeable sediment). In contrast, sediment whose resistivity is less than 300 ohm-m and conductivity is greater than 30 mS/m likely has a combined content of silt and clay ≥50 percent. Beds of sand and fine gravel interbedded with silty and clayey fine sand would explain the numerous and pronounced changes in resistivity recorded over short vertical distances in the upper 40 m (130 ft) of both wells V and Y. Conversely, freshwater-saturated sediment containing large amounts of silt and clay have lower resistivity and higher conductivity than sandy sediment, a condition evident in the lower parts of wells V and Y. The strata containing large amounts of silt and clay accumulated in a lake that occupied much of the northern San Luis Valley from Pliocene to middle Pleistocene time. Siebenthal (1910) was the first to describe this lake and the sediment that accumulated in it, which he named the Alamosa Formation. Note, the tops of wells V and Y are at different altitudes; hence, the depth to the inferred top of the Alamosa Formation differs between these wells.

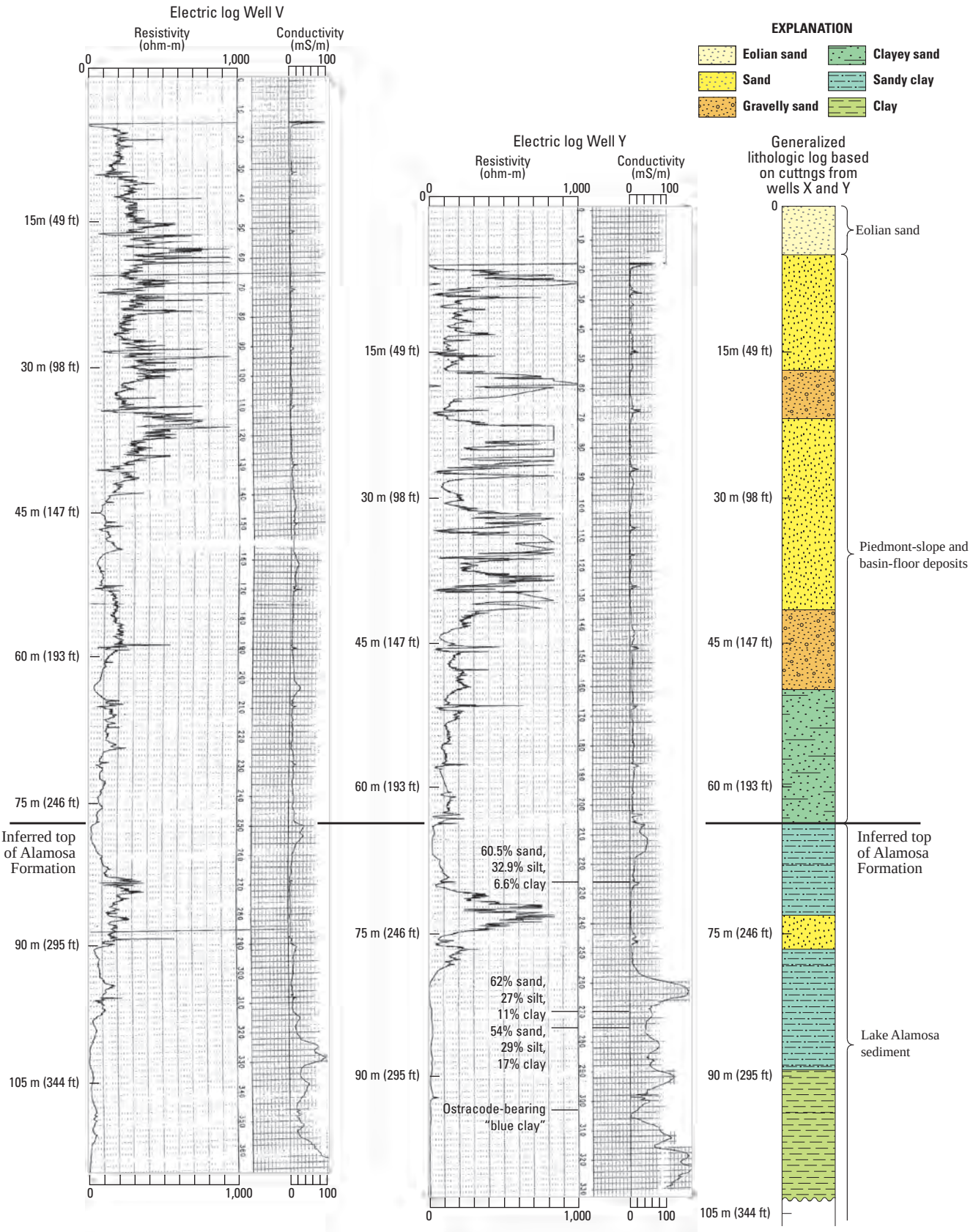
Electric log Well V
Resistivity (ohm-m)
Conductivity (mS/m)
0
1,000
0
100
15m (49 ft)
30 m (98 ft)
45 m (147 ft)
60 m (193 ft)
75 m (246 ft)
90 m (295 ft)
105 m (344 ft)
Inferred top of Alamosa Formation
Electric log Well Y
Resistivity (ohm-m)
Conductivity (mS/m)
60.5% sand, 32.9% silt, 6.6% clay
62% sand, 27% silt, 11% clay
54% sand, 29% silt, 17% clay
Ostracode-bearing "blue clay"
EXPLANATION
Eolian sand
Sand
Gravelly sand
Clayey sand
Sandy clay
Clay
Generalized lithologic log based on cuttngs from wells X and Y
Eolian sand
Piedmont-slope and basin-floor deposits
Inferred top of Alamosa Formation
Lake Alamosa sediment

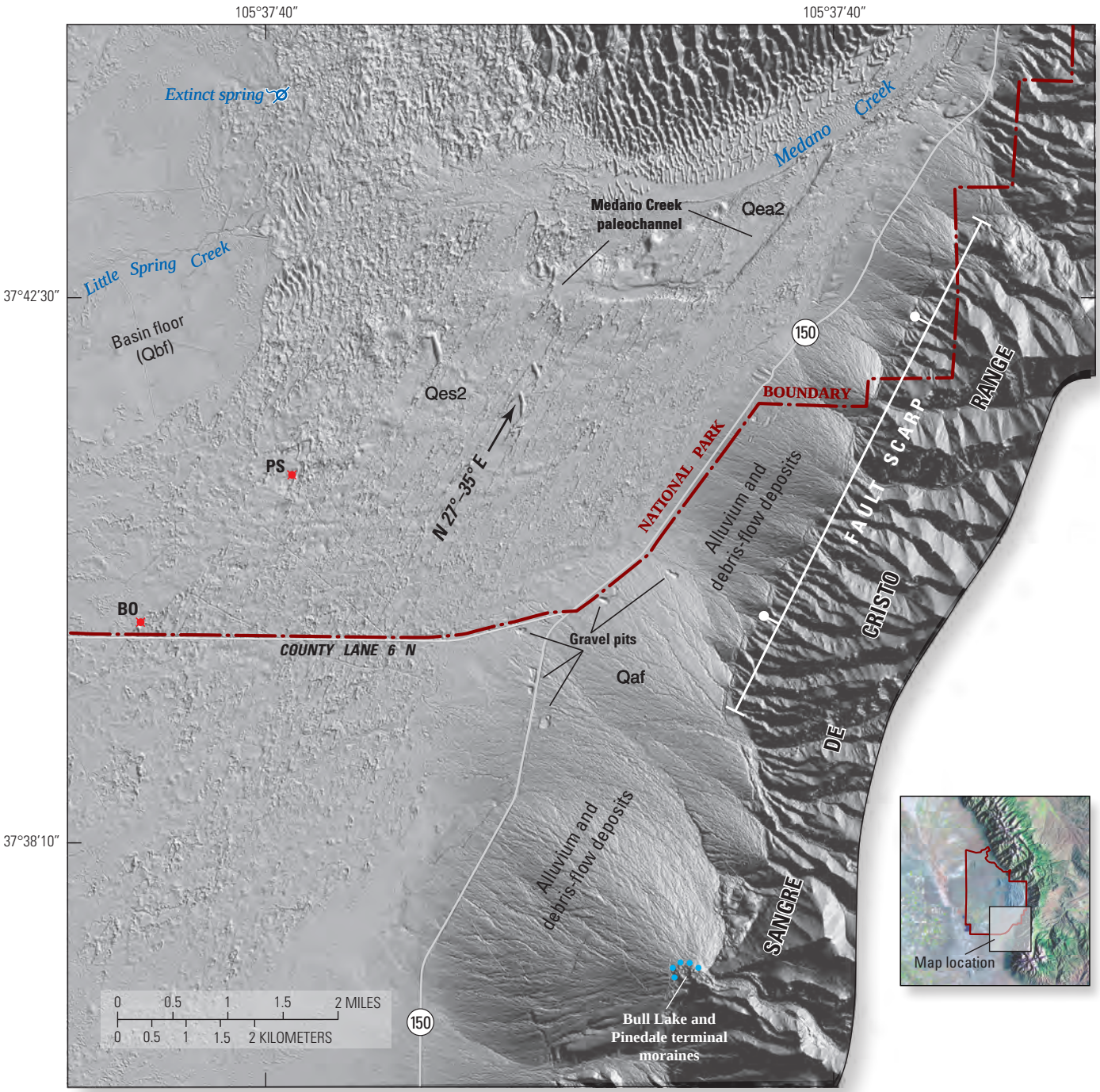


Lidar base from USGS Earth Resources Observation and Science (EROS) Center acquired 2013 at https://eros.usgs.gov/remote-sensing
Universal Transverse Mercator, zone 13; North American Datum 1983 (NAD 83)

**Figure 6.** Lidar image of the southeastern part of the map area shows numerous hairpin-shaped parabolic dunes of unit Qes2 trending between N.27°E. and N.35°E. The dune sand was derived from the southern (lowest) end of the trough southwest of the map area (fig. 2). South of the Great Sand Dunes, eolian sand does not bury parts of unit Qaf as it does east and north of the Great Sand Dunes because here sand transport was nearly parallel rather than perpendicular to the Sangre de Cristo Range. A forest of mainly piñon (*Pinus edulis*) and Rocky Mountain juniper (*Sabina scopulorum*), which does not show on lidar imagery, covers the massive fan deposits. Letters BO and PS (red symbol) denote radiocarbon-age locations of samples described in table 1. The fault scarp (white line) shows the distance over which a range-front fault breaks the surface. The fault scarp is slightly northwest of the white line; ball and bar symbol indicates that displacement is down on the northwest side of the scarp.

In most places on the floor of the closed basin (fig. 2), the water table is within 4 m of the land surface, and the unconfined aquifer (defined as water-bearing material that has a water table and is connected to the atmosphere via pores) is between 15 and 60 m thick (Emery and others, 1971; Huntley, 1976). The unconfined aquifer is separated from deeper confined aquifers by strata that Emery and others (1971) refer to as the "clay series" (although silt is likely more abundant than clay) and local water-well drillers call "blue clay." Collectively, these clayey strata are 3–24 m thick and present throughout much of the central and northern San Luis Valley.

Wurster and others (2003) and Rupert and Plummer (2004) used stable isotopes ($^{2}H$ and $^{18}O$) to show that the unconfined aquifer in the vicinity of the Great Sand Dunes is recharged chiefly by snowmelt runoff from streams draining the Sangre de Cristo Range. Furthermore, Rupert and Plummer (2004) determined that some of the precipitation on basin-floor sediment evaporates before it can affect recharge of the unconfined aquifer, a conclusion that differs somewhat from previous interpretations (see for example Emery and others, 1971). Conversely, precipitation on the Sangre de Cristo Range undergoes little evaporation after reaching the land surface. The composition of stable isotopes ($^{2}H$ and $^{18}O$) in groundwater at the eastern edge of the Great Sand Dunes is similar to that of snowmelt runoff from the Sangre de Cristo Range. In addition, Wurster and others (2003) demonstrated that a series of wet and dry cycles that occurred between 1936 and 1995 affected groundwater level in the Great Sand Dunes area. During dry cycles, groundwater level declined by as much as 1.3 m and interdunal wetlands shrank in size or dried up. During intervening wet cycles, groundwater level rose and interdunal wetlands reappeared or expanded.

Surface water is scarce in the map area. It is present in wetlands and marshes, which are sustained by groundwater discharge, and a few streams that are mostly ephemeral. The streams are of two distinctly different kinds: (1) those that originate in drainage basins high on the west flank of the Sangre de Cristo Range and (2) those that emerge from springs and marshes several kilometers west of the mountain front. Discharge in streams draining the west flank of the Sangre de Cristo Range is controlled primarily by snowmelt, and flow is perennial until it reaches the mountain front, beyond which streams begin losing water via infiltration at a high rate. Even streams originating in the larger drainage basins, such as Sand and Medano Creeks, generally do not extend much more than 4 km beyond where they exit the mountains. That these streams extend even that far is because they flow on beds of coarse gravel (inset in eolian sand) that constrain or reduce the rate at which water is lost to infiltration. The perennial parts of these streams and the gallery forests (mostly cottonwood trees, *Populus deltoides* ssp. *deltoides*) that they sustain terminate where the channel bed changes from gravel to sand. Sediment in terrace deposits along Sand Creek indicates that in the past the transition from gravel to sand has occurred in the same general area. Downstream from this point, the channel is dry most of the year except for short periods following thunderstorms. Peak discharge in streams that originate in the mountains occurs in late spring and early summer, after which it practically ceases for the rest of the year.

Groundwater discharge streams like Big Spring Creek contrast in most respects with streams that drain from the mountains. Big Spring Creek flows on a sand bed, and its discharge increases rather than decreases in a downstream direction, as long as its channel is lower than the water-table level in adjacent areas, which it is until the creek reaches the basin floor. In addition, flow in Big Spring Creek tends to be perennial rather than seasonal, as is the case for streams draining from the mountains. Groundwater discharge at Indian Spring was sufficient at times to sustain perennial streams that carved valley floors that are tens of meters wide (fig. 8). The fact that the valley of Big Spring Creek contains a sequence of cut-and-fill terraces indicates that water-table, which is the local base level for groundwater discharge streams, has fluctuated over time.

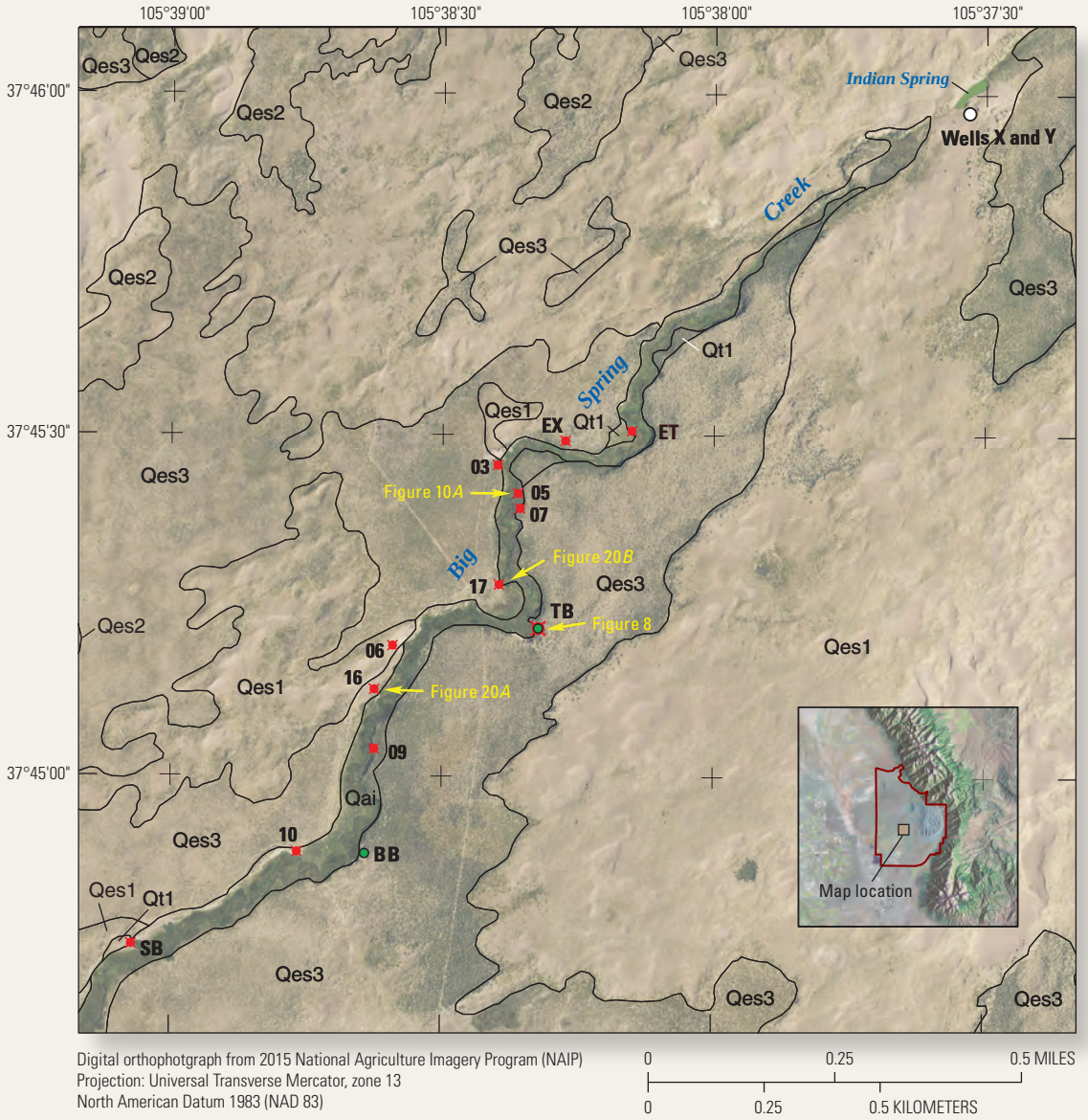


**Figure 7.** Orthophotograph image of upper Big Spring Creek showing the locations of Indian Spring, wells X and Y, and localities (designated by letters and numbers) where important stratigraphic and geochronologic data were obtained (see tables 1 and 2). Red symbol indicates radiocarbon-age locality (table 1), and green symbol indicates infrared stimulated luminescence (IRSL) and optically stimulated luminescence-age (OSL) locality (table 2). Yellow arrows indicate view directions of photographs. Locality TB has both radiocarbon and stimulated luminescence data.


**Figure 8.** Photograph looking west down the valley of Big Spring Creek from locality TB (see fig. 7). This instream wetland is sustained by groundwater discharge from Indian Spring. The valley floor is covered by unit Qai and flanked by units Qt1 and Qt2. The dense greasewood (*Sarcobatus vermiculatus*) and saltbush (*Atriplex canescens*) shrubland in areas adjacent to the wetland is typical of the vegetation cover on unit Qes3. *Photograph by R.F. Madole, July 12, 2001.*

## Hydrogeology, Vegetation, and Sand-Surface Stability

Understanding the effect that water-table fluctuations have on vegetation is necessary to decipher the chronology of Holocene eolian sand deposits in the Great Sand Dunes area. Changes in water-table depth cause the kind and quantity of vegetation to change, which in turn affects the stability of surficial deposits, especially those susceptible to wind erosion. Shrubs like greasewood (*Sarcobatus vermiculatus*) and saltbush (*Atriplex canescens*), which commonly grow in thick stands and have root systems that can penetrate several meters below the ground surface, inhibit wind erosion (fig. 8). Thus, in almost all areas where the oldest Holocene eolian sand unit (Qes3) is preserved, these two species dominate the vegetation cover. Note that these species and unit Qes3 are most prevalent in the topographically lower parts of the map area; namely, the areas closest to the trough and areas flanking instream wetlands like Big Spring Creek (fig. 2). During intervals of declining water table, these shrubs survived in places where root growth kept pace with a declining water table. Where their root systems were unable to keep pace with or reach the declining water table, the shrubs died, after which wind eroded and reshaped sandy substrates into new bed forms (dunes and sand sheets).

The relation between declining water table and plant die off described here is based on several studies of riparian plant communities in arid and semiarid parts of western North America (Scott and others, 1999, 2000, and references therein). These studies show that die off in riparian forests can occur in as little time as a year or two in response to declining water table. Even large woody plants like the plains cottonwood (*Populus deltoides* ssp. *monilifera*) growing on valley floors in eastern Colorado died in a relatively short time when water table declined below the lower limit of root growth (Jonathan Friedman, USGS, personal commun., 2015). Changes in water-table level can have several causes, both natural (channel-incising floods, drought, and climate change), and human (gravel mining, groundwater pumping, and stream diversions). A sustained shift to greater aridity following a period of a high water table can be particularly devastating to plant communities, even to those that root deeply, such as greasewood, because during the time when water table was high, the plants developed shallow root systems. Then when the water table fell, root systems were unable to grow downward fast enough for the plants to survive.

## Great Sand Dunes Area

About 80 percent of the 437 km$^2$ encompassed by the Great Sand Dunes National Park is blanketed by eolian sand. This sand is part of a larger body of eolian sand that extends along the western edge of the Sangre de Cristo Range for about 60 km (fig. 2). The entire eolian sand area covers about 625 km$^2$. The Great Sand Dunes cover only 72 km$^2$ of this area, and sand sheets and tracts of low (3–8 m high) dunes cover the remaining 553 km$^2$ (Madole and others, 2008). Although the Great Sand Dunes occupy only about 12 percent of the eolian sand area, they contain more than half of the sand in it (estimated to be 10–13 billion cubic meters [m$^3$]±430 million m$^3$ of sand). This is because the Great Sand Dunes are as much as 200–230 m thick in some places, whereas the sand sheets and low dunes are less than 8 m thick in most places.

The Great Sand Dunes accumulated in an embayment formed where the trend of the Sangre de Cristo Range changes from southeasterly to southwesterly (figs. 1 and 2). A combination of factors including the proximity of the sand supply (the trough, fig. 2), range-front geometry, topography, and wind regime caused eolian sand to pile higher in the embayment than anywhere else along the east edge of the closed basin. In the embayment area, the crest of the Sangre de Cristo Range lowers by as much as 780 to 930 m. This produces a pronounced saddle on the range crest that is about 14 km long (fig. 2). The saddle is bounded on the north by a cluster of high peaks, two of which, Crestone Peak and Kit Carson Mountain, rise higher than 4,300 m. Blanca Peak (4,354 m) and four other peaks ranging in elevation from 4,163 m to 4,280 m bound the saddle on the south. Prevailing winds in the San Luis Valley are southwesterly and westerly, but during the summer, wind frequently blows through the range-crest saddle from the east. This complex wind regime has produced a variety of dune types, the most common of which are parabolic, transverse, reversing, and star (Andrews, 1981; Madole and others, 2008).

Large areas of low-relief (3–8 m) parabolic dunes are present both north and southwest of the Great Sand Dunes. On the north, the average trend of dune arms and axes is about N.65°E. (fig. 9), which is nearly normal to the axis of the Sangre de Cristo Range north of the Great Sand Dunes. Thus, in this area, wind has drifted sand high onto alluvial fans and adjacent mountain slopes, including the steep, rugged terrain between Little Medano Creek and Sand Creek. In contrast, the trend of most parabolic dunes southwest of the Great Sand Dunes is between N.27°E. and N.35°E., which is nearly parallel to the mountain front (fig. 6). Here, wind transported sand northeastward toward the Great Sand Dunes rather than onto the footslopes of the Sangre de Cristo Range.

Most deposits of eolian sand, regardless of age, have similar physical properties and mineralogy because they were derived from the same proximate source, namely, the floor of the trough (fig. 2). Most eolian sand is grayish-brown to brown and well sorted. Analyses of particle-size distributions in 15 samples obtained from deposits of three different ages (map units Qes1, Qes2, and Qes3) indicate that sand, mostly fine and medium sizes (that is, mostly grains ranging in size from 125 to 500 micrometers [μm]) make up 95–100 percent of all the samples. Silt and clay combined constitute 0–5 percent. The mineralogy of the eolian sand reflects the original source of the sand grains, namely, the rocks in adjacent mountain ranges. Surprisingly though, most of the sand in the Great Sand Dunes came from the San Juan Mountains, 80 km or more to the west, rather than from the nearby Sangre de Cristo Range. Early on, Endlich (1875, 1877) noted that the Great Sand Dunes contain grains that came from the San Juan Mountains, an observation later supported by Burford (1960) and by Hutchison (1968, p. 92), who quantified the provenance (place of origin) of the minerals in the dunes. Hutchison concluded that “the sands of the Great Sand Dunes consist mainly of minerals derived from rocks in the central and southwestern parts of the San Juan Mountains” but also contain minor amounts of minerals derived from the Sangre de Cristo Range. More recently, Aleinikoff (*in* Madole and others, 2008) used uranium-lead (U-Pb) ages of detrital zircons to determine that most of the sand (as much as 70 percent) in the Great Sand Dunes was derived from rocks in the San Juan Mountains and the rest of the sand was derived from rocks in the Sangre de Cristo Range. These data are consistent with Wiegand’s (1977) findings that sand in and near the Great Sand Dunes is made up of about 52 percent volcanic rock fragments, 28 percent quartz, and 20 percent other minerals.

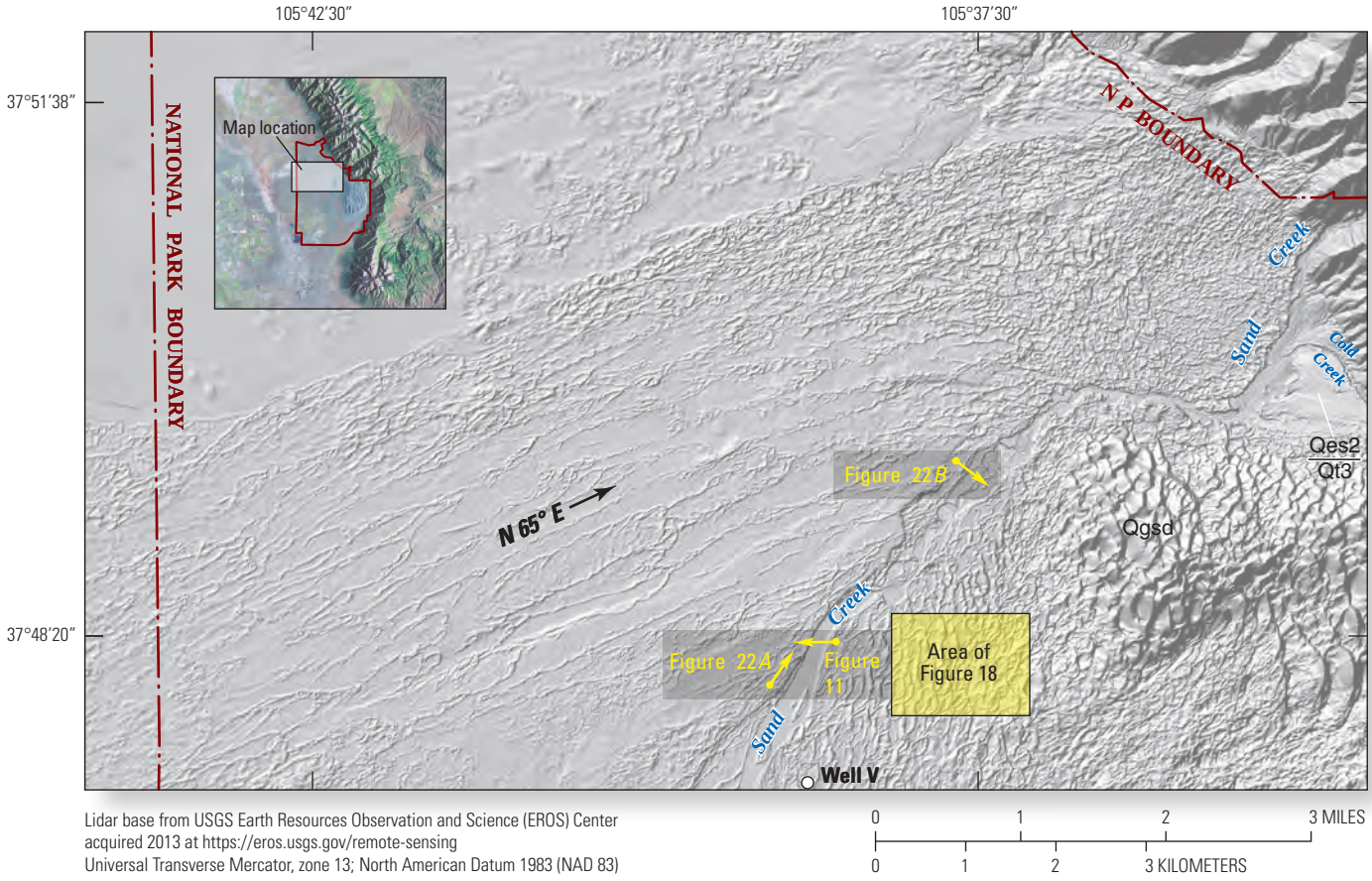


**Figure 9.** Lidar image shows the extensive area of hairpin-shaped parabolic dunes north of the Great Sand Dunes. On average, the axes and arms of these dunes trend N.65°E. This trend is basically normal to that of the Sangre de Cristo Range. Consequently, wind has drifted sand high onto alluvial fans and adjacent mountain slopes, covering sizeable areas underlain by units Qpf and Qaf. The label Qes2/Qt3 (right center) identifies an area where a thin cover of eolian sand conceals a thick sequence of alluvium. The sand is not shown on the map in order to document the presence of an important alluvial deposit that is exposed in only a few places because of the pervasive eolian sand cover. Lidar imagery, however, reveals the morphology of the underlying alluvium. Yellow arrows indicate view directions for figures 11, 22*A*, and 22*B*. The square indicates the location of figure 18.

## Chronology of Eolian Sand Deposits

Deposits of eolian sand cover most of the Great Sand Dunes National Park. These deposits are divided into four units (Qes1, Qes2, Qes3, and Qgsd) on the basis of four sets of attributes: (1) stratigraphic relations (chiefly superposed and crosscutting strata); (2) geomorphic relations (that is, position in the landscape and differences in topographic expression, such as, sharpness of dune crests, flanks, and slip faces); (3) the quantity and kind of vegetation cover; and (4) the presence or absence of secondary (post-depositional) calcium carbonate in the upper 1–1.5 m of the deposit. Degree of weathering, which commonly is used to distinguish age differences among surficial deposits, is not useful for that purpose here. Soil development is entirely absent in some eolian sand deposits and barely discernible in others, possibly in part because wind tends to rework sand surfaces from time to time, especially after wildfires.

Even though numerical ages of Holocene deposits have been determined at several localities in the Great Sand Dunes area—in this study as well as others (Madole, 2001, 2005; Marín and others, 2005; Forman and others, 2006; Madole and Mahan, 2007)—the chronology of Holocene eolian activity remains poorly defined. Topographic and stratigraphic relations indicate that all eolian sand units are products of multiple episodes of activity, but the number and timing of these episodes are unclear. Strata of separate episodes of activity usually are difficult to distinguish, and exposures that reveal stratigraphic relations are scarce. Even where exposures are present, they can contain disconformities and crosscutting relations that have no temporal significance because, as dunes migrate, deposition can occur in some places while erosion simultaneously occurs in other places. This aspect of eolian sand stratigraphy can confound the reliability of luminescence dating. Likewise, the utility of radiocarbon dating is limited because of the rarity of buried soils or other dateable materials in eolian sand deposits.

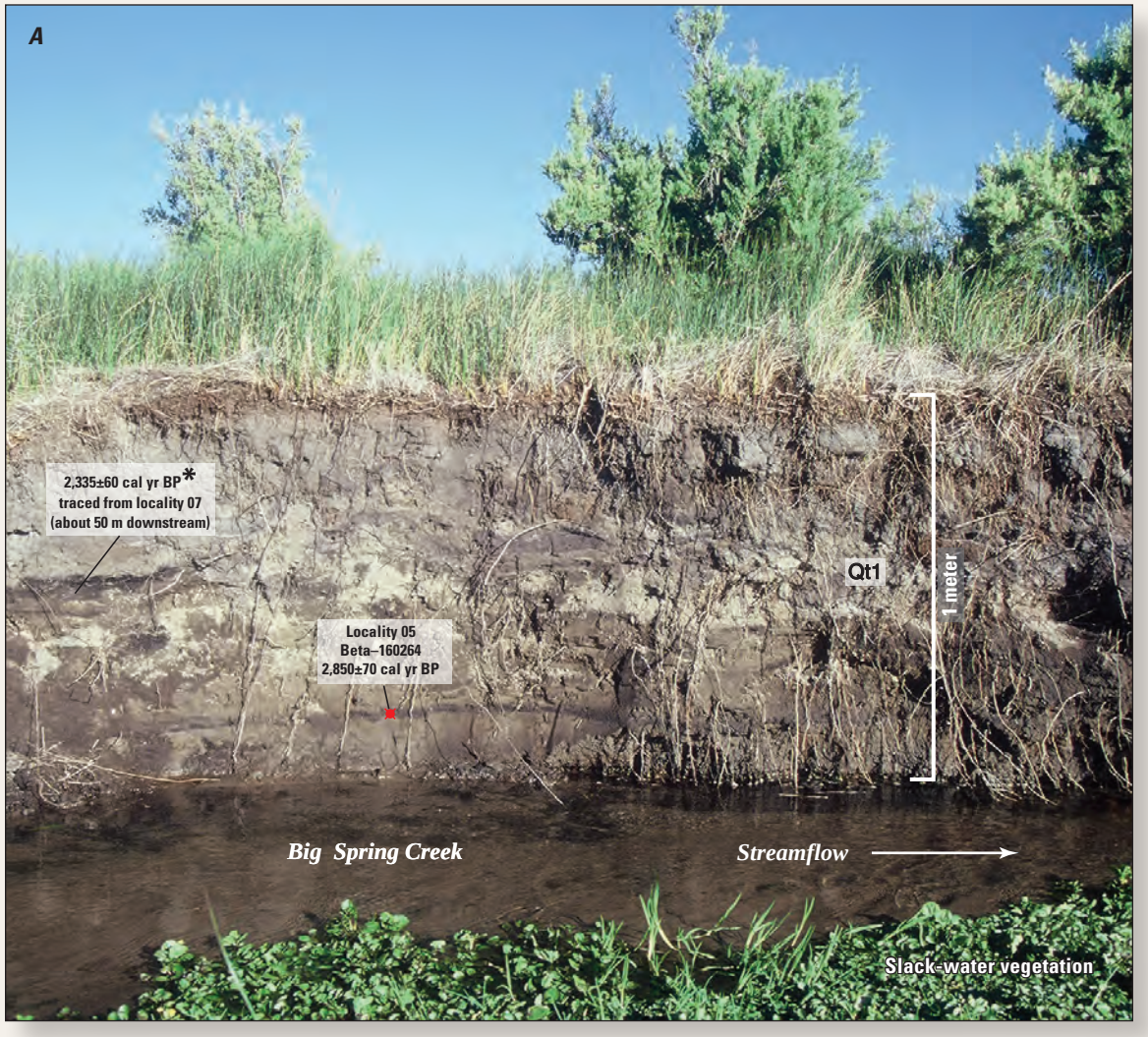


**Figure 10 (pages 18 and 19).** *A*, Photograph of unit Qt1 alluvium in the east bank of Big Spring Creek at locality 05 (see fig. 7, table 1). Similar Qt1 strata are exposed in cutbanks at several places along Big Spring Creek. Note that the terrace height and stratigraphy of Qt1 along Big Spring Creek, a groundwater discharge stream, is similar to that of Qt1 along Deadman Creek (fig. 10*B*), a stream that originates in the mountains. Also, note that deposits of eolian sand and sheetwash alluvium do not overlie Qt1 alluvium, as they typically do unit Qt2 (figs. 20*A*, 20*B*, and 20*C*). The asterisk and leader indicate that the radiocarbon age, although obtained from the same stratum, was collected from a similar cutbank at locality 07 (fig. 7, table 1). The shrubs here are greasewood (*Sarcobatus vermiculatus*). *Photograph by R.F. Madole, June 14, 2001. B*, Photograph of lower Deadman Creek looking east from a point about 1.3 kilometers (km) east of the western park boundary. Here, as in most places along this stream, terrace deposits are present at two levels. The lower terrace deposit (Qt1) is visible in the foreground and the upper deposit (Qt2) underlies the slightly higher surface that crosses the center of the image from left to right. *Photograph by R.F. Madole, September 4, 2009.*


Because of the limitations of numerical methods for dating eolian sand, the age limits suggested here for units Qes2 and Qes3 rely heavily on geomorphic and stratigraphic relations in addition to numerical ages of alluvial, palustrine, and lacustrine deposits that can be related to specific eolian sand units. A basic premise in interpreting these data is that episodes of widespread eolian deposition are initiated by a decline in water-table level. As discussed in the section on hydrogeology and sand-surface stability, a sustained decline in water-table level negatively affects the kind and quantity of vegetation present in the affected area and increases the susceptibility of sandy sediment to wind erosion. Similarly, a rise in water-table level that is sustained alters the kind and quantity of vegetation cover in ways that inhibit wind erosion.

A sustained decline in water-table level is recorded geomorphically and stratigraphically in two ways: (1) incision of stream channels and the formation of terraces and (2) desiccation of marshes and lakes. Conversely, a sustained rise in water-table level produces the opposite effects, namely, aggradation on valley floors and the formation of marshes and lakes in topographically low areas. Because water-table level controls the depth of channel incision, terrace heights are the same regardless of whether they flank groundwater discharge streams (such as Big Spring Creek) or streams that originate in the Sangre Cristo Range (Deadman Creek, for example) (figs. 10*A* and 10*B*).

## Great Sand Dunes Unit (Qgsd)

The Great Sand Dunes are treated as a separate map unit even though they are covered by a thin layer of active sand (unit Qes1) because most of this massive body of sand (volume estimated to be between 10 and 13 billion $m^3$±430 million $m^3$) is a complex of deposits that accumulated episodically for more than 130,000 years (yr) (Madole and others, 2008, 2013). In addition, Pleistocene eolian sand likely underlies much of the Holocene eolian sand in areas flanking the Great Sand Dunes. This presumed presence of Pleistocene eolian sand is based on a few isolated exposures in stream banks (for example, see fig. 11), blowouts, and excavations and by the presence of Folsom-age artifacts in eolian sand just below the base of unit Qes2 at Stewart's Cattle Guard site. The Cattle Guard site was a bison kill and processing camp excavated and described by Jodry (1987) and Jodry and Stanford (1992). Also, collectors have reported finding Clovis and Folsom artifacts at several localities in the map area (Jodry, 1999). The Clovis culture existed in many parts of North America between about 13,300 and 12,800 calibrated years before the present (cal yr BP) (Before Present) (Sanchez and others, 2014), and the Folsom culture was present between about 12,800 and 12,280 cal yr BP (D.J. Stanford, Smithsonian Museum of Natural History, personal commun., 2005). In addition, mammoth bones (known as the Medano mammoth site) were found in a blowout near Indian Spring a few km west of the Great Sand Dunes. Finally, two optically stimulated luminescence (OSL) ages of eolian sand in steeply dipping (24°–26°) beds in a 10–12-m-high cutbank on Medano Creek opposite the south edge of the Great Sand Dunes (Madole and others, 2013) indicate that eolian sand was present in this area prior to 60 ka (kilo annum, or thousand years ago). Cross-bedded dune sand, overlain by about 5 m of unit Qt3, occupies a similar position along Sand Creek near the north edge of the Great Sand Dunes (fig. 11).

## Eolian Sand Unit 3 (Qes3)

Deposits of unit Qes3 are present only in the topographically lower (western) part of the park. Collectively, they cover about 10 percent of the map area. Most deposits are on or adjacent to the basin floor or blanket areas flanking instream wetlands. In these areas, two plant species—greasewood and saltbush—dominate the vegetation cover. These shrubs have root systems that can penetrate several meters below the ground surface, and they typically form relatively thick stands that inhibit wind erosion (fig. 8). During intervals of low or declining water table, these shrubs survived in places where root growth could reach or keep pace with a declining water table. Were it not for this, it is likely that unit Qes3 would not have been preserved.

Stratigraphic data and radiocarbon ages obtained from auger holes in palustrine and lacustrine deposits (units Qbf and Qw) and alluvium in cutbanks along Big Spring Creek indicate that the water table in this area was higher than it is today during the early Holocene and early part of the middle Holocene (the part prior to the deposition of unit Qes3). At present, the water table is about 1 m lower than the land surface over much of the basin floor. According to radiocarbon ages of dark gray to black organic-rich clayey sediment obtained at three localities (fig. 12, localities LN, LP, and PL, table 1), water table in this area was near or at the land surface between 9,455±35 and 7,200±40 cal yr BP. Similarly, several radiocarbon ages of organic-rich alluvium from the banks of Big Spring Creek record a progressive rise in water table that began sometime prior to 9,490±30 cal yr BP and continued to be higher than at present until at least 7,350±70 cal yr BP (figs. 13, 20*A*, and 20*B*). In addition, a radiocarbon age of organic matter obtained from lacustrine sediment at locality DC, which is 8.5 km south of San Luis Lake, indicates that a lake was present in the central part of the trough (fig. 2) about 8,480±60 cal yr BP (table 1). Paleontological data (primarily fossil fish) at locality BP, which is 4 km north of locality DC and about 4 km south of San Luis Lake, coupled with a high-accuracy Global Positioning System (GPS) survey of lacustrine strata between these localities (R.F. Madole and J.S. Honke, USGS, written commun., 2008) indicate that this lake might have been as long as 10 km and as deep as 6–7 m. This lake is unrelated to Lake Alamosa, which occupied most of the northern San Luis Valley from Pliocene to middle Pleistocene time (Siebenthal, 1910), but drained (ended) about 440,000 yr ago (Machette, 2004; Machette and Marchetti, 2006). A high or shallow water table during early Holocene time and the early part of middle Holocene time likely supported a vegetation cover that prevented deflation of surface sediment, which might explain why eolian sand deposits of early Holocene age were not recognized in this study.

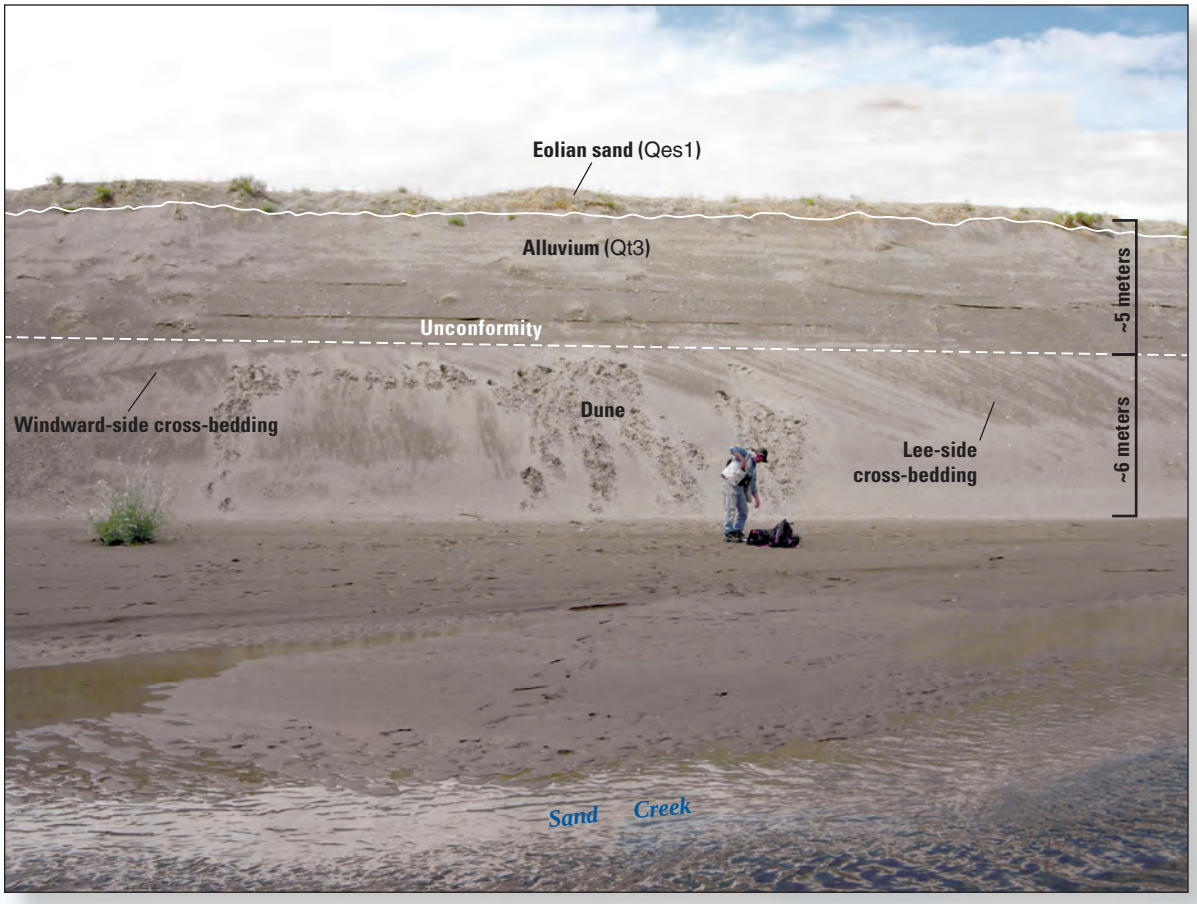


**Figure 11.** Photograph looking westward from the Qt3 terrace (see fig. 9). In most places, a thin cover of Qes1 sand of variable thickness blankets the terrace. The underlying alluvium (Qt3) is about 5 meters thick, and it overlies a surface that truncates the crests of dunes that likely are of middle Pleistocene age. *Photograph by R.F. Madole, August 10, 2008.*

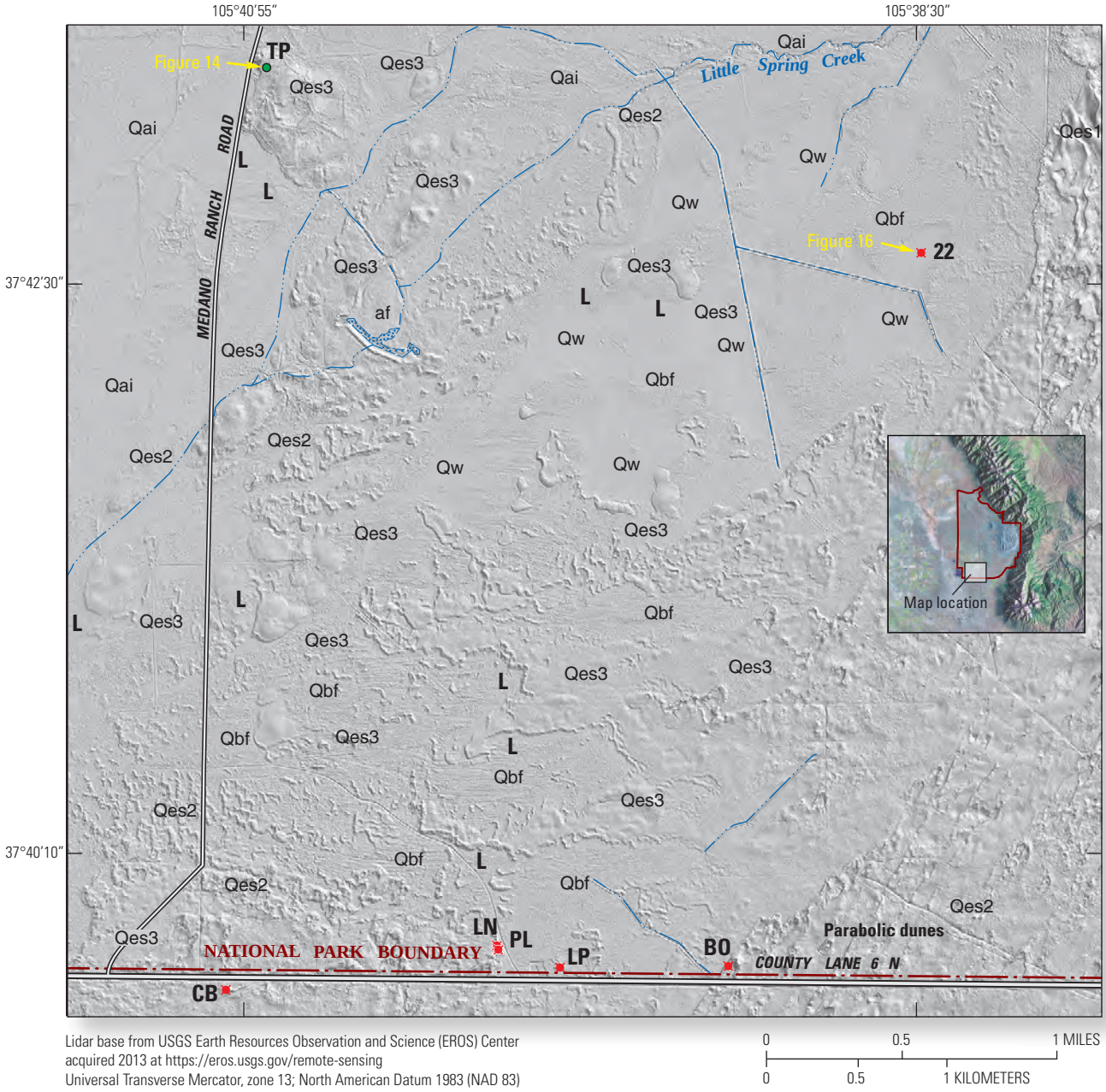


**Figure 12.** This lidar image shows the complexity of the surficial geology in the southwestern part of the park. Wet-meadow deposits (Qw), which are the result of groundwater discharge, occupy widely scattered topographic lows (light-gray areas). The narrow, sharply defined curvilinear and arcuate-shaped landforms are deposits of late Holocene eolian sand (Qes2), which unlike most Qes2 deposits are slightly calcareous in this area. Some deposits are calcareous because they were derived from Qes3 sand that was not transported far enough for ballistic impacts and abrasion to completely remove the carbonate coatings on grains. Other deposits of Qes2 sand are slightly calcareous because calcium carbonate-rich sediment was blown onto them from nearby basin-floor deposits (Qbf). This is particularly true of the lunette dunes (denoted by the letter L) that are banked against the windward (southwest) sides of mounds or dunes of unit Qes3. On the map sheet, a broken-block pattern identifies deposits of Qes2 that are slightly calcareous. Alluvium of groundwater discharge streams (unit Qai), related primarily to Big Spring Creek, is particularly extensive in the westernmost part of the area. The letters CB, BO, LN, PL, LP, and TP are places where numerical ages were acquired, and the yellow arrows show the location and view direction of figures 14 and 16. Red symbol indicates radiocarbon-age locality (table 1), and green symbol indicates infrared stimulated luminescence (IRSL) and optically stimulated luminescence-age (OSL) locality (table 2).

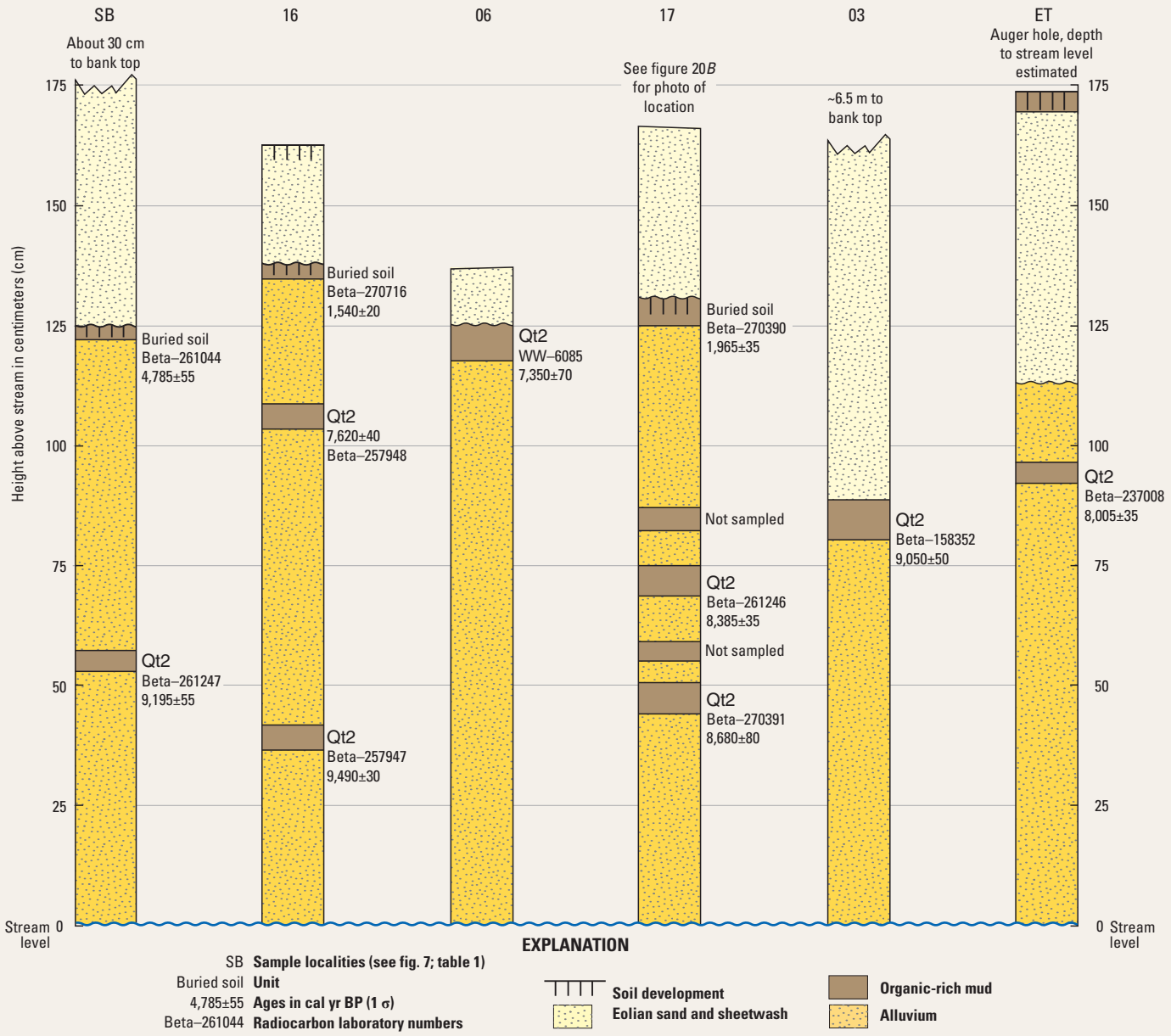


**Figure 13.** Diagram of unit Qt2 stratigraphy along Big Spring Creek (see fig. 7 for site locations). Deposits of middle Holocene eolian sand and sheetwash alluvium tend to obscure Qt2 alluvium in most places. Unit Qt2 alluvium aggraded during a period when groundwater level was rising. The water table began to rise prior to 9,490±30 calibrated years before the present (cal yr BP) and remained higher than it is today until at least 7,350±70 cal yr BP (table 1, localities 16 and 06).

Deposition of unit Qes3 likely began about 7,200 yr BP in response to a regional decline in water-table level, and deposition ended about or before 3,500 yr BP in response to a rise in water-table level. The beginning date is based primarily on a radiocarbon age (table 1, locality PL, 7,200±40 cal yr BP) of palustrine sediment collected from directly beneath the bottom of unit Qes3. Persistence of a low water table is indicated by the radiocarbon ages of (1) charred fish bones (5,825±75 cal yr BP) at locality BP and (2) charcoal (6,055±50 cal yr BP) from a nearby hearth (M.A. Jodry, Smithsonian Museum of Natural History, written commun., 2005). These ages indicate that by about 6,000 cal yr BP the lake that existed between localities DC and BP during early Holocene time had shrunk to a depth of not more than 1–1.5 m. This level is about 5.5 m lower than the high stand reached during the early Holocene. However, although much reduced in size, the lake still supported a population of buffalo fish (*Ictiobus* sp. and *Ictiobus bubalus*), some of which might have been as long as 40–60 cm, and possibly Rio Grande chub (*Gila elegans*) (L.M. Snyder and C.R. Falk, Smithsonian Museum of Natural History, written commun., 2002).

Numerical ages suggest that deposition of unit Qes3 was episodic. However, the large measurement errors associated with luminescence ages and the limited spatial distribution of radiocarbon ages make it difficult to date individual episodes of eolian activity. A radiocarbon age of charcoal at locality TP (see fig. 12) indicates that at least 4 m of Qes3 sand had accumulated by the time the charcoal was emplaced, which was about 6,060±110 cal yr BP (table 1), and an additional 2 m was deposited after the charcoal was emplaced. An OSL age from nearly the same level as the charcoal, but about 15 m farther south (fig. 14), indicates that the eolian sand there was deposited or reworked about 3,640±270 yr ago (table 2). This situation is not as inconsistent as it might seem because lidar imagery shows that lunette dunes have accreted in shingle-like fashion against the southwest sides of sand mounds at locality TP and elsewhere in the southwestern part of the map area (see fig. 12). A somewhat similar situation exists at locality TB on Big Spring Creek (see fig. 7). Here, a hearth was constructed in the upper part of Qes3 sand about 4,205±55 cal yr BP (table 1), but about 15 m to the south, sand at the top of this unit has an OSL age of 2,920±230 yr and an infrared stimulated luminescence (IRSL) age of 3,770±360 (table 2). The difference between the radiocarbon and OSL ages might not be relevant because the OSL age indicates when the sand was buried rather than when it was deposited. Also, the OSL age comes from near the top of a 10-m-high stream bank that is subject to ongoing erosion and deposition of sand deflated from the surface of the steep, unvegetated bank.

The end date suggested for unit Qes3 is based on evidence that indicates the water table began to rise by or before about 3,500 yr BP. This rise affected the landscape in various ways: it caused (1) alluvium (unit Qt1) to aggrade on valley floors (figs. 10*A*, 10*B*, and 15); (2) organic-rich silty, clayey, and peaty sand (unit Qw) to accumulate in marshes (fig. 16); (3) dry playas to become lakes; (4) vegetation cover to change; and (5) deposition of unit Qes3 to end. OSL ages (blue-light quartz and IRSL) of sediment from about 1 m below the basin floor 1.4 km south of San Luis Lake (locality DE, table 2) suggest that standing water might have been present here as long ago as 3,780±610 yr or as recently as 3,185±830 yr ago. In addition, organic detritus concentrated from lake sediment at locality DA (1.3 km south of San Luis Lake) has a radiocarbon age of 3,310±20 cal yr BP (table 1). Given that the detritus came from the uppermost part of the lake sediment, it is likely that the lake formed prior to 3,300 cal yr BP. Together, these numerical ages suggest that the water table in this area had risen to a level that caused lakes to form and deposition of unit Qes3 to cease by, if not prior to, 3,500 yr BP. Additional support for this conclusion is provided by a radiocarbon age of charcoal (table 1; 3,160±70 cal yr BP) in a hearth embedded in Qes3 sand at locality SB (see fig. 7). Obviously, the hearth postdates deposition of unit Qes3 at this locality by an unknown amount of time.

## Eolian Sand Unit 2 (Qes2)

Eolian sand unit 2 (Qes2) covers nearly half (47 percent) of the map area, which makes it by far the most extensive surficial deposit in the park. According to radiocarbon ages of organic-rich sediment in alluvial and palustrine deposits and of charcoal in basal sand deposits of Qes2, deposition of this unit began sometime between 1,500 and 1,300 cal yr BP. Deposition began in response to a declining water table, which is inferred to have altered the kind and quantity of vegetation cover and initiated wind erosion over much of the map area. One of the better records of this decline is preserved in the geomorphology and alluvial stratigraphy of Big Spring Creek. As water table lowered, this spring-fed stream deepened its channel, thus abandoning its former valley floor. Remnants of that valley floor, now a low terrace, are shown on the map as unit Qt1. Except for at least one interval (about 930–760 cal yr BP), the water table likely remained low for many centuries. Although the end date for deposition of Qes2 is unknown, it seems reasonable to assume, given the importance of snowmelt runoff to the hydrogeology of the closed basin, that the growth of cirque glaciers and formation of the Grenadier moraines in the nearby San Juan Mountains (Carrara and Andrews, 1975) was a time of increased recharge and rising water table in the closed basin. In other words, deposition of Qes2 likely ended with the onset of the Little Ice Age, which occurred between the 16$^{th}$ and mid-19$^{th}$ centuries (Mann, 2002). The preservation in some places of a weakly developed soil A-horizon in unit Qes2 indicates that for a time the vegetation cover on this unit was greater than it is today.

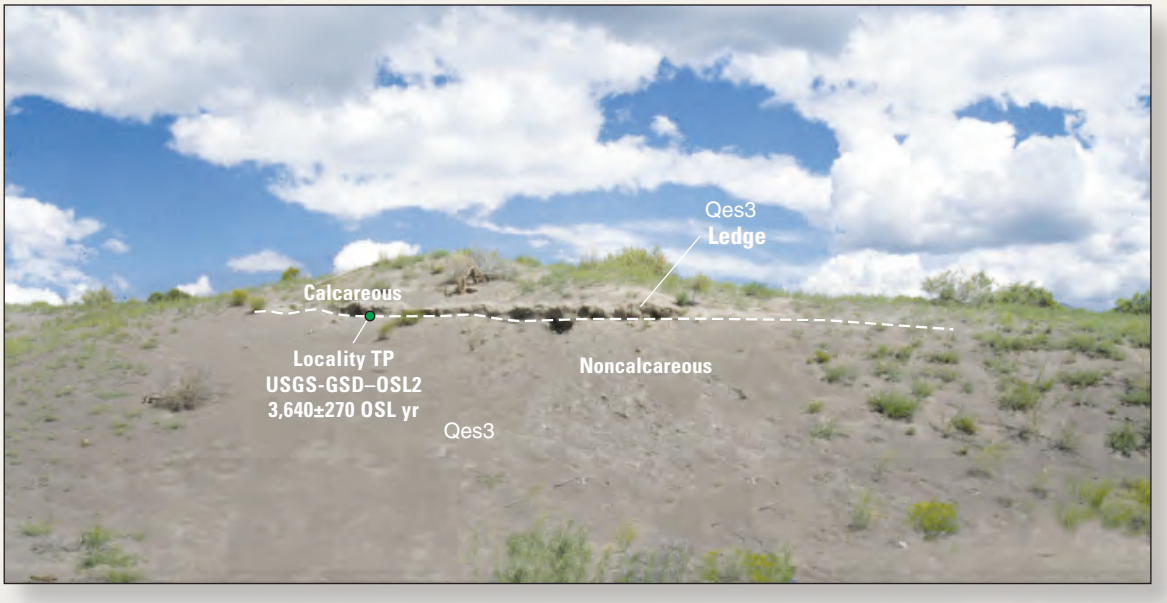


**Figure 14.** Photograph looking east at locality TP (fig. 12, table 2) showing a ledge of calcium carbonate-bonded Qes3 sand that crops out between 1.2 and 1.5 meters (m) below the ground surface. The ledge marks the maximum depths reached by downward percolating water (rain and snowmelt). All eolian sand above the base of the ledge is calcareous, whereas that below the ledge is noncalcareous. The ledge is about 6 m higher than the base of the slope in the foreground. The calcium carbonate-enriched zone parallels the land surface across topographically high and low areas, which indicates that it is of pedogenic rather than groundwater origin. The zone is distinctly visible only when sand is dry or case hardened. The optically stimulated luminescence (OSL) age of noncalcareous sand collected 30 centimeters below the calcium carbonate ledge is dated at 3,640±270 yr. *Photograph by R.F. Madole, July 18, 2001.*

Radiocarbon ages of 1,490±60 and 1,540±20 cal yr BP of organic-rich wetland sediment in unit Qt1 along Big Spring Creek at localities 10 and 16 (see figs. 7, 20*A*, and table 1) indicate that about 1,500 yr ago the floor of this instream wetland was at least 1 m higher than it is today. Two other radiocarbon ages—1,270±20 cal yr BP of charcoal from rabbitbrush (*Ericameria nauseosa*) collected from the base of Qes2 sand at locality TB (fig. 7, table 1) and 1,310±20 cal yr BP of charcoal-coated sand (likely cultural in origin) at locality CB (fig. 12, table 1)—indicate that deposition of Qes2 was occurring by 1,300 cal yr BP. Together, these radiocarbon ages indicate that the creek began incising its channel after about 1,500 cal yr BP but prior to 1,300 cal yr BP in response to a declining water table, which is inferred to have altered the kind and quantity of vegetation cover in this area and consequently initiated the eolian activity that produced unit Qes2.

De Lanois (1993) obtained stratigraphic data and radiocarbon ages from a 1.6-m-long core extracted from San Luis Lake that when combined with information from other localities in the map area suggest that water table rose enough between about 930 and 760 cal yr BP to form cienegas in the topographically lowest (southwestern) part of the map area. The core contained a 56-cm-thick interval of clayey silty sand at a depth of 56–112 cm below the lake floor. The particle-size distribution in the lower part of this interval is 56 percent sand, 21 percent silt, and 23 percent clay, and in the upper part of the interval it is 70 percent sand, 12 percent silt, and 18 percent clay (De Lanois, 1993). These particle-size distributions are similar to those of slack-water deposits sampled along Big Spring Creek and are markedly different from the particle-size distributions in eolian sand deposits, which as noted previously are typically 95 percent or more sand and 0–5 percent silt and clay combined. Sand percentages greater than 77 percent were not found in any of 20 samples from other depositional environments (alluvial, paludal, and lacustrine) in the map area. Therefore, the particle-size distribution of the 56-cm-thick interval beneath the floor of San Luis Lake suggests that when this sediment was accumulating, the basin containing San Luis Lake (which it should be noted is maintained with water from the Closed Basin Project canal) would not have been a source of sand for dunes like those shown in figure 17 because mud or damp sand resists deflation.

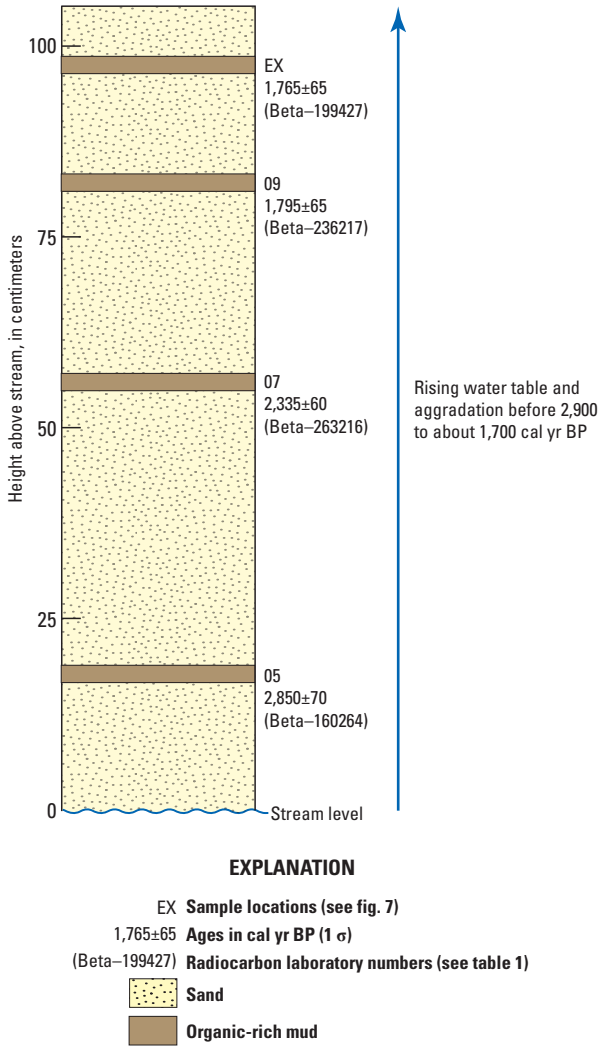


**Figure 15.** Composite diagram of Qt1 stratigraphy exposed at four localities on Big Spring Creek (fig. 7, localities 05, 07, 09, and EX). Radiocarbon ages of thin beds of organic-rich mud at these localities document the progress of aggradation of Qt1 alluvium between 2,850±70 and 1,765±65 calibrated years before the present (cal yr BP) (table 1). Aggradation occurred during this time because the water table in the closed basin, which is the local base level for Big Spring Creek, was rising. The alluvial fill became a terrace sometime after 1,765±65 cal yr BP when a declining water-table level caused Big Spring Creek to incise its channel.


**Figure 16.** Photograph looking east across locality 22, one of several widely scattered mesic wetlands on the basin floor, in the western part of the park (fig. 12, table 1). The Great Sand Dunes are visible in the distance. At present, the water table in this area is between 85 and 105 centimeters (cm) below the ground surface depending on the season. Organic-rich mud (mixture of silt, fine sand, and some clay) collected from between 50 and 65 cm below the wetland surface shown here has a radiocarbon age of 3,150±70 calibrated years before the present (cal yr BP). *Photograph by M.A. Jodry, August 30, 2000.*

Organic-rich strata at depths of about 70 and 90 cm below the floor of San Luis Lake have radiocarbon ages of 928±45 and 920±60 $^{14}$C yr BP, respectively (De Lanois, 1993). When calibrated to the one-sigma confidence level, the ages are 855±65 and 845±85 cal yr BP (table 1, locality SL). The radiocarbon ages of the silty, clayey organic-rich strata at locality SL indicate that sometime between 980 and 760 cal yr BP the area was moist, if not wet, and thus was not susceptible to wind erosion. Evidently, Qes2 sand mantling the surface shown in figure 17 postdates this time. According to the radiocarbon age of organic-rich sediment that accumulated in an interdunal pond about 6 km southwest of the Great Sand Dunes (see fig. 6, locality PS), renewed deposition of Qes2 sand at that location likely began sometime after 760±30 cal yr BP (table 1, locality PS). A radiocarbon age of charcoal collected from silty sand 1 m below the base of a prominent lunette dune (7.3 m high) at locality BP 4 km south of San Luis Lake has an age of 980±60 cal yr BP (table 1). Finally, charcoal in eolian sand exposed 6 m below the ground surface in a blowout in an area of prominent parabolic dunes (fig. 12, locality BO) has a radiocarbon age of 1,015±45 cal yr BP (table 1).

## Eolian Sand Unit 1 (Qes1)

Eolian sand unit 1 (Qes1) is defined simply by the fact that it is presently active. Although sand on the surface of the Great Sand Dunes also is active, it is not included in unit Qes1 because it is merely a thin cover on a much larger body of eolian sand most of which is of Pleistocene age (Madole and others, 2008, 2013). Note that the International Commission on Stratigraphy set the upper limit of Pleistocene time at 11,700 yr BP (Cohen and others, 2015). Examination of several generations of aerial photography acquired between 1936 (the first aerial photography ever obtained) and 2012 and satellite and lidar (light detection and ranging) imagery obtained since 2014 indicates that the margins of unit Qes1 have changed slightly (moving primarily east and northeast) over time in many places.

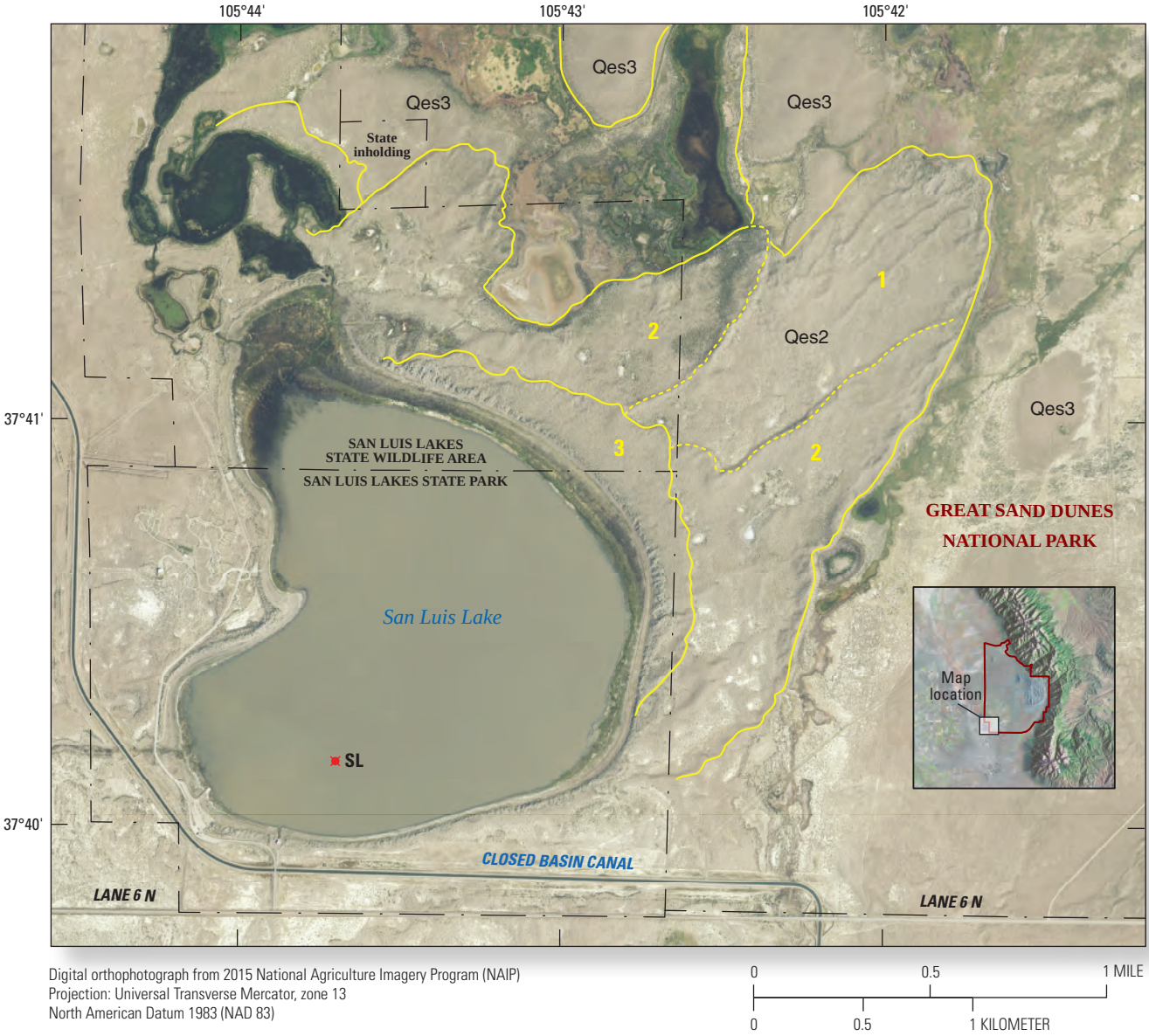


**Figure 17.** Compound parabolic dunes extend 2.3 kilometers (km) northeast (downwind) from San Luis Lake (see fig. 2 for lake location). Deflation of this sand created the present basin of San Luis Lake and at the same time deepened other basins between San Luis Lake and the Dry Lakes area (fig. 2). Crosscutting relations among these dunes suggest the occurrence of at least three episodes of activity during late Holocene time (1 denotes the oldest dunes and 3 denotes the youngest dunes). Stratigraphic relations and radiocarbon ages indicate that all three episodes occurred sometime after about 980 years ago and therefore postdate earlier episodes of Qes2 deposition. Red symbol indicates radiocarbon-age locality.

# DESCRIPTION OF MAP UNITS

The geologic map of the Great Sand Dunes National Park is essentially a surficial geologic map because just two bedrock units are present at the surface (units IPm and Xgn), and combined these units cover barely 2 percent of the map area. On the other hand, surficial deposits cover 98 percent of the map area and are divided into 19 units. Unlike bedrock units, which are defined by their lithologic properties, surficial deposits are defined and identified on the basis of their bounding unconformities rather than their lithic characteristics and stratigraphic position (North American Commission on Stratigraphic Nomenclature, 1983).

Most bedrock units in the map area were formally defined and named long ago and are present in other parts of Colorado. Surficial deposits, on the other hand, are referred to by informal names based on either genesis (process of formation) or landform, and their names are intended to apply only to a particular map area. Use of the same informal names in different map areas does not imply that the respective units have the same properties or are of the same age, as is the case with formally named stratigraphic units. The terminology used here for divisions of Pleistocene time adheres to the standard adopted by the International Commission on Stratigraphy (Cohen and others, 2015). The same is not true, however, for divisions of Holocene time, which are informal and undefined. As used here, early, middle, and late Holocene refer to the intervals between 11.7 and 8.0 ka, 8.0 and 4.0 ka, and 4.0 and 0 ka, respectively.

The sizes of the particles that compose the various map units are described according to the modified Wentworth scale (Ingram, 1989). Gravel includes all particles that are somewhat rounded and larger than 2 mm (that is, pebbles, cobbles, and boulders). Terms used to describe sorting (a measure of the range in particle sizes present) are those of Folk and Ward (1957). However, other than eolian sediment and alluvium derived from eolian sand, most surficial deposits are poorly sorted to extremely poorly sorted. Because sorting generally is not a distinguishing characteristic it is not mentioned in most unit descriptions. Furthermore, because exposures of surficial deposits are few and shallow, the thickness of many map units is unknown. Consequently, deposit thickness for those map units is not mentioned in unit descriptions. R.F. Madole mapped the geology of the Great Sand Dunes National Park during part or all of most field seasons between the years 2000 and 2014. Mapping was accomplished using satellite (Landsat) imagery, lidar (Light Detection and Ranging) imagery, and several generations of aerial photography obtained from the U.S. Forest Service, the Bureau of Reclamation, the U.S. Geological Survey, and the National Park Service. Aerial photography was acquired for all or part of the map area during 16 different years between 1936 and 2005. No photography was obtained during the 1940s, but otherwise photography was acquired every two to five years. The scale of the base map governs the minimum size of the deposits shown. With few exceptions, deposits that have minimum dimensions of less than 45 m are not shown on the map. Also, deposits that are less than 1.5 m thick were not mapped, except where they compose landforms whose boundaries are evident on aerial photography or lidar imagery. Initially, contacts between map units were plotted on aerial photography in the field using a pocket stereoscope and later transferred to orthophoto quadrangles and digitized. Late in the study, lidar imagery of the area became available. In some places, the acquisition of lidar resulted in revisions to map units whose boundaries are distinguished wholly or partly by topographic or geomorphic expression, which is the case for most deposits of eolian sand.

The Great Sand Dunes National Park is accessible only by a few two-track lanes, most of which are closed to the public, and about 12 km of paved highway in the southeastern part of the park (Colorado Highway 150) that provides public access to the Great Sand Dunes. Off-road vehicular travel, including two-track lanes in remote areas of the park is prohibited. Therefore, geologic mapping of the park required hundreds of kilometers of traverses on foot that were made to verify interpretations based on stereoscopic examination of aerial photography and lidar imagery, or to obtain detailed stratigraphic information and geochronologic data in selected areas. A variety of laboratory studies were made including particle-size analyses, X-ray diffraction (XRD) identification of salts and other minerals, trace element and heavy mineral analyses, identification of ostracode fauna and diatom flora, and acquisition of 48 radiocarbon ages and 18 OSL ages, not all of which are described in this publication. In addition, subsurface stratigraphy was examined in logs of more than 250 wells and borings (Madole and others, 2013).

Eolian sand covers nearly 80 percent of the map area, and alluvial, lacustrine, and palustrine sediment combined cover nearly 20 percent of the area. Lacustrine and palustrine deposits are generally small, widely scattered, and mostly in the southwestern part of the map area, which is where the park extends into the trough (fig. 2). Mass-wasting deposits, most of which are the result of debris flows, cover less than 1 percent of the map area. These deposits are concentrated along the mountain front in the eastern part of the map area and are interbedded with alluvium in fan-shaped deposits derived from canyons carved into the west flank of the Sangre de Cristo Range (fig. 6).

# SURFICIAL DEPOSITS

## ANTHROPOGENIC DEPOSITS

af **Artificial fill (latest Holocene)**—Earth materials emplaced or shaped by humans, principally to construct earthen dams, roadbeds, embankments, and well-drilling sites

## EOLIAN DEPOSITS

The term eolian derives from Aeolus (Greek god of the winds) and refers to all landforms and deposits produced by wind. Windblown deposits of silt (called loess) are common in the map area, but not in amounts that are sufficiently extensive or thick enough to show at the scale of this map.

Qes1 **Eolian sand unit one (latest Holocene)**—Active, loose, noncalcareous sand mostly in the form of dunes that have well-defined crests, flanks, and slip faces, and are between 3 and 8 m high. Deposits of this unit are devoid of vegetation except for the odd tuft of Indian ricegrass (*Achnatherum hymenoides*) or wild prairie sunflowers (*Helianthus petiolaris*) because it is difficult for plants to become established on active sand (fig. 18). Because the sand is active, unit boundaries have changed slightly in some places since the imagery used to map the area was acquired, and doubtless, some boundaries will continue to change. Stratigraphic relations in the western part of the map area, and in the vicinity of Big Spring Creek (fig. 7), indicate that most Qes1 sand was derived from older sand deposits, namely, units Qes3 and Qes2. In most places, Qes1 sand is loose and particularly difficult to traverse by vehicle

Qes2 **Eolian sand unit two (late Holocene)**—Noncalcareous sand in sheets and dunes, mostly parabolic forms, that are between 3 and 8 m high and have well-defined, narrow crests and steep flanks (figs. 6 and 9). The stipple pattern overlain on deposits of unit Qes2 along the mountain front northwest of the Great Sand Dunes denotes areas where the unit is not thick enough to conceal the hummocky debris-fan deposits that it overlaps. Although soil maps (Pannell and others, 1973; Yenter, 1984) indicate that soils of the Cotopaxi series are developed in unit Qes2, in most places evidence of soil formation is negligible. Where preserved, the Cotopaxi soil consists simply of an A/C-horizon profile wherein the A-horizon is generally less than 15 cm thick. Unit Qes2 supports a thin, relatively continuous cover of vegetation that contrasts with the much thicker, shrub-dominated vegetation cover on deposits of unit Qes3 (see figs. 8 and 19). Vegetation on unit Qes2 is composed chiefly of grasses, forbs, and rabbitbrush. Unit Qes2 was derived primarily by re-activation of unit Qes3; thus in most places, it is downwind (east and northeast) from deposits of unit Qes3. Most re-activation of unit Qes3 is inferred to have occurred when the water table lowered faster than plant roots could grow downward. Even shrubs like greasewood and saltbush, which have root systems that can penetrate several meters below the ground surface, die off when the decline in water-table level outpaces root growth (see the section on "Hydrogeology, Vegetation, and Sand-Surface Stability" for references and a more detailed discussion of this process). Unit Qes2 is noncalcareous, except locally in the southwestern part of the map area. Here, slightly calcareous deposits of unit Qes2 are depicted using a broken-block pattern. These deposits are slightly calcareous for two reasons: (1) calcium carbonate-rich sediment from adjacent basin-floor deposits was blown onto them, and (2) in some places Qes3 sand was reshaped into new bed forms, but the sand was not transported far enough for ballistic impacts and abrasion among moving sand grains to completely remove the films of calcium carbonate that coated them. Deposition of this unit began sometime between 1,500 and 1,300 cal yr BP and likely ended with the onset of the Little Ice Age in the 16$^{th}$ century. Although bulk densities were not measured, it is obvious that Qes2 sand is much less compact than Qes3 sand and is thus more difficult to traverse by vehicle

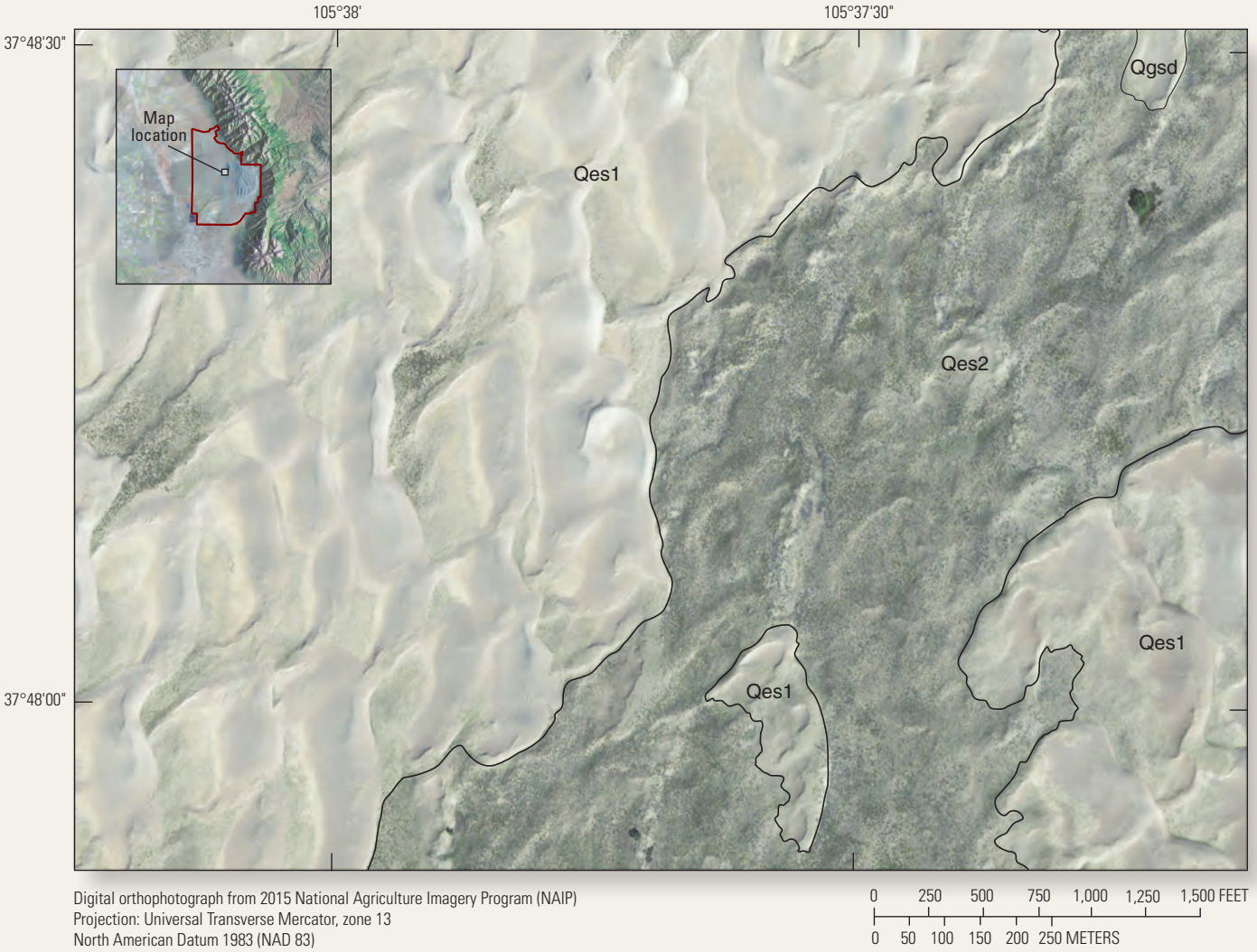


**Figure 18.** Orthophotograph image shows active, unvegetated sand of unit Qes1 overlapping inactive vegetation-covered sand of unit Qes2 near the northeastern edge of the Great Sand Dunes (see fig. 9 for location of image). Although these two units differ markedly in amount of vegetation cover (because it is difficult for vegetation to become established on active sand), they have similar morphologic expression (suggestive that the age difference between them is small) and thus are difficult to distinguish on lidar imagery because lidar does not "see" (detect) vegetation.

**Figure 19.** Photograph looking northeast toward the Great Sand Dunes of vegetation typically found on deposits of unit Qes2. Rabbitbrush (*Ericameria nauseosa*), grasses, forbs, and cacti are the dominant plants. Viewed at an angle, as in this image, vegetation appears denser than it actually is. Regardless, vegetation on unit Qes2 is much sparser than on unit Qes3; for example, compare the vegetation in this scene with that shown in figure 8. *Photograph by R.F. Madole, August 11, 2001.*

Qes3 **Eolian sand unit three (late Holocene? and middle Holocene)**—Sand in sheets, clusters of low (3–6 m high) dunes, and a small number of oval sand mounds (a few of which are 9–10 m high and more than 1 km long) in the southwestern part of the map area. Typically, Qes3 dunes have broader crests and flatter side slopes than Qes2 dunes because they have been inactive for a longer time during which erosion, deposition, and creep modified their form (figs. 12 and 17). Besides topographic expression, the most diagnostic properties of unit Qes3 are (1) the presence of calcium carbonate in the upper 1.0–1.5 m of sediment (fig. 14), and (2) it supports a relatively dense plant cover dominated by halophytic (salt tolerant) woody shrubs, notably greasewood and saltbush, which generally grow in thick stands (fig. 8). Neither of these shrubs is common on deposits of unit Qes2. Soils of the Space City series are developed in unit Qes3 (Pannell and others, 1973; Yenter, 1984). Typically, soil profiles consist of a weakly developed A-horizon, 9–20 cm thick, overlying a calcareous C-horizon that is 100–150 cm thick. This unit is present mainly in the topographically lower parts of the map area, which mostly border the trough and areas flanking instream wetlands in the southwestern part of the map area (figs. 2 and 8). Comparable deposits of Qes3 sand are not present along the western (upwind) margin of the trough, which indicates that Qes3 sand was transported from the trough by southwesterly and westerly winds. Deposition of unit Qes3 began about 7,200 yr BP and ended about or before 3,500 yr BP. Unlike younger sand units, unit Qes3 is compact and easily traversed by vehicle or on foot.

Qgsd **Great Sand Dunes (latest Holocene to middle Pleistocene)**—Well-sorted eolian sand in dunes that have the following characteristics: they are more than 10 m high, contiguous, presently active, have identifiable slip faces, and contain bedding that dips at greater than 20°. Dunes at the edge of the active sand mass that do not quite meet these criteria are included in the Great Sand Dunes if they are contiguous with them. The exceptional heights of the Great Sand Dunes are due mostly to (1) their proximity to a sand source that was replenished periodically (the trough, fig. 2), (2) a complex wind regime, and (3) the Sangre de Cristo Range, which prevented continued eastward migration of dune sand by prevailing southwesterly and westerly winds. Although the sand on the surface of the Great Sand Dunes is presently active, the boundary of the unit has not changed appreciably since the first aerial photographs of the area were taken in 1936. The sand at and near the surface of the Great Sand Dunes is equivalent in age to unit Qes1 (latest Holocene), but most of this massive body of sand (volume estimated to be between 10 and 13 billion $m^3$±430 million $m^3$, Madole and others, 2008) is a complex of deposits that accumulated episodically for more than 130,000 yr (Madole and others, 2008, 2013). The onset of dune formation occurred sometime after Lake Alamosa began to drain, which according to Machette and others (2007) was about 440 ka. The elapsed time between the end of Lake Alamosa and the beginning of the Great Sand Dunes is unknown. However, it was long enough for a thick wedge of piedmont-slope deposits to prograde westward over sediment of Lake Alamosa for a distance of at least 23 km. This wedge was as much as 60 m thick at a point 10 km west of the Sangre de Cristo Range (Madole and others, 2013)

## EOLIAN AND ALLUVIAL DEPOSITS

Qea1 **Younger eolian sand and alluvium (latest Holocene)**—Eolian sand overlying alluvium mostly in the run-out zones of Sand Creek and Medano Creek, the two largest drainage basins on the west flank of the Sangre de Cristo Range in the map area. As used here, run-out zone refers to places where annual snowmelt-driven peak flows and floods caused by severe thunderstorms dissipate due to infiltration and development of distributary channels. Floods transport sand to the run-out zones, sometimes in such quantities that dam-like masses are left on the channel floor when floodwaters dissipate. For most of the year, however, stream channels are dry and susceptible to wind erosion. Sand eroded from dry channels is deposited over older alluvium in areas near the channels. In some places, unit Qea1 includes active dunes overlying unit Qa1 on channel floors, particularly along Medano Creek. The distribution of unit Qea1 is particularly complex and dynamic in the run-out zone of Sand Creek. Thus, it is impractical to map unit Qea1 in detail in this area

Qea2 **Older eolian sand and alluvium (late Holocene)**—Eolian sand in dunes and sheets overlying alluvium on the floor of a prominent paleochannel formerly occupied by Medano Creek. The channel floor is as much as 400-m-wide near its upstream (northeast) end and tapers to a width of 150 m over a distance of about 5 km. Alluvium is within 0.5 to 1.5 m of the ground surface near the upstream end of the paleochannel, but Qes2 sand thickens downvalley and completely buries the west (downstream) end of the channel (fig. 6). Either stream piracy or avulsion (an abrupt change in course) or a combination of these processes likely caused Medano Creek to abandon its former course. The alluvium underlying the paleochannel floor consists of interbedded sand and fine to coarse gravel. The gravel consists mostly of Precambrian granitic and gneissic rock derived from the core of the Sangre de Cristo Range. The thickness of the alluvium is unknown beyond the fact that where augured near the upstream end of the paleochannel it is greater than 1 m

## ALLUVIAL DEPOSITS

Qa1 **Younger alluvium (latest Holocene)**—Alluvium deposited by streams draining from the Sangre de Cristo Range. In mountain canyons, unit Qa1 consists of clast-supported gravel ranging in size from pebbles to boulders. Westward from the mountain front, the larger streams continue to flow on gravel, but clast size decreases progressively in a downstream direction. The distance to the point where gravel ceases to be a constituent is proportional to drainage basin size. The transition from gravel bed to sand bed is abrupt. Downstream from where gravel ends, unit Qa1 consists of sand derived mostly from the eolian sand that bounds it. In some places, most notably along Deadman Creek in the northern part of the map area, deposits of unit Qt1 are included in map unit Qa1 because although the terrace deposits are morphologically distinct and extensive, they are too narrow to show separately at the scale of this map. During floods, Sand Creek commonly entrains more sand in its upper reaches than it can transport through its lower reaches because of the reduction in stream energy resulting from diminished discharge. Stratigraphic and geomorphic relations indicate that at times Sand Creek, and to lesser extent Medano Creek, were self-damming and prone to avulsion, which is one reason why unit Qa1 occupies multiple channels in the lower reaches of both streams

Qa2 **Older alluvium (latest Holocene)**—Alluvium that is physically similar to unit Qa1 because it was derived from the same source areas. Deposits of unit Qa2 are mainly in abandoned paleochannels in the lower reaches of Sand Creek. Most paleochannels are 1.0–1.5 m higher than the present channel of Sand Creek. The distribution of these deposits indicates that in its lower reaches Sand Creek occupied a broad range of locations during Holocene time. Stream avulsion likely accounts for most of the changes in channel location, and most changes likely occurred during exceptionally large floods

Qt1 **Lower terrace alluvium (late Holocene)**—Alluvium underlying a terrace that is about 1 m higher than channel level along all streams regardless of whether they drain from the mountains or from springs (figs. 10*A* and 10*B*). Many deposits of unit Qt1, particularly along Deadman Creek and Big Spring Creek, are either too small or too narrow to show at the scale of the map. However, examples of this unit are visible in figures 7 and 8. Near the mountain front, Qt1 alluvium consists chiefly of cobble and pebble gravel, but farther west it is made up mostly of fine- to medium-size sand. Stratigraphic and geomorphic relations suggest that Qt1 alluvium began to accumulate sometime about or after 3,500 yr BP and ceased to accumulate by or about 1,500 yr BP. Several radiocarbon ages indicate that most aggradation occurred between about 2,900 and 1,700 cal yr BP (figs. 10*A* and 15)

Qt2 **Middle terrace alluvium (middle and early Holocene and latest Pleistocene?)**—Alluvium underlying a terrace that, depending on drainage basin size and distance from the mountain front, is 1.7–3 m higher than adjacent stream channels (figs. 20*A*, 20*B*, and 20*C*). Terrace height is higher near the mountain front and in large drainage basins. This unit is most extensive along Deadman Creek and similar valleys (Cottonwood Creek, for example) north of the park. In this area, runoff from the cluster of high peaks east of Crestone (some of which have altitudes in excess of 4,000 m) is sufficient to maintain channels westward all the way across the map area. Deposits of unit Qt2 also exist along Sand Creek but are more difficult to discern because eolian sand overlies them in most places. The same is true along Medano Creek, where eolian sand buries nearly all terrace deposits. Cottonwood Creek, Deadman Creek, and an unnamed channel draining from Cedar Canyon (fig. 21) are underfit streams; that is, they appear to be too small to have eroded the valleys in which they presently flow. Also, the discharges required to form such broad valleys were too great to have occurred in the Holocene, yet the lack of a distinct weathering profile and the presence of calcium carbonate indicates that most of the Qt2 alluvium exposed in cutbanks is Holocene (fig. 20*C*). However, the gravel in the lower part of the unit suggests that it might have begun to accumulate during latest Pleistocene time when stream discharge was greater. Aggradation likely was in progress prior to 9,490±30 cal yr BP and continued at least until 7,350±70 cal yr BP (fig. 13, table 1)

Qt3 **Upper terrace alluvium (middle Pleistocene)**—Chiefly poorly sorted sand, gravelly sand, and gravel in terrace remnants that are 10–11 m higher than the floors of Sand Creek, Cold Creek, and Deadman Creek (figs. 11, 22*A*, and 22*B*). In some places near the mountain front, this unit also includes debris-flow deposits. The number and thickness of gravel beds, gravel size, and height above stream level all decrease with increased distance from the mountain front. Deposits of Qt3 alluvium along Sand Creek are at least 11 m thick near the mountain front, but only about half as much Qt3 alluvium is exposed 7 km west of the mountain front (fig. 11). Eolian sand overlies unit Qt3 in much of the area; thus, in some places, unit boundaries are based on terrace morphology. For example, the morphology of Qt3 alluvium at the confluence of Cold Creek and Sand Creek is clearly visible on lidar imagery even though it is blanketed by eolian sand that, except for a few small dunes, is 1.0–1.5 m thick (fig. 9). A pit near the south side of Sand Creek about 3.5 km downstream from the mountain front exposes a 6-m-thick section of Qt3 gravel. The gravel consists of cobbles and lesser amounts of pebbles and a few small boulders in a coarse sandy matrix. The gravel is deeply oxidized (1–2 m) and clasts are highly weathered. This depth of oxidation contrasts markedly with the 1–36 cm depth of oxidation on nearby alluvial fans that are correlated with the Pinedale (latest Pleistocene) glaciation (McCalpin, 1982). Therefore, unit Qt3 is most likely of middle Pleistocene age.

Qau **Alluvium, undivided (Holocene and late Pleistocene)**—Deposits of mostly sandy alluvium that are correlative with units Qa1, Qa2, Qt1, and Qt2, but are undifferentiated because they are either too small to show separately at the scale of this map, or are too difficult to distinguish because of the basinward (westward) convergence of their surfaces. These limitations apply only in valleys that originate in small canyons in the northern part of the map area

Qai **Alluvium of groundwater discharge streams (late Holocene)**—Alluvium deposited primarily by streams that flowed from springs and marshes. Most deposits consist of poorly sorted stratified sand and a few thin, discontinuous beds of dark-gray, organic-rich mud. The mud accumulated in slack-water areas along stream margins (for example, see figs. 8, 10*A*, and 20*A*). Typically, these beds are composed of mixtures of sand (38–59 percent), silt (35–60 percent), and clay (7–9 percent).The age of unit Qai is uncertain beyond the fact that it postdates unit Qt1

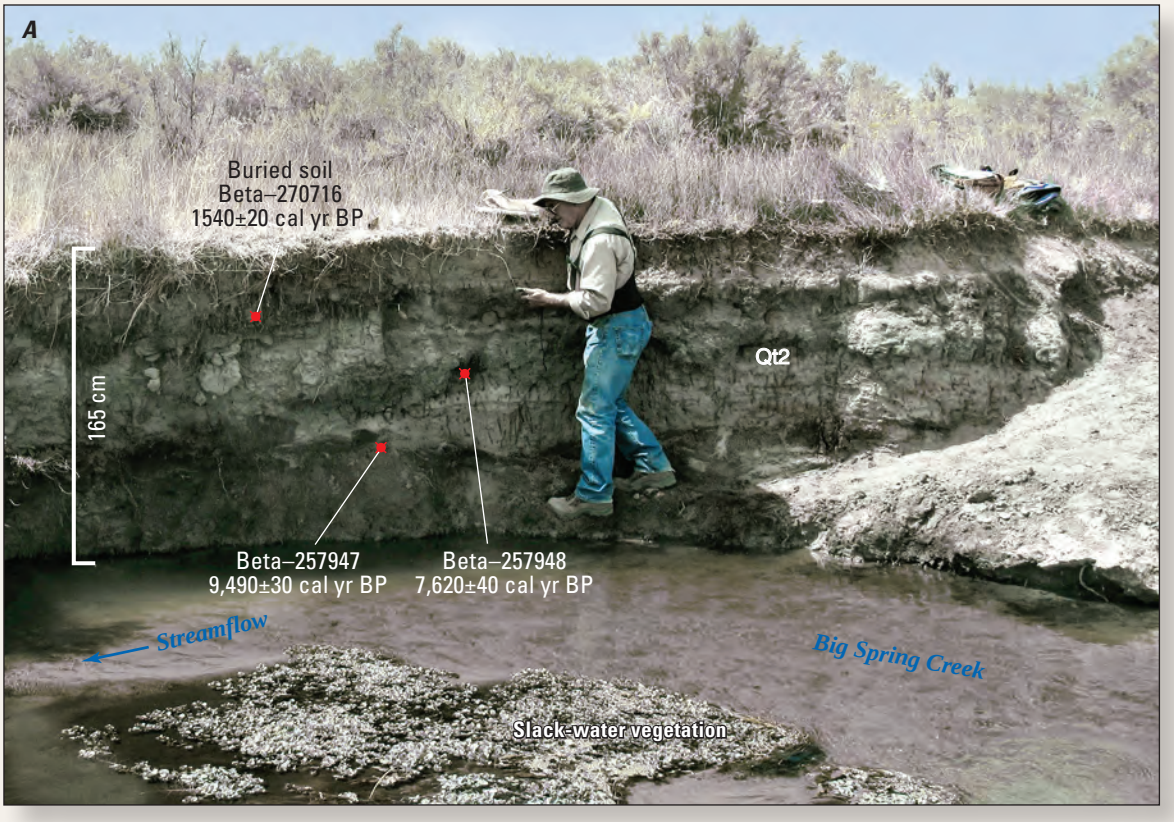
A
Buried soil
Beta–270716
1540±20 cal yr BP
165 cm
Qt2
Beta–257947
9,490±30 cal yr BP
Beta–257948
7,620±40 cal yr BP
Streamflow
Big Spring Creek
Slack-water vegetation


B
Buried soil
(Beta-270390)
1,965±35 cal yr BP
Qt2
8,385±35 cal yr BP
(Beta-261246)
8,680±80 cal yr BP
(Beta-270391)
165cm
Streamflow
Big Spring Creek

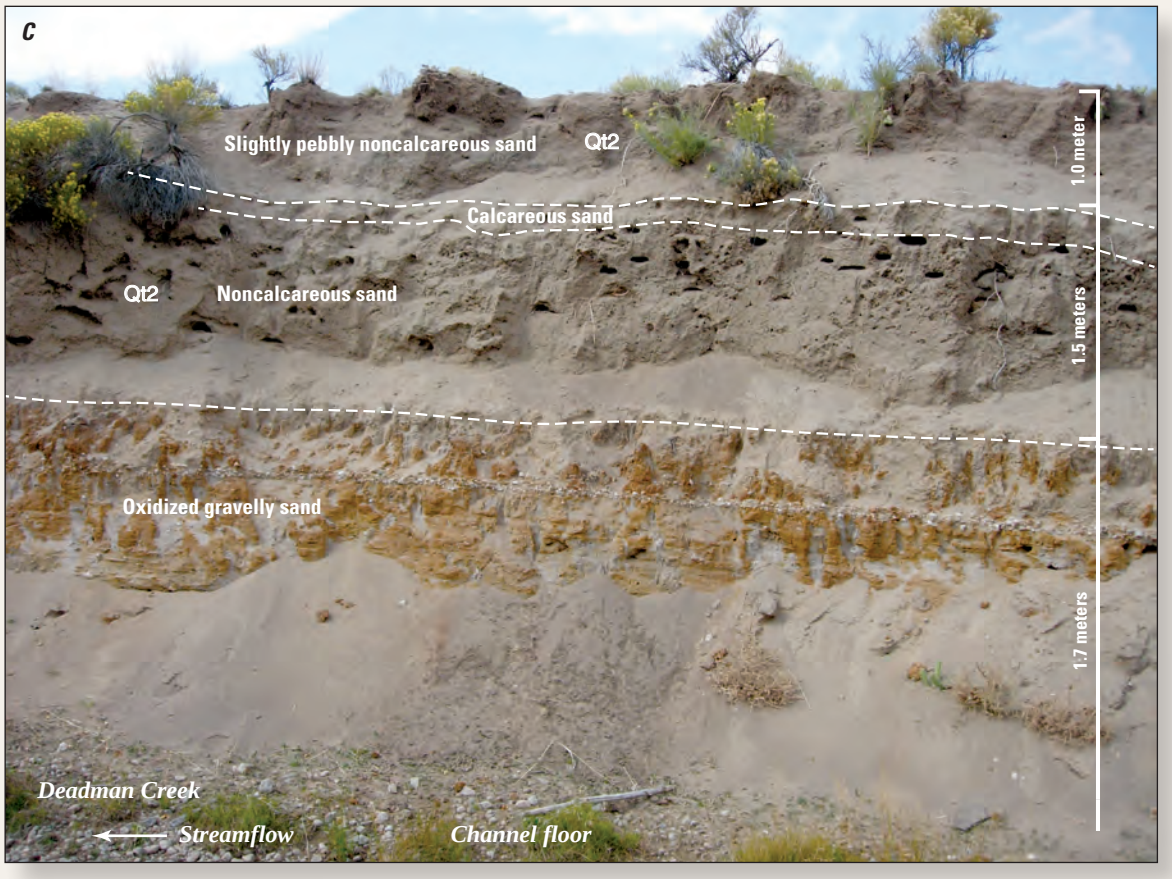


**Figure 20 (pages 36 and 37).** *A*, Photograph of the Qt2 terrace at locality 16 on Big Spring Creek (fig. 7, table 1). Here the Qt2 terrace is capped by 25 centimeters (cm) of calcareous, sandy slopewash alluvium derived from unit Qes3, which mantles the adjacent upland. Radiocarbon ages indicate that Qt2 alluvium began aggrading sometime prior to 9,500 calibrated years before the present (cal yr BP) and continued to aggrade until sometime after 7,600 cal yr BP (fig. 13). The landscape at this locality was stable prior to 1,500 calibrated years before the present (cal yr BP), long enough for a 15-cm-thick soil to develop before being buried by slopewash alluvium. The area of aquatic plants (slack-water vegetation) shown here is the depositional environment that produced the black, organic-rich layers of mud that were sources of radiocarbon ages here and elsewhere along Big Spring Creek (for example, localities 05 and 17, shown in figs. 10*A* and 20*B*). *Photograph by R.F. Madole, September 4, 2009. B*, Photograph of the Qt2 terrace at locality 17 on Big Spring Creek (fig. 7, table 1). Here, the terrace is capped by a thin (typically about 13 cm) layer of noncalcareous sediment overlying about 20 cm of calcareous silty sand derived from unit Qes3 on adjacent uplands. The buried soil possibly correlates with the buried soil shown in figure 20*A*. Thin beds of dark-gray to black, organic-rich mud (the source of radiocarbon ages) are slack-water deposits of ancestral Big Spring Creek. Typically, these beds are composed of mixtures of sand (38–59 percent; mostly very fine to medium sizes), silt (35–60 percent), and clay (7–9 percent). *Photograph by R.F. Madole, September 4, 2009. C*, Photograph of Qt2 strata exposed in the north bank of Deadman Creek about 3.3 kilometers (km) east of the western park boundary. Here, secondary calcium carbonate is concentrated in a zone that is 30–40 cm thick. The iron-oxide coated (and locally cemented) pebbly sand in the lower part of the section is the result of a time when the water table was higher than the present-day channel of Deadman Creek. *Photograph by R.F. Madole, September 8, 2005.*

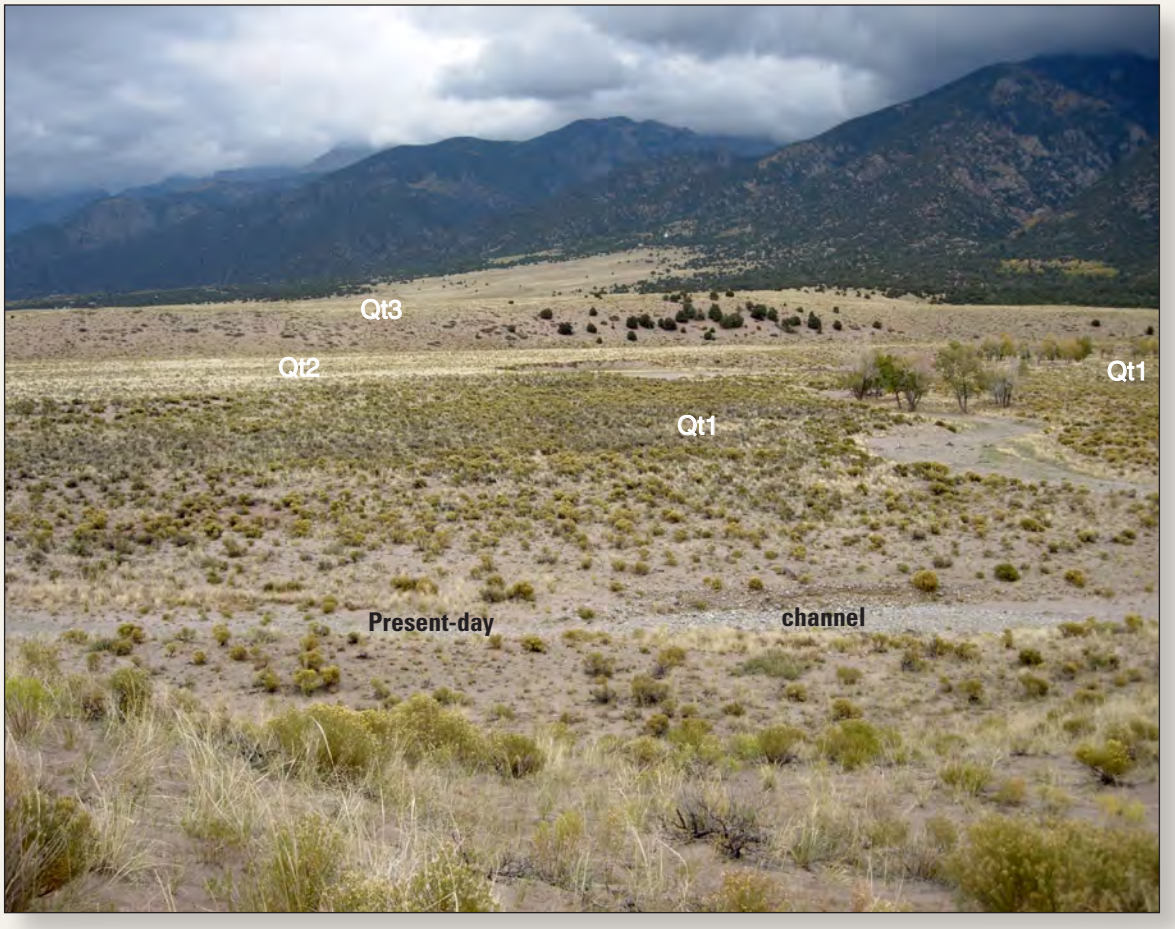


**Figure 21.** Photograph northeast across the valley of the unnamed creek between and approximately parallel to Cottonwood and Deadman Creeks. This view shows the extent and spatial relations of units Qt1, Qt2, and Qt3. Eolian sand several meters thick overlies unit Qt3 here, as it does elsewhere along the mountain front. Exposures of Qt3 large enough to show at the scale of this map are limited to particularly high stream banks, most of which are near the mountain front in places where streams have cut deeply into the edge of the upper piedmont slope. Notice that the present-day stream is ephemeral and markedly underfit, that is, it is much too small to have eroded the broad valley in which it flows. *Photograph by R.F. Madole, October 4, 2005.*

---

**Figure 22 (facing page).** *A*, Photograph of the Qt3 terrace looking northeast from a location shown in figure 9. Here, the terrace is about 10–11 m higher than the floor of Sand Creek, and pebbles litter its surface, which is remarkably flat except where dunes have drifted over it. Unit Qt3 extends along the north side of Sand Creek to the gallery forest in the distance (right center). In most places, however, eolian sand covers Qt3 alluvium (for example, see fig. 11). Patches of the terrace surface, such as shown here, typically are too small to show at the scale of the geologic map. Thus, in most places, the boundaries of unit Qt3 are based on terrace morphology rather than sediment (see for example, Qes2/Qt3 on fig. 9). *Photograph by R.F. Madole, September 8, 2005.* *B*, Photograph of typical Qt3 alluvium exposed in the bank of Sand Creek (see fig. 9 for photo location). *Photograph by R.F. Madole, September 8, 2005.*

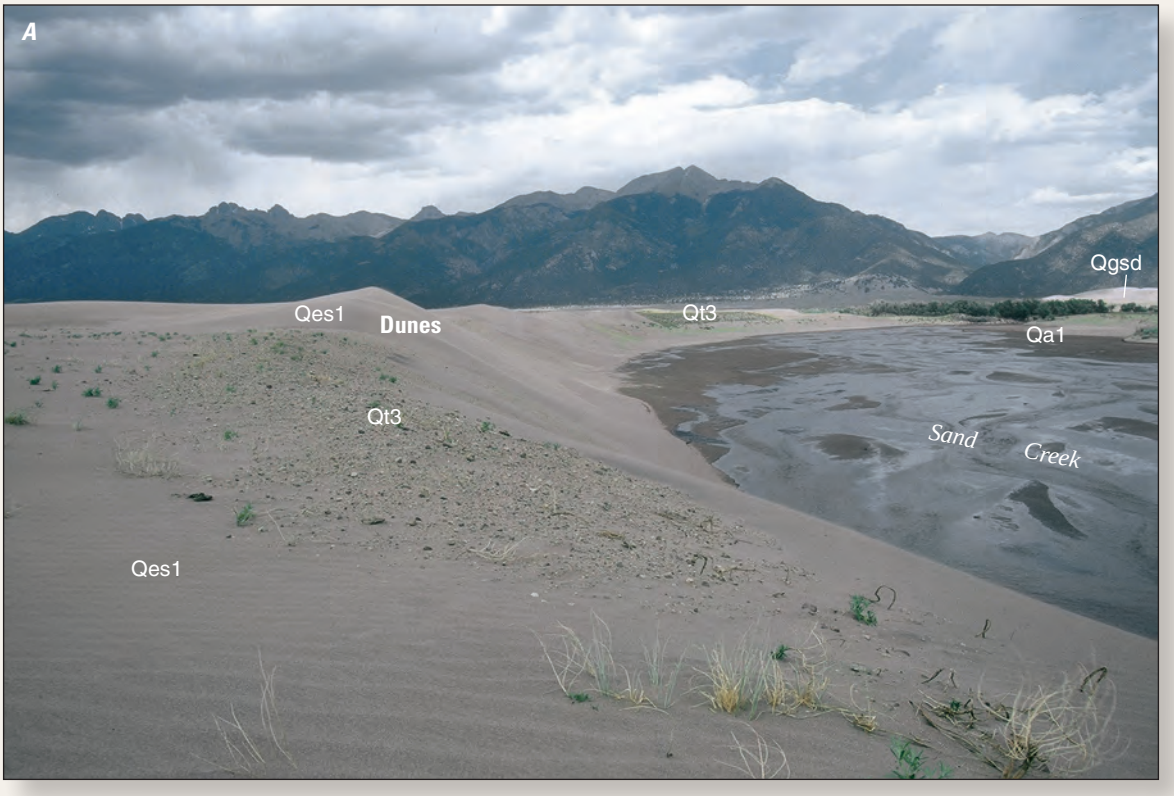
A
Qgsd
Qes1
Dunes
Qt3
Qa1
Qt3
Sand
Creek
Qes1


B
Qt3
0.5 meter
Qf3

## ALLUVIAL AND MASS-WASTING DEPOSITS

Deposits of alluvial and mass-wasting origins are widespread and generally interbedded along the junction of mountain fronts and the upslope edge of adjacent piedmont slopes. Mass-wasting deposits differ from alluvial deposits in that the force of gravity was the primary cause of their movement. That is, mass-wasting deposits move as a mass rather than as individual fragments borne along by a transporting medium such as flowing water, as is the case with alluvium. Although water is an important constituent of most mass wasting and commonly triggers movement, water is part of the moving mass rather than the transporting agent.

Qaf **Alluvial-fan deposits (late Holocene to early Pleistocene?)**—Chiefly coarse-grained alluvium composed of gravel and sand, interbedded with debris-flow deposits and sheetwash alluvium. Cobbles of all sizes are the dominant constituents, but boulders also are abundant in many places. The deposits were derived primarily from Precambrian gneiss and granitic rock in canyons on the west flank of the Sangre de Cristo Range. Fans emanate from canyons and merge laterally with other fans to form a nearly continuous zone of bouldery detritus along the mountain front (fig. 6). Fans south of the map area contain large amounts of clast-supported gravel of glaciofluvial origin, but those in the map area do not contain glaciofluvial sediment because here the range was not high enough to be glaciated. At the mountain front, unit Qaf is at least 330–460 m thick based on the difference in altitude between the tops of fans and the basin floor to the west. However, the full thickness and maximum age of unit Qaf are unknown because the position of its basal contact has not been determined (Brister and Gries, 1994). At the surface, deposits range in age from late Holocene to middle Pleistocene. However, the stratigraphic relations of unit Qaf and the underlying deposits of the upper Santa Fe Group (Pleistocene to Miocene) are unknown

Qpf **Piedmont-fan deposits (late Holocene to early Pleistocene?)**—Sediment underlying the piedmont fan (that is, the merged lower slopes of adjacent mountain-front alluvial fans) consists chiefly of alternating beds of poorly sorted sand and gravel. The quantity and size of gravel clasts decrease downslope. Well-log data indicate that at times clasts as large as 6.5 cm were transported as far as 10 km from the mountain front. In much of the map area, eolian sand buries the lower piedmont slope (fig. 6). Well-log data suggest that alluvium underlying the lower piedmont slope is at least 60 m thick. The unit is presumed to be of the same age as unit Qaf

## MASS-WASTING DEPOSITS

Qdf **Debris-flow deposits (late Holocene to late Pleistocene?)**—Nonsorted, heterogeneous mixtures of surficial materials and fragmented rock debris in a wide range of sizes, including large boulders. The deposit matrix (material less than 2 mm in size) and the lithologies and sizes of rock fragments vary according to the kind of bedrock from which the debris was derived. Levees formed by recent small debris flows (too small to show at the scale of this map) are visible in several places along Colorado Highway 150. Debris-flows occur frequently along the mountain front and sediment transported by them is present on both units Qaf and Qpf. Only large debris-flow deposits are mapped separately. These deposits are estimated to be less than 40 m thick

## ALLUVIAL, EOLIAN, LACUSTRINE,AND PALUSTRINE DEPOSITS

Qbf **Basin-floor sediment (late Holocene to middle Pleistocene)—**Chiefly poorly sorted sandy alluvium, some thin beds of clayey silt, and minor amounts of gravelly sand. The unit is at the surface only in the topographically lowest (southwestern) part of the map area (figs. 6 and 12). Thin beds of loess consisting mostly of windblown silt and very fine sand derived from dry playas and lakes during the Holocene cover unit Qbf in some places, as do thin deposits of silty and clayey lacustrine sediment, also of Holocene age. Both the loess and lacustrine deposits are too small or thin to show at the scale of this map. Deposits of loess typically are 50–80 cm thick and highly calcareous. The upper part of the Laney soil series is developed in loess and the lower part is developed in alluvium. The soil profile typically consists of an A/AC/C/ B2b/B3b/IIC2/IIIC3 horizon sequence (Pannell and others, 1973). Most lacustrine deposits also are 1 m or less thick. They are the parent material of the Hooper clay loam, which unlike other soils in the map area includes a heavy clay loam Bt horizon that typically is 20–25 cm thick (Pannell and others, 1973; Yenter, 1984). According to well-log data, unit Qbf is several tens of meters thick

Qw **Wet-meadow sediment (late Holocene)—**Chiefly sand, silty sand, and thin beds of very dark-gray to black clayey silty sand. Unit Qw is present in areas where groundwater discharge sustains or formerly sustained wetlands and sub-irrigated meadows (fig. 16). Fluctuations in water-table level during Holocene time caused the locations of groundwater discharge points to shift. They shifted upslope (northeast in most places) when the water table rose and downslope when the water table lowered. Thus, deposits of unit Qw are present in a zone that is 3–6 km wide. The zone trends roughly northwest–southeast across the topographically lowest (southwestern) part of the map area. Deposits of Qw are common at the upslope (northeast) ends of several now defunct instream wetlands (unit Qai). Soils of the Medano series are developed in unit Qw (Pannell and others, 1973; Yenter, 1984). These soils are the only Mollisols—thick dark-colored soils typically associated with lush grasslands—present in the map area. Their contrast in color and character with the generally pale brown and brown sandy Aridisols that dominant the area is noteworthy

Qps **Ponded sediment (Holocene)**—Well-sorted fine sand, chiefly of eolian origin, and variable amounts of extremely poorly sorted sand and matrix-supported gravel that are of fluvial and mass-wasting origin. Unit is present in small areas along the mountain front north of Medano Creek where ridges of eolian sand dam the mouths of minor canyons (fig. 23). Only the upper 2 m (the depth limit of auguring) of unit Qps were examined. Given the porous nature of unit Qps, impoundment of runoff in areas underlain by it is likely short-lived and episodic, occurring mainly during and for a short time after thunderstorms and periods of heavy snowmelt


**Figure 23.** View of unit Qps looking northwest along the west edge of the Sangre de Cristo Range from a locality about 0.5 kilometer (km) northwest of Little Medano Creek. A vegetation covered dune of unit Qes2 (lower left), trending approximately parallel to the mountain front, impounds sediment (unit Qps) transported from a small, unnamed drainage basin that flows primarily during rainstorms and periods of snowmelt runoff. The taller trees in the background are Ponderosa pine (*Pinus ponderosa*), and the shorter conifers to the right, far left, and growing up the mountain front are mostly junipers (*Juniperus* sp.). The yellow flowering shrubs at the bottom of the photograph are rabbitbrush (*Ericameria nauseosa*). Grasses and forbs grow in the center of the small basin. *Photograph by R.F. Madole, September 16, 2014.*

## BEDROCK

### PALEOZOIC ROCKS

**IPm** **Minturn Formation (Middle Pennsylvanian)**—Chiefly gray arkosic sandstone, conglomerate, siltstone, shale, and minor limestone (Bruce and Johnson, 1991) that crops out in a small area along the park boundary in the southeastern part of the map area. These sedimentary rocks are relics of sediment eroded from the Ancestral Rocky Mountains (Kluth and Coney, 1981).

### PROTEROZOIC ROCKS

**Xgn** **Mixed gneiss (Paleoproterozoic)—**Unit consists chiefly of interlayered mafic and felsic gneisses, and micaceous schist that are intruded by several bodies of non-foliated igneous rocks of unknown age. Layering is complex, variable in proportion, discontinuous, and rarely traceable in outcrop for more than 0.5 km (Johnson and others, 1989; Bruce and Johnson, 1991). These authors determined that unit Xgn was of Early Proterozoic age, which the updated International Chronostratigraphic Chart (Cohen and others, 2015) reassigns to Paleoproterozoic time.

**Table 1.** Radiocarbon ages of Holocene eolian sand, alluvium, and palustrine deposits in Great Sand Dunes area, Colorado.

[RAD, radiometric; AMS, accelerator mass spectrometer; –, indicates no data; years BP, years before present; cal yr BP, calibrated years before the present; ‰, parts per 1,000; δ $^{13}C$ value, the delta of carbon-13. Plants fractionate atmospheric $CO_2$, and have less $^{13}C$ than the atmosphere; hence, the negative delta $^{13}C$ values listed here; Sigma (σ), denotes the standard deviation of the measured population. There is a 95 percent probability that a given $^{14}C$ age is between the two-sigma limits listed for it]

| Deposit | Locality[1] | Laboratory number[2] | Method | Material sampled | Measured $^{14}C$ age | δ $^{13}C$ ‰ | Conventional $^{14}C$ age (yr B.P.)[3] | Cal yr BP (1σ)[4] | Cal yr BP (2-σ range)[4] |
|---|---|---|---|---|---|---|---|---|---|
| – | PS | Beta–245014 | AMS | sediment[5] | 820±40 | -22.6 | 860±40 | 760±30 | 910–690 |
| Palustrine and lacustrine | SL | A–5607 | RAD | sediment | – | -25.0[6] | 920±60 | 845±85 | 935–700 |
| | SL | AA–7769 | RAD | sediment | – | -25.0[6] | 928±45 | 855±65 | 930–735 |
| | 22 | WW–6159–LT[5] | AMS | sediment | – | -23.1 | 2,990±40 | 3,150 ±70 | 3,330–3,060 |
| – | DA[7] | Beta-297989 | AMS | pollen | 3,060±30 | -23.8 | 3,080±30 | 3,310±20 | 3,370–3,230 |
| | BP[8] | Beta–276512 | AMS | burned bone | 5,040±40 | -22.8 | 5,080±40 | 5,825±75 | 5,920–5,730 |
| | PL | Beta–237009 | AMS | sediment[9] | 6,180±40 | -21.1 | 6,240±40 | 7,200±40 | 7,260–7,020 |
| | LP | WW–6160–LT[5] | RAD | sediment[9] | – | -22.9 | 7,450±40 | 8,270±40 | 8,370–8,180 |
| | DC[7] | Beta–314103 | AMS | pollen | 7,640±40 | -22.6 | 7,680±40 | 8,480±60 | 8,550–8,400 |
| | LN | WW–5324–LT[5] | AMS | sediment[9] | – | -25.4 | 8,410±60 | 9,455±35 | 9,530–9,290 |
| Qes2 | BP[8] | Beta–199426 | RAD | charcoal[10] | 1,010±70 | -22.5 | 1,050±70 | 980±60 | 1,080–790 |
| | BO | Beta–329573 | RAD | charcoal | 1,080±30 | -22.9 | 1,110±30 | 1,020±50 | 1,060–960 |
| | TB | Beta-145016 | AMS | charcoal | 1,340±50 | -24.7 | 1,340±50 | 1,270±20 | 1,320–1,175 |
| | CB | Beta–236218 | AMS | charcoal | 1,340±40 | -21.7 | 1,390±40 | 1,310±20 | 1,350–1,270 |
| Qes3 | SB | Beta–288473 | AMS | charcoal[10] | 2,950±40 | -23.2 | 2,980±40 | 3,160±70 | 3,270–3,030 |
| | TB | Beta–199428 | AMS | charcoal | 3,770±40 | -22.0 | 3,820±40 | 4,205±55 | 4,390–4,090 |
| | TP | Beta–236219 | AMS | charcoal | 5,100±40 | -14.6 | 5,270±40 | 6,060±110 | 6,180–5,930 |
| Qt1 | 10 | Beta–270389 | AMS | buried soil | 1,550±40 | -21.0 | 1,620±40 | 1,490±60 | 1,600–1,410 |
| | 16 | Beta–270716 | AMS | buried soil | 1,610±40 | -23.3 | 1,640±40 | 1,540±20 | 1,620–1,420 |
| | 17 | Beta-270390 | AMS | buried soil | 1,990±40 | -22.9 | 2,020±40 | 1,965±35 | 2,100–1,880 |
| | EX | Beta–199427 | RAD | sediment[9] | 1,790±60 | -23.0 | 1,820±60 | 1,765±65 | 1,880–1,580 |
| | 09 | Beta–236217 | AMS | sediment | 1,840±60 | -23.7 | 1,860±40 | 1,795±65 | 1,880–1,710 |
| | 07 | Beta–263216 | RAD | sediment | 2,300±60 | -24.5 | 2,310±60 | 2,335±60 | 2,460–2,160 |
| | 05 | Beta–160264 | RAD | sediment | 2,760±60 | -25.0 | 2,760±60 | 2,850±70 | 2,980–2,760 |
| Qt2 | 10 | Beta–245012 | AMS | sediment | 3,860±40 | -24.7 | 3,860±40 | 4,295±105 | 4,420–4,150 |
| | SB | Beta–261044 | AMS | buried soil | 4,150±40 | -20.6 | 4,220±40 | 4,785±55 | 4,850–4,640 |
| | 10 | Beta–245013 | AMS | sediment[9] | 3,910±40 | -22.4 | 3,950±40 | 4,420±10 | 4,520–4,290 |
| | 06 | WW–6085 | AMS | sediment | – | -25.0 | 6,415±40 | 7,350±70 | 7,420–7,260 |
| | 16 | Beta–257948 | AMS | sediment | 6,760±40 | -24.5 | 6,770±40 | 7,620±40 | 7,680–7,570 |
| | ET | Beta–237008 | RAD | sediment | 7,200±60 | -24.0 | 7,210±60 | 8,005±35 | 8,170–7,940 |
| | 17 | Beta–261246 | RAD | sediment | 7,570±70 | -24.8 | 7,580±70 | 8,385±35 | 8,520–8,220 |
| | DC | Beta-314103 | AMS | pollen | 7,640±40 | -22.6 | 7.680±40 | 8480±60 | 8,550–8400 |
| | 17 | Beta–270391 | AMS | sediment | 7,900±50 | -25.8 | 7,890±50 | 8,680±80 | 8,980–8,580 |
| | 03 | Beta–158352 | RAD | peaty sed. | 8,120±60 | -25.6 | 8,110±60 | 9,050±50 | 9,240–8,980 |
| | SB | Beta–261247 | AMS | sediment | 8,210±50 | -26.9 | 8,230±50 | 9,195±55 | 9,400–9,020 |
| | 16 | Beta–257947 | RAD | sediment | 8,480±50 | -26.1 | 8,460±50 | 9,490±30 | 9,540–9,420 |

[1]See figs. 6, 7, 12, and 17 for localities.

[2]Beta, Beta Analytic Inc.; WW, U.S. Geological Survey; A and AA, University of Arizona.

[3]Conventional $^{14}C$ age indicates (1) the age was calculated using a $^{14}C$ half-life of 5,568 years; (2) $\delta^{13}C$ was determined and used to correct for isotopic fractionation; and (3) AD 1950 is the base (zero) year.

[4]Calibrations were made using INTCAL98 and INTCAL04.

[5]Low temperature combustion.

[6] $^{13}C/^{12}C$ ratio is estimated.

[7]Locality DA is 1.3 kilometers south of San Luis Lake. Locality DC is 8.5 kilometers south of San Luis Lake

[8]Locality BP is on the north side of a large playa about 4 kilometers south of San Luis Lake.

[9]Organic-rich mud (clayey silty sand).

[10]Charcoal fragments and sediment heavily coated by charcoal ash.

**Table 2.** Infrared stimulated luminescence (IRSL )and optically stimulated luminescence (OSL) data, Great Sand Dunes area, Colorado.

[Ages were determined in the U.S. Geological Survey laboratory, Denver, Colo., Shannon A. Mahan, Director. %, percent; K, potassium; U, uranium; Th, thorium; ppm, parts per million; yr, year; Gy, dose; Gy/ka, dose per thousand years; –, no data]

| Locality | Method | % Water content[1] | K (%)[2] | U (ppm)[2] | Th (ppm)[2] | Cosmic dose (Gy/ka)[3] | Total Dose rate (Gy/ka)[3] | Equivalent dose (Gy) | n[4] | Age (yr)[5] |
|---|---|---|---|---|---|---|---|---|---|---|
| DE[6] | OSL | 8 (42) | 3.36±0.02 | 3.04±0.13 | 10.4±0.27 | 0.29±0.03 | 4.26±0.07 | 16.1±1.28 | 10 (13) | 3,780±610 |
| | IRSL | | | | | | 5.78±0.09[7] | 18.4±2.32[7] | – | 3,185±830[7] |
| TB | OSL | 1 (26) | 3.26±0.03 | 3.07±0.11 | 11.3±0.26 | 0.24±0.02 | 3.71±0.07 | 10.8±0.39 | 20 (48) | 2,920±230 |
| | IRSL | | | | | | 6.15±0.09[7] | 23.2±1.04[7] | – | 3,770±360[7] |
| BB | OSL | 4 (25) | 3.37±0.05 | 3.18±0.17 | 11.6±0.43 | 0.28±0.02 | 4.57±0.11 | 19.1±0.76 | – | 4,170±500 |
| TP | OSL | 2 (22) | 3.42±0.02 | 3.52±0.12 | 12.1±0.28 | 0.28±0.02 | 4.72±0.08 | 16.9±1.01 | – | 3,640±270 |

[1]Field moisture, with figures in parentheses indicating the complete sample saturation percent. Ages calculated using 20 percent of full moisture saturation values.

[2]Analyses obtained using laboratory gamma spectrometry (low resolution sodium iodide [NaI] detector).

[3]Cosmic doses and attenuation with depth were calculated using the methods of Prescott and Hutton (1994). See text for details.

[4]Number (n) of replicated equivalent dose ($D_e$) estimates used to calculate the mean. Figures in parentheses indicate total number of measurements made including failed runs with unusable data.

[5]Dose rate and single-aliquot regenerative-dose (SAR) age for fine-grained 250–180 or 180–90 micrometers (µm) quartz sand. Linear + exponential fit used on age, errors to 1 sigma (σ).

[6]Locality DE is approximately 1.4 kilometers south of San Luis Lake.

[7]Dose rate and multiple-aliquot additive-dose (MAAD) feldspar age from fine-grains of 4 to 11 µm. Exponential fit used for equivalent dose. Errors 1 sigma. Fade tests indicate 5 percent–7.5 percent correction.

## References Cited


Andrew, R.L., Kane, N.C., Baute, G.J., Grassa, C.J. and Rieseberg, L.H., 2013, Recent nonhybrid origin of sunflower ecotypes in a novel habitat: Molecular Ecology, v. 22, is. 3, 799–813.

Andrews, Sarah, 1981, Sedimentology of Great Sand Dunes, Colorado: Society of Economic Paleontologists and Mineralogists Special Publication 31, p. 279–291.

Brister, B.S., 1990, Tertiary sedimentation and tectonics: San Juan sag-San Luis Basin region, Colorado and New Mexico: New Mexico Institute of Mining and Technology, Socorro, Ph.D. dissertation, 267 p.

Brister, B.S., and Gries, R.R., 1994, Tertiary stratigraphy and tectonic development of the Alamosa basin (northern San Luis basin), Rio Grande rift, south-central Colorado, *in* Keller, G.R. and Cather, S.M., eds., Basins of the Rio Grande rift—Structure, stratigraphy, and tectonic setting: Boulder, Colo., Geological Society of America Special Paper 291, p. 39–58.

Bruce, R.M., and Johnson, B.R., 1991, Reconnaissance geologic map of parts of the Zapata Ranch and Mosca Pass quadrangles, Alamosa and Huerfano Counties, Colorado: U.S. Geological Survey Miscellaneous Field Studies Map MF–2168, scale, 1:24,000. [Available at http://ngmdb.usgs.gov/Prodesc/proddesc_5797.htm.]

Burford, A.E., 1960, Geology of the Medano Peak area, Sangre de Cristo Mountains, Colorado: Ann Arbor, University of Michigan, Ph.D. dissertation, 201 p.

Carrara, P.E., and Andrews, J.T., 1975, Holocene glacial/periglacial record—Northern San Juan Mountains, southwestern Colorado: Zeitschrift fûr Gletscherkunde und Glazialgeologie, v. 11, p. 155–174.

Chapin, C.E., 1971, The Rio Grande rift, Part 1—Modifications and additions: New Mexico Geological Society, 22nd Field Conference Guidebook, p. 191–202.

Chapin, C.E., and Cather, S.M., 1994, Tectonic setting of the axial basins of the northern and central Rio Grande rift, *in* G.R Keller, and S.M. Cather, eds., Basins of the Rio Grande rift—Structure, stratigraphy, and tectonic setting: Boulder, Colo., Geological Society of America Special Paper 291, p. 5–25.

Cohen, K.M., Finney, S.C., Gibbard, P.L., and Fan, J. -X., 2015, The ICS International Chronostratigraphic Chart: Episodes, v. 36, p. 199–204. [Also available at http://www.stratigraphy.org/ICSchart/ChronostratChart2015-01.pdf.]

De Lanois, J.L., 1993, Climatic change during the late Holocene from a south central Colorado lake: Tucson, University of Arizona, Master's thesis, 50 p.

Emery, P.A., Boettcher, A.J., Snipes, R.J., and McIntyre, H.J., Jr., 1971, Hydrology of the San Luis Valley, south-central Colorado: U.S. Geological Survey Hydrologic Investigations Atlas HA–381, scale 1:250,000. [Also available at http://pubs.er.usgs.gov/publication/ha381.]

Endlich, F.M., 1875, San Luis Valley: U.S. Geological and Geographical Survey of the Territories, Ninth Annual Report, Pt. I—Geology, chap. II, p. 140–149.

Endlich, F.M., 1877, Geological report on the Southeastern District, *in* Hayden, F.V., Report of progress of the exploration for the year 1875: U.S. Geological and Geographical Survey of the Territories, Ninth Annual Report, p. 103–236.

Folk, R.L., and Ward, W.C., 1957, Brazos River bar—A study in the significance of grain size parameters: Journal of Sedimentary Petrology, v. 27, p. 3–26.

Forman, S.L., Spaeth, M., Marìn, Liliana, Pierson, J.M., Gómez, Jeaneth, Bunch, Fred, and Valdez, Andrew, 2006, Episodic late Holocene dune movements on the sand-sheet area, Great Sand Dunes National Park and Preserve, San Luis Valley, Colorado, USA: Geomorphology, v. 66, p. 97–108.

Hayden, F.V., 1873, From Fort Garland to South Park: United States Geological Survey of the Territories, embracing Colorado and New Mexico: U. S. Geological Survey, Third Annual Report, chap. IX, p. 175–181.

Hudson, M.R., and Grauch, V.J.S., 2013, Introduction, *in* Hudson, M.R., and Grauch, V.J.S., eds., New perspectives on Rio Grande Rift Basins—From Tectonics to Groundwater: Geological Society of America Special Paper 494, p. 1–20

Huntley, D.L., 1976, Ground water recharge to the aquifers of northern San Luis Valley, Colorado—A remote sensing investigation: Colorado School of Mines Remote Sensing Report 76–3, 313 p.

Hutchison, D.M., 1968, Provenance of sand in the Great Sand Dunes National Monument, Colorado: Morgantown, West Virginia University, Ph.D. dissertation, 132 p.

Ingram, R.L., 1989, Grain-size scales, *in* Dutro, J.T., Jr., Dietrich, R.V., and Foose, R.M., compilers, AGI data sheets—For geology in the field, laboratory, and office, (3d ed.): Alexandria, Va., American Geological Institute, sheet 29.1.

Jodry, M.A., 1987, Stewart's Cattle Guard site—A Folsom site in southern Colorado: Austin, University of Texas, M.A. thesis, 247 p.

Jodry, M.A., 1999, Paleoindian stage, chap. 6 *of* Colorado prehistory—A context for the Rio Grande basin: Denver, Colo., Council of Professional Archaeologists, p. 45–114.

Jodry, M.A., and Stanford, D.J., 1992, Stewart's Cattle Guard site—An analysis of bison remains in a Folsom kill-butchery campsite, *in* Stanford, D.J., and Day, J.S., eds., Ice age hunters of the Rockies: Niwot, Colo., Denver Museum of Natural History and University of Colorado Press, p. 101–168.

Johnson, B.R., Bruce, R.M., and Lindsey, D.A., 1989, Reconnaissance geologic map of the Medano Pass quadrangle and part of the Liberty quadrangle, Alamosa, Huerfano, and Saguache Counties, Colorado: U.S. Geological Survey Miscellaneous Field Studies Map MF–2089, scale, 1:24,000. [Also available at http://ngmdb.usgs.gov/Prodesc/proddesc_5693.htm.]

Keller, G.R., and Cather, S.M., 1994, Introduction, *in* G.R Keller, and S.M. Cather, eds., Basins of the Rio Grande rift—Structure, stratigraphy, and tectonic setting: Boulder, Colo., Geological Society of America Special Paper 291, p. 1–3.

Kluth, C.F., and Coney, P.J., 1981, Plate tectonics of the ancestral Rocky Mountains: Geology, v. 9, p. 10–15.

Kluth, C.F., and Schaftenaar, C.H., 1994, Depth and geometry of the northern Rio Grande rift in the San Luis basin, south-central Colorado, *in* Keller, G.R. and Cather, S.M., eds., Basins of the Rio Grande rift—Structure, stratigraphy, and tectonic setting: Boulder, Colo., Geological Society of America Special Paper 291, p. 27–37.

Lipman, P.W., 2007, Incremental assembly and prolonged consolidation of Cordilleran magma chambers—Evidence from the Southern Rocky Mountain volcanic field: Geosphere, v. 3, p. 42–70.

Lipman, P.W., and Mehnert, H.H., 1975, Late Cenozoic basaltic volcanism and development of the Rio Grande depression in the southern Rocky Mountains, *in* Curtis, B.F., ed., Cenozoic history of the southern Rocky Mountains: Geological Society of America Memoir 144, p. 119–154.

Machette, M.N., 2004, New evidence for ancient Lake Alamosa in the San Luis basin of Colorado [abs.], *in* Denver Annual Meeting, Nov. 7–10, 2004: Denver, Colo., Geological Society of America Abstracts with Programs v. 36, no. 5, p. 530.

Machette, M.N., and Marchetti, D.W., 2006, Pliocene to middle Pleistocene evolution of the upper Rio Grande, northern New Mexico and southern Colorado [abs.], *in* Rocky Mountain Section, 58th annual meeting May 17–19, 2006: Gunnison, Colo., Geological Society of America Abstracts with Program v. 38, no. 6, p. 36.

Machette, M.N., Marchetti, D.W., and Thompson, R.A., 2007, Ancient Lake Alamosa and the Pliocene to middle Pleistocene evolution of the Rio Grande, chap. G, *of* Machette, M.N., Coates, M-M., and Johnson, M.J., eds., 2007 Rocky Mountain section friends of the Pleistocene field trip—Quaternary geology of the San Luis Basin of Colorado and New Mexico, September 7–9, 2007: U.S. Geological Survey Open-File Report 2007–1193, p. 157–167. [Also available at http://pubs.usgs.gov/of/2007/1193/.]

Madole, R.F., 2001, Preliminary report on the Quaternary geology and geomorphology of the Indian Spring area, Alamosa and Saguache Counties, Colorado: Boulder, Colo, Madole and Associates, 35 p. [Document prepared for and on file with the Great Sand Dunes National Park and Preserve].

Madole, R.F., 2005, Quaternary geology and geomorphology, chap 4 *of* Woodlands to wetlands—Human occupation and use of the Great Sand Dunes eolian system: Colorado State Historic Fund Project 2001–02–069, p. 45–61. [Also available from the Office of the State Archeologist, the Colorado Historical Society]

Madole, R.F., and Mahan, S.A, 2007, Overview of Quaternary stratigraphy in the Great Sand Dunes area, chap. A, Stop A6.1, *of* Machette, M.N., Coates, M-M., and Johnson, M.J. eds., Quaternary geology of the San Luis Basin, southern Colorado and Northern New Mexico— 2007 Rocky Mountain Section Friends of the Pleistocene Field Trip—Quaternary geology of the San Luis Basin of Colorado and New Mexico, September 7–9, 2007: U.S. Geological Survey Open-File Report 2007–1193, p. 31–34. [Also available at http://pubs.usgs.gov/of/2007/1193/.]

Madole, R.F., Mahan, S.A. Romig, J.H., and Havens, J.C., 2013, Constraints on the age of the Great Sand Dunes, Colorado, from subsurface stratigraphy and OSL ages: Quaternary Research, v. 80, p. 435–446, doi:10.1016/j.yqres.2013.09.009.

Madole, R.F., Romig, J.H., Aleinikoff, J.N., VanSistine, D.P., and Yacob, E.Y., 2008, On the origin and age of the Great Sand Dunes, Colorado: Geomorphology, v. 99, p. 99–119, doi:10.1016/j.geomorph.2007.10.006.

Mann, M.E., 2002, Little Ice Age, The Earth system—Physical and chemical dimensions of global environmental change, v. I, MacCracken, M.C. and Perry, J.S., and Munn, Ted, eds., *in* Encyclopedia of global environmental change: Chichester, UK, John Wiley & Sons, Ltd, p. 504–509.

Marín, Liliana, Forman, S.L., Valdez, Andrew, and Bunch, Fred, 2005, Twentieth century dune migration at the Great Sand Dunes National Park and Preserve, Colorado, relation to drought variability: Geomorphology, v. 70, p. 163–183, doi:10.1016/j.geomorph.2005.04.014.

Mast, M.A., 2007, Assessment of historical water-quality data for National Park units in the Rocky Mountain network, Colorado and Montana, through 2004: U.S. Geological Survey Scientific Investigations Report 2007–5147, 80 p. [Also available at http://pubs.usgs.gov/sir/2007/5147/.]

McCalpin, J.P., 1982, Quaternary geology and neotectonics of the west flank of the northern Sangre de Cristo Mountains, south-central Colorado: Colorado School of Mines Quarterly, v. 77, no. 3, 97 p.

North American Commission on Stratigraphic Nomenclature, 1983, North American stratigraphic code: American Association of Petroleum Geologists Bulletin, v. 67, p. 841-875. North American Commission on Stratigraphic Nomenclature. [Also available at http://www.nacstrat.org/.]

Pannell, J.P., Yenter, J.M., Woodyard, S.O., and Mayhugh, R.E., 1973, Soil survey of Alamosa area, Colorado: U.S. Department of Agriculture, Soil Conservation Service, in cooperation with Colorado Agricultural Experiment Station, 122 p.

Pineda, P.M., and Kondratieff, B.C., 2003, Natural History of the Colorado Great Sand Dunes Tiger Beetle, *Cicindela theatina* Rotger: Transactions of the American Entomological Society v. 129, .no. 3/4, p. 333–360.

Powell, W.J., 1958, Groundwater resources of the San Luis Valley, Colorado: U.S. Geological Survey Water-Supply Paper 1379, 284 p. [Also available at http://pubs.er.usgs.gov/publication/wsp1379.]

Prescott, J.R., and Hutton, J.T., 1994, Cosmic ray contributions to dose rates for luminescence and ESR dating: large depths and long-term time variations: Radiation Measurements, v. 23, p. 497–500.

Rupert, M.G., and Plummer, L.N., 2004, Groundwater flow direction, water quality, recharge sources, and age, Great Sand Dunes National Monument, south-central Colorado, 2000–2001: U.S. Geological Survey Scientific Investigations Report 2004–5027, 28 p. [Also available at http://pubs.usgs.gov/sir/2004/5027/.]

Sanchez, Guadelupe, Holliday, V.T., Gaines, E.P., Arroyo-Cabrales, Joaquin, Martínez-Tagüeña, Natalia, Kowler, Andrew, Lange, Todd, Hodgins, G.W.L., Mentzer, S.M., and Sanchez-Morales, Ismael, 2014, Human (Clovis)–gomphothere (*Cuvieronius* sp.) association ~13,390 calibrated yr BP in Sonora, Mexico: Proceedings of the National Academy of Sciences, v. 111, p. 10972–10977. [Also available at http://www.pnas.org/content/111/30/10972.full.]

Scott, M.L., Gregory, C. L., and Auble, G.T., 2000, Channel incision and patterns of cottonwood stress and mortality along the Mojave River, California: Journal of Arid Environments, v. 44, p. 399–414.

Scott, M.L., Shafroth, P.B., and Auble, G.T., 1999, Responses of riparian cottonwoods to alluvial water table decline: Environmental Management, v. 23, p. 347–358.

Siebenthal, C.E., 1910, Geology and water resources of the San Luis Valley, Colorado: U.S. Geological Survey Water-Supply Paper 240, 128 p., 1 pl. [Also available at https://pubs.er.usgs.gov/publication/wsp240.]

Tweto, Ogden, 1979, The Rio Grande rift system in Colorado, *in* Riecker, R.E., ed., Rio Grande Rift—Tectonics and Magmatism: Washington, D.C., American Geophysical Union, p. 33–56, doi: 10.1029/SP014p0033.

Wallace, A.R., 2004, Evolution of the southeastern San Luis basin margin and the Culebra embayment, Rio Grande rift, southern Colorado, *in* Brister, B.S, Bauer, P.W., Reed, A.S., and Lueth, V.W., eds., Geology of the Taos region, fifty-fifth field conference, September 22–25, 2004: New Mexico Geological Society Guidebook, 55th Field Conference, p. 181–192.

Walton-Day, Katherine, 1996, Colorado wetland resources, *in* Fretwell, J.D., Williams, J.S., and Redman, P.J., compilers, National water summary on wetland resources: U.S. Geological Survey Water-Supply Paper 2425, p. 135–140.

Wiegand, J.P., 1977, Dune morphology and sedimentology at Great Sand Dunes National Monument: Fort Collins, Colorado State University, M.S. thesis, 165 p.

Wurster, F.C., Cooper, D.J., and Sanford, W.E., 2003, Stream/aquifer interactions at Great Sand Dunes National Monument, Colorado—Influences on interdunal wetland disappearance: Journal of Hydrology, v. 271, p. 77–100.

Yenter, J.M., 1984, Soil survey of Saguache County area, Colorado: U.S. Department of Agriculture, Soil Conservation Service, 203 p.

# Glossary

Some terms in this glossary have multiple meanings or are defined differently by different scientific disciplines. The definitions listed here are for this publication, and are not necessarily all-inclusive. Several definitions have been adapted from the Glossary of Geology (Gary and others, 1972; Bates and Jackson, 1995). Glossary modified from Madole and others, 1998 and 2005.

## A

**A horizon** A soil layer at the ground surface, or underlying an O horizon (organic litter), that is characterized by humified organic matter mixed with the mineral fraction of soil.

**AB horizon** A transitional horizon between A and B soil horizons. It has properties of both horizons, but those of the A horizon are dominant.

**AC horizon** A transitional horizon between A and C soil horizons. It has properties of both horizons, but those of the A horizon are dominant.

**aggradation** A term meaning the raising of ground level. It is commonly used to describe streams that build up the levels of their channels or flood plains because they receive (accumulate) more sediment than they can transport.

**alluvium** Sediment deposited by streams or by unconfined runoff, such as sheet flow.

**alluvial terrace** An abandoned flood-plain surface underlain by alluvium that was deposited by an aggrading stream. The surface was abandoned when hydraulic variables changed and caused the stream to degrade (incise) its channel.

**AMS age** A radiocarbon age based on the quantitative determination of the amount of $^{14}C$ remaining in a sample of organic material using an accelerator mass spectrometer.

**aquifer** Any rock unit or surficial deposit that is partly or fully saturated with groundwater and has sufficient permeability and porosity to yield groundwater to a well or spring at a rate sufficient to meet a specific purpose.

**aridisol** Soil that forms in arid environments and has a low content of organic-matter content and a high content of salts. Thus, Aridisols tend to be light-colored and sparsely vegetated by drought- or salt-tolerant plants.

**avulsion** The term as applied to fluvial processes, refers to a rapid change in the course or position of a stream channel. It occurs most commonly during floods.

## B

**base level** The level below which a stream cannot degrade its bed. Sea level is the ultimate base level, but few streams reach this level. Most streams are controlled by local base levels, which might be either temporary or long-lasting.

**B horizon** A soil layer that underlies an O, A, or E horizon that is dominated by obliteration of all or much of the original rock structure, including stratification in unconsolidated sediment, and development of various properties that distinguish several kinds of B horizons (Soil Survey Division Staff, 1993). Only those kinds of B horizons referred to in the pamphlet are defined in this glossary. For definitions of other kinds of B horizons see Soil Survey Division Staff (1993) and Birkeland (1999).

**blowout dune** A circular or bowl-shaped dune that is primarily a feature of deflation. Its form is apparently controlled more by partial stabilization by vegetation and (or) moisture, than by wind strength or direction (after McKee, 1979).

**Bt horizon** A soil layer characterized by the accumulation of silicate clay that either formed in place or was translocated downward within or into the horizon. A Bt horizon has more clay than the deposit in which it formed (parent material).

## C

**C horizon** A soil layer in various stages of weathering, excluding bedrock, that lacks properties of A and B horizons (after Birkeland, 1999).

**$^{14}$C yr BP** An abbreviation for radiocarbon years before present. The base (zero) year for the present is AD 1950, or, in other words, before present is defined as before AD 1950 (see definition of conventional $^{14}$C age).

**cal yr BP** An abbreviation for calendar years before the present. Calendar years are determined by calibrating (with tree-rings or corals, for example) a radiocarbon age to correct for the fluctuations in the production of atmospheric radiocarbon that occur over time. As with the abbreviation $^{14}$C yr BP, before present is defined as before AD 1950.

**clast** A rock fragment derived from the disintegration of a larger rock mass.

**clast-supported** Deposits composed of clasts and matrix (particles smaller than 2 mm), in which clasts are dominant and in point contact.

**clay** A particle size that in the Wentworth scale (used by geologists) is smaller than 1/256 millimeter or 4 microns and in the USDA (U.S. Department of Agriculture) scale (used by soil scientists) is smaller than 2 microns. This term also is used for a complex group of layered silicate minerals formed chiefly by the alteration of primary silicate minerals. Clay minerals are characterized by small particle size (colloidal) and the capacity to adsorb significant amounts of water and ions on their surfaces.

**closed basin** An enclosed area having no outflow of surface water; water leaves the enclosure only by infiltration and evaporation.

**Clovis** A culture identified by the association of several distinct tool types, including well-made, fluted spear points, used in many parts of North America between about 12,000 and 10,600 $^{14}$C yr BP (age range from Dennis Stanford, oral commun., 2005).

**coarse sand** A geologic term (Wentworth scale) for sand particles having a diameter in the range of 0.5–1.0 millimeter (500–1,000 microns).

**cobble** A clast that is at least somewhat rounded having a diameter between 64 mm and 256 mm (2.5-10 inches).

**complex dune** Two or more dunes of different types that overlap or are superimposed on one another (after McKee, 1979).

**compound dune** Two or more dunes of the same type that overlap or are superimposed on one another (after McKee, 1979).

**confined aquifer** A material that stores and transmits water and is separated from the atmosphere by material that water cannot pass through (that is, impermeable material).

**conglomerate** A sedimentary rock consisting of subangular to rounded clasts in a matrix of mostly sand and silt; the lithified equivalent of gravel.

**contact** Boundary between two different types or ages of rocks or surficial deposits.

**conventional $^{14}$C age** A term that implies that the age determination involved all of the following: (1) the use of the 5,568-yr half-life of $^{14}$C, (2) assumed constancy of atmospheric $^{14}$C in the past, (3) the use of oxalic acid as a standard, (4) the $\delta^{13}$C value was determined and used to correct for isotopic fractionation, and (5) AD 1950 is the base (zero) year (after Stuiver and Polach, 1977). The term is not a synonym for either radiometric $^{14}$C age or AMS (accelerator mass spectrometer) $^{14}$C age.

**Cox horizon** The upper part of a C horizon (soil parent material) that is more oxidized than the parent material lower in the profile, but does not meet the requirements of a B horizon.

**crystalline rock** A rock consisting entirely of intergrown crystals or fragments of crystals. Term is most commonly used in referring to bodies of igneous and metamorphic rocks.

## D

**deflation** The sorting, lifting, or removal of particles by wind.

**$\delta^{13}C$ value** The ratio between the $^{13}C/^{12}C$ of the radiocarbon sample and the $^{13}C/^{12}C$ of the PDB standard (a fossil belemnite from the Peedee Formation in South Carolina) expressed as per mil (‰). This value indicates the degree to which the isotopic composition of the sample varies from the PDB standard. It is used to adjust $^{14}C$ ages to correct for isotopic fractionation.

**degradation** The lowering of a bottomland surface through the process of erosion; conceptually it is the opposite of the vertical component of aggradation and is most frequently applied to sediment removed from a channel bed or other low-lying parts of a stream channel (Osterkamp, 2008).

**detrital** An adjective pertaining to detritus, which is a collective term for loose rock or mineral material that was eroded from older rocks and transported from its place of origin.

**distal** With respect to landforms and deposits, pertains to the part away from or more distant from the source.

**drought** A relative term that is defined in different ways by meteorologists, hydrologists, agronomists, and others. Common to most definitions of drought is the notion that conditions are drier than average over a specific area for longer than is normal or expected (see Beaudoin, 2002, for a useful discussion of the characterization of drought).

**dune field** Informal term for localities where dunes are extensive, but cover small areas compared to sand seas whose volumes are large and measured in cubic kilometers (after Lancaster, 1995).

## E

**end moraine** A ridge or embankment of drift (sediment deposited from glacier ice) that accumulated along the margin of a glacier.

**eolian** Pertains to the wind and materials moved, shaped, or deposited by wind.

**extrusive rock** An igneous rock formed from molten material that flowed on or was ejected onto the surface of the earth.

## F

**feldspar** The most abundant group of minerals in the Earth's crust. All members are closely related in form and physical properties, but fall into two subgroups, orthoclase and plagioclase.

**fine sand** A geologic term (Wentworth scale) for sand particles having a diameter in the range of 0.125–0.25 millimeter (125–250 micrometers).

**flood plain** Flat area adjacent to a stream channel that was constructed by the stream in the present climate and that is flooded frequently (after Dunne and Leopold, 1978).

**fluvial** Pertains to stream processes, deposits, and landforms.

**Folsom** A culture that overlapped and followed the Clovis culture but was less widespread. It existed between about 10,900 and 10,400 $^{14}C$ yr BP (Dennis Stanford, oral commun., 2005) and is identified by the association of several tool types, including distinctive, fluted spear points.

## G

**geomorphology** The scientific study of landscapes and the processes that shape them (Bloom, 1998).

**glaciofluvial** Pertains to the processes, deposits, and landforms produced by meltwater streams flowing from glacier ice.

**gneissic** Pertains to the texture or structure of gneiss, a foliated (banded) metamorphic rock.

**granitic** Pertains to light-colored, coarse-grained, intrusive igneous rock composed chiefly of feldspar and quartz.

**gravel** A deposit that consists chiefly of abundant subangular to rounded clasts larger than 2 millimeters, but also containing variable amounts of matrix (material smaller than 2 millimeters).

**groundwater** A term for water that is below the water table.

## H

**$^{3}H$** An isotope of hydrogen having an atomic weight of three, also known as tritium.

**hydrogeology** The study of groundwater with emphasis on its chemistry, mode of migration, and relation to the geologic environment (Davis and DeWiest, 1966).

## I

**igneous rock** A rock that solidified from molten material.

**infrared stimulated luminescence (IRSL)** A method of optically stimulated luminescence dating that uses photons of infrared wavelengths (1.4 eV excitation) to stimulate luminescence from potassium feldspars (after Aitken, 1998). See definition of luminescence dating.

**intrusive rock** An igneous rock formed from the intrusion or emplacement of molten rock within the crust of the earth.

**isotope** Any of two or more species of atoms of the same chemical element; that is, they have the same atomic number and place in the periodic table and nearly identical chemical behavior, but have a different atomic mass and different physical properties.

## K

**ka** An abbreviation for kilo-annum (1,000 years).

## L

**lacustrine** A term that refers to anything produced by, formed in, deposited in, or living in a lake or lakes.

**leeside** The side away from the wind, or downwind; also called leeward.

**loam** Soil material that contains 7 to 27 percent clay, 28 to 50 percent silt, and less than 50 percent sand.

**lidar** An acronym for light detection and ranging, which is an imaging technique that generates a surface using lasers to measure distances.

**lithologic** A term that pertains to the description of rocks and sediment and their properties or characteristics.

**loess** A surficial deposit of windblown origin that consists chiefly of silt (dust), which where unweathered, is typically pale brown, homogeneous, and nonstratified.

**luminescence dating** A general term for methods that determine the time elapsed since buried mineral grains were last exposed to sunlight or intense heat. The methods utilize luminescence from the release of electrons trapped in defects in quartz or feldspar. The electrons were trapped after being displaced by radioactivity in the surrounding sediment. Luminescence is stimulated by heat (TL, also known as thermoluminescence) or photon bombardment (OSL, also known as optically stimulated luminescence). These dating methods require that the electron traps be emptied by exposure to light or heat prior to burial.

**lunette dune** A broad, low concentric (convex downwind) dune bordering the downwind sides of playas or playa lakes. These dunes are composed of sand that was derived from the lake floor when the lake basin was dry or nearly dry.

## M

**Ma** An abbreviation for Mega-annum (1,000,000 years).

**massive** As applied to stratified rocks and sediment, massive denotes thick, homogeneous layers in which stratification or other internal structures, such as minor joints or laminations, are not present or are obscure.

**mass-wasting** Processes by which earth materials are moved primarily by gravity; differs from other modes of material transport in that the material moves as a mass rather than as individual fragments borne along by a transporting medium such as wind or flowing water.

**matrix** The material in gravel or gravelly deposits that is smaller than 2 millimeters.

**matrix-supported** Pertains to deposits composed of matrix and clasts, in which clasts comprise less than half of the deposit and are separated and surrounded by matrix.

**medium sand** A geologic term (Wentworth scale) for sand particles having a diameter in the range of 0.25–0.5 millimeter (250–500 microns).

**metamorphic rock** A rock transformed from pre-existing rock by mineralogical, chemical, and structural changes, essentially in the solid state and below the zone of surface weathering, induced by changes in temperature, pressure, and chemically active fluids.

**mollisol** Thick, dark-colored soil typically associated with areas that support abundant tall grasses, as opposed to the short grasses that are dominant in semi-arid regions.

## N

**numerical age** The age of a material or feature calculated and expressed in units of time, usually years.

## O

**optically stimulated luminescence (OSL)** An umbrella term for luminescence dating that uses photons to stimulate luminescence (after Aitkin, 1998). The term implies a signal can be related directly to the trapped-charge population via stimulation with light. See also the definition of luminescence dating.

## P

**palustrine** A term pertaining to material growing in or deposited in a marsh or marsh-like environment (Gary and others, 1972).

**parabolic dune** A sand dune that approximates a parabola in plan view. The convex front of the parabola faces downwind and the arms trail upwind toward the open end of the parabola.

**particle size** The diameter of a particle measured along the intermediate axis generally expressed in millimeters or phi units.

**particle-size distribution** The distribution of the various size-fractions of sand, silt, and clay defined by the Wentworth (1922) that are present in sediment.

**pebble** A rock fragment that is at least somewhat rounded having a diameter between 2 and 64 millimeters (0.17 and 2.5 inches).

**playa** A dry, vegetation-free, flat area at the lowest part of an undrained desert basin. It is a location where temporary lakes can form during wet periods.

**piedmont slope** Relatively gently sloping surface between a mountain front and an adjoining basin or valley floor that typically is underlain by sediment of both alluvial and mass-wasting origin derived primarily from the mountains.

## Q

**quartz** Crystalline silica ($SiO_2$); next to feldspar, it is the most common rock-forming mineral.

**Quaternary geology** Commonly used as a synonym for surficial geology; term refers to a broad range of geologic topics (materials, processes, history, and so forth) that formed or occurred during Quaternary time. The Quaternary Period includes the Pleistocene Epoch (2.58 Ma to 11.7 ka) and the Holocene Epoch (11.7 ka to the present).

## R

**radiocarbon age** An age expressed in years and calculated from the quantitative determination of the amount of $^{14}C$ remaining in a sample of organic material (after Gary and others, 1972).

**radiometric age** An age that is determined from nuclear decay and is expressed in years. Age estimates in years are derived from equations that relate the ratio of decay products to the parent products in the sample.

## S

**sand** Geologic term (Wentworth scale) for particles having a diameter in the range of 4 to 0.63 millimeters.

**sedimentary rock** A rock formed of sediment, organic matter, or material precipitated from solution that was deposited or accumulated on the earth's surface.

**shale** A thinly bedded sedimentary rock formed from mud (mainly silt- and clay-size particles).

**sheetwash alluvium** Sediment deposited by unconfined runoff or sheet flow, also called overland flow.

**silt** Geologic term (Wentworth scale) for particles having a diameter in the range of 1/16 to 1/256 millimeter (62–4 microns), which is smaller than very fine sand and larger than clay.

**simple dune** Single or individual dunes of any of the basic types that are not in contact with other dunes (see definitions for compound and complex dunes).

**slack-water deposit** A term for fine-textured sediment that settles from suspension in a body of water because the velocity of stream flow has slowed to or reached zero. In terms of sediment size and stratification, slack-water deposits resemble some lacustrine deposits.

**slip face** The steeply sloping surface on the downwind side of a dune, standing at or near the angle of repose of loose sand, and advancing downwind by a succession of slides wherever the angle is exceeded (Gary and others, 1972).

**soil horizon** A layer of soil approximately parallel to the ground or soil surface having properties produced by soil-forming processes, and some of the properties are not like those of the layers just above or beneath it (after Soil Survey Division Staff, 1993). Horizons may be distinguished from adjacent layers (horizons) by properties such as color, texture, structure, consistence, and the presence or absence of carbonates.

**soil profile** A vertical section of soil that includes all of its horizons and the parent material. Parent material is not soil, but is part of the soil profile.

**soil series** A group of soils having horizons that, except for the texture of the A or surface horizon, are similar in all profile characteristics and in arrangement in the soil profile.

**sorting** Processes by which particles of similar size, shape, or specific gravity are separated from dissimilar particles. Better sorting indicates a greater similarity among particles. Sorting is a measure of the range in particle sizes present and provides information about conditions of sediment transport and deposition.

**star dune** A dune type that has three or more sharp-crested ridges that radiate from a central peak. They form in areas where the wind blows from multiple directions, and they tend to remain in the same place for exceptionally long periods and to grow vertically to exceptional heights.

**stratigraphy** The definition, description, and interpretation of stratified rocks and sediment in terms of a variety of attributes including their properties, origin, age, and spatial distribution.

**stream piracy** The natural diversion of one stream into the channel of another stream that has greater erosional activity and flows at a lower level. Also referred to as stream capture or beheading.

**stream terrace** A two-dimensional surface or landform that is higher than the flood plain.

**surficial deposit** Unconsolidated to moderately consolidated sediment that was transported or translocated (as in mass-wasting) and deposited on other surficial deposits or bedrock.

**surficial geology** The study of the age, origin, and properties of generally loose, unconsolidated or moderately consolidated sediment that either formed in place or was transported and overlies bedrock. The term is synonymous with Quaternary geology.

## T

**terminal moraine** An end moraine formed at or near the point of farthest advance of a valley glacier.

**terrace deposit** A surficial deposit, usually alluvium, underlying a terrace.

**transverse dune** A barchanoid-type dune that forms long, commonly wavy, strongly asymmetric ridges oriented perpendicular to the direction of prevailing winds (after McKee, 1979). These dunes have a gentle windward slope and a steep leeward slope that is at or near the angle of repose (that is, the angle at which sliding may be initiated).

**two sigma (2σ)** Sigma (σ) is used in statistics to denote the standard deviation of the measured population. In this publication, the two-sigma (two standard deviations) limits of several conventional $^{14}C$ ages are listed in tables and discussed in the text. There is a 95 percent probability that a given $^{14}C$ age is between the two-sigma limits listed for it.

## U

**unconfined aquifer** Water-bearing material that has a water table and is connected to the atmosphere via pores.

**unconformity** A gap or interruption in stratigraphic succession.

**U-Pb age** A radiometric dating method that utilizes two decay chains, the uranium series $^{238}U$ to $^{206}Pb$, which has a half-life of 4.47 billion years, and the actinium series from $^{235}U$ to $^{207}Pb$, which has a half-life of 710 million years. Each decay chain involves a series of alpha- and beta-particle emissions.

## V

**very coarse sand** A geologic term (Wentworth scale) for sand particles having a diameter in the range of 1–2 millimeters.

**very fine sand** Geologic term (Wentworth scale) for sand particles having a diameter in the range of 0.0625–0.125 millimeters (62.5–125 microns).

**volcanic rock** A fine-grained crystalline or glassy (that is, noncrystalline) igneous rock resulting from volcanic action at or near the earth's surface.

## W

**water table** A theoretical surface that is approximated by the elevation of water surfaces in wells or borings that penetrate into the saturated zone; also defined as the upper surface of water-saturated material or the upper limit of ground-water saturation.

**weathering** A general term for several processes operating at or near the earth's surface that cause the physical disintegration and (or) chemical decomposition of rock and surficial materials.

**windward** Term for the side facing the wind or in the direction from which the wind is blowing.

## X

**x-ray diffraction (XRD)** A scientific technique involving the scattering of X-rays by the atoms of a crystal that is useful in obtaining and interpreting information about the molecular structure of the crystal.

## Z

**zircon** A silicate mineral ($ZrSiO_4$) that is a minor but common constituent of crystalline rocks, particularly igneous and metamorphic rocks, and also is common in sediment and sedimentary rocks derived from crystalline rocks.

## Glossary References

Aitken, M.J., 1998, An introduction to optical dating—The dating of Quaternary sediments by the use of photon-stimulated luminescence: Oxford, Oxford University Press, 267 p.

Bates, R.L., and Jackson, J.A., 1995, Glossary of geology, 3d ed.: Alexandria, Va., American Geological Institute, 805 p.

Birkeland, P.W., 1999, Soils and geomorphology 3d ed.: New York, Oxford University Press, 430 p.

Bloom, A.L., 1998, Geomorphology: A systematic analysis of late Cenozoic landforms, 3d ed.: Upper Saddle River, New Jersey, Prentice–Hall, Inc., 482 p.

Beaudoin, A.B., 2002, On the identification and characterization of drought and aridity in postglacial paleoenvironmental records from the northern Great Plains, *in* Wolfe, S.E. and Running, G.L. IV, eds., Drylands: Holocene climatic, geomorphic and cultural change on the Canadian prairies: Géographie physique et Quaternaire, v. 56, p. 229–246.

Davis, S.N., and DeWiest, R.J.M., 1966, Hydrogeology: New York, NY, John Wiley and Sons, Inc., 463 p.

Dunne, T., and Leopold, L.B., 1978, Water in environmental planning: San Francisco, W.H. Freeman and Company, 818 p.

Gary, Margaret, McAfee, Robert., Jr., and Wolf, C.L., eds., 1972, Glossary of geology, 1st ed.: Washington, D.C., American Geological Institute, 857 p.

Lancaster, N., 1995, Geomorphology of desert dunes: New York, NY, Routledge, 290 p.

McKee, E. D., 1979, Introduction to a study of global sand seas, *in* McKee, E.D., ed., A study of global sand seas: U.S. Geological Survey Professional Paper 1052, p. 1–19.

Madole, R.F., VanSistine, D. Paco, and Michael, J.A., 1998, Pleistocene glaciation in the upper Platte River drainage basin, Colorado: U.S. Geological Survey Geologic Investigations Series, I–2644.

Madole, R.F., VanSistine, D.P., and Michael, J.A., 2005, Distribution of Late Quaternary wind-deposited sand in eastern Colorado: U.S. Geological Survey Scientific Investigations Map 2875, scale 1:700,000, 49 p. pamphlet.

Osterkamp, W.R., 2008, Annotated definitions of selected geomorphic terms and related terms of hydrology, sedimentology, soil science and ecology: U.S. Geological Survey Open-File Report 2008–1217, 49 p.

Soil Survey Division Staff, 1993, Soil survey manual: U.S. Department of Agriculture Handbook no. 18, 437 p.

Stuiver, M., and Polach, H.A., 1977, Reporting of 14C data: Radiocarbon, v. 19, p. 355–363.

Wentworth, C.K., 1922, A scale of grade and class terms for clastic sediments: Journal of Geology, v. 30, p. 377–392.

# Photograph Credits

## Page

| | |
|---|---|
| **Cover 1** | **Star dunes with gold aspen**—*Courtesy of the National Park Service* |
| **Cover 2–i** | **Star dunes with gold aspen**—*Courtesy of the National Park Service* |
| **iii** | **Dune closeup**—*Courtesy of the National Park Service* |
| **iv** | **Autumn trees and dunes**—*Courtesy of the National Park Service* |
| **v** | **Aspen tree**—*PixelSquid object—TurboSquid, Inc.—Royality free license* |
| **ix** | **Snow on dunes**—*Courtesy of the National Park Service* |
| **x–1** | **Cleveland Peak with cottonwoods**—*Courtesy of the National Park Service* |
| **2–3** | **Dune closeup**—*Courtesy of the National Park Service* |
| **8–9** | **Sunset on dunes and Crestone Peak**—*Courtesy of the National Park Service, flickr, Patrick Myers* |
| **12** | **Creekbed**—*Photograph by Lisa Binder, USGS* |
| **20–21** | **Sand dune panoramic**—*Photograph by Footwarrior—Wikimedia Commons; Creative Commons Attribution, Share Alike 3.0* |
| **25** | **Sand dunes and vegetation**—*Courtesy of the National Park Service* |
| **35** | **Coyote**—*Photograph by Richard F. Madole, USGS* |
| **42–43** | **Prairie sunflowers, dunes, and Crestone Peak**—*Courtesy of the National Park Service, flickr, Patrick Myers* |
| **45** | **Hiker on top of dune**—*Courtesy of the National Park Service, flickr, Scott Hansen* |
| **57** | **Kangaroo rat**—*Courtesy of the National Park Service* |
| **58–Cover 3** | **Bison photographs**—*Photographs by Richard F. Madole, USGS* |

## Map

**A** **Star dune**—*Photograph by Bob Rozinski. Used with permission. © Wendy Shattil/Bob Rozinski www.dancingpelican.com*

**B** **Aerial view of dunes**—*Photograph courtesy of National Aeronautics and Space Administration (NASA)*

**C** **Dune movement**—(left) *Photograph courtesy of USGS*

**D** **Dune movement**—(right) *©2011 DigitalGlobe*

**E** **Tiger beetle**—*Photograph by Phyllis Pineda Bovin, National Park Service, April 2006*

**F** **Bison and dunes**—*Photograph courtesy of National Park Service*

**G** **Bison herd**—*Photograph courtesy of National Park Service*

**H** **Sandhill crane**—*Photograph by Manjith Kainickara—Wikimedia Commons; Creative Commons Attribution, Share Alike 2.0*

**I** **Rufous hummingbird**—*Image Courtesy of www.naturespicsonline.com*

**J** **Large sunflowers**—*Photograph by Phyllis Pineda Bovin, National Park Service, 2007*

**K** **Sunflowers and dunes**—*Photograph courtesy of National Park Service*

**L** **Lightning over dunes**—*Photograph by Jon-Pierre Lasseigne, 2014, courtesy of the National Park Service.*

**M** **Fulgurite**—*Photograph courtesy of National Park Service*

**N** **Medano Creek**—*Photograph courtesy of L.J. Binder, USGS*

**O** **Beaver**—*Photograph by Steve—Wikimedia Commons; Creative Commons Attribution, Share Alike 2.0*

**P** **Kangaroo rat**—*Photograph courtesy of National Park Service*

**Q** **Great Sand Dunes National Park entrance sign**—*Photograph courtesy of L.J. Binder, USGS*

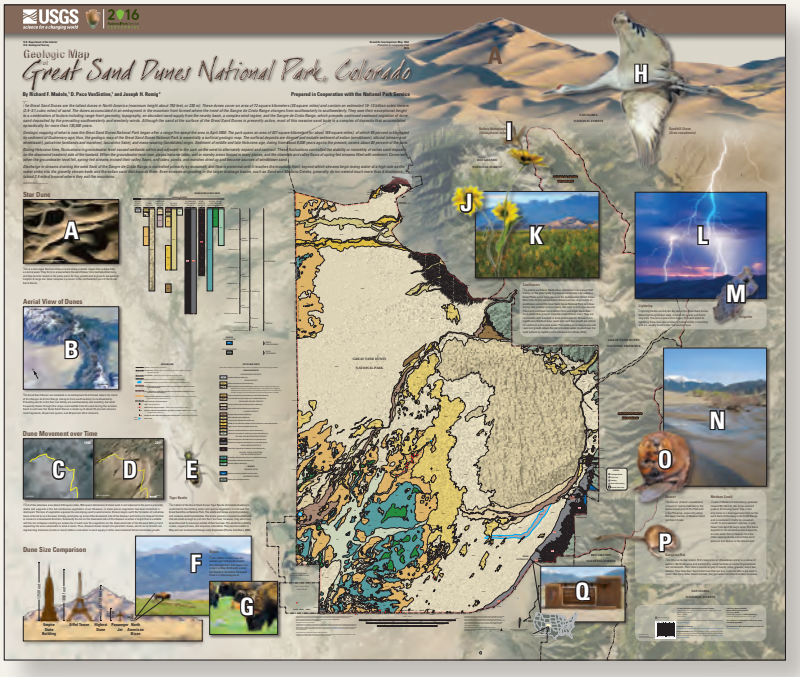


Topographic base modified from U.S. Geological Survey US Topo 1:24,000-scale maps, 2013: Beck Mountain, Crestone, Crestone Peak, Liberty, Medano Pass, Medano Ranch, Mosca Pass, Sand Camp, and Zapata Ranch, Colorado.
Projection: Universal Transverse Mercator, zone 13; North American Datum 1983 (NAD 83)
National Geodetic Vertical Datum of 1988 (NGVD 88)
Road data on US Topo from ©TomTom

Shaded relief base created from U.S. Geological Survey 1-meter resolution lidar elevation data, accessed September 2011 at http://nationalmap.gov/. Orthophotograph background image from the U.S. Department of Agriculture National Agricultural Imagery Program (NAIP) accessed 2013 at https://gdg.sc.egov.usda.gov/. National Park and Preserve boundaries from the National Park Service, accessed December 2015 at https://irma.nps.gov/ , National Forest boundaries from the U.S. Department of Agriculture U.S. Forest Service accessed May 2016 at http://data.fs.usda.gov/geodata/. State park boundaries from Colorado Parks and Wildlife accessed on September 2015 at http://cpw.state.co.us/. Other boundaries modified from The National Map at http://viewer.nationalmap.gov/basic/

Private inholdings may exist within Federal or State reservations

This map is not a legal document. Public lands are subject to change and leasing, and may have access restrictions; check with appropriate offices. Obtain permission before entering private lands

# Great Sand Dunes National Park, Colorado

**Publishing support provided by:**
**Denver Publishing Service Center**
Edited by **L.J. Binder**
Graphic design and layout by **Carol A.Quesenberry**
Manuscript approved for publication July 25, 2016

Madole and others—**Geologic Map of Great Sand Dunes National Park**—Pamphlet to Accompany Scientific Investigations Map 3362, Version 1.1, August 2018



ISBN 978-1-4113-4072-5

ISSN 2329-1311 (print)
ISSN 2329-132X (online)
https://doi.org/10.3133/sim3362

Printed on recycled paper